

NFATc1 as a Therapeutic Target in **Burkitt's Lymphoma**

**NFATc1 – ein Angriffspunkt zur Therapie des
Burkitt-Lymphoms**



Aus dem Institut für Pathologie der Universität Würzburg

Vorstand: Prof. Dr. Andreas Rosenwald

Dissertation

zur Erlangung der Doktorwürde der Medizinischen Fakultät der
Julius-Maximilians-Universität Würzburg

vorgelegt von Hendrik Eike Fender

Geboren am 6.8.1988 in Göttingen

Würzburg, Mai 2015

Referent: Prof. Dr. Dr. Edgar Serfling

Korreferent: Prof. Dr. Max Topp

Berichterstatter: Prof. Dr. Ralf Bargou

Dekan: Prof. Dr. Matthias Frosch

Tag der mündlichen Prüfung: 27.4.2016

Der Promovend ist Arzt

Abbreviations

α	anti
AICD	activation induced cell death
AID	activation-induced deaminase
ATR	Ataxia telangiectasia and Rad3 related
ATRA	all-trans retinoic acid
BAFF	B cell activation factor of the TNF family
BCL6	B-cell lymphoma 6
BCR	B cell receptor
bHLH	basic helix-loop-helix
BL	Burkitt's lymphoma
BLNK	B cell linker Protein
Btk	Bruton's tyrosine kinase
cAMP	cyclic adenosine monophosphate
CD	cluster of Differentiation
CDK	cyclin-dependent kinase
CK1 α	casein kinase 1 α
CN	calcineurin
CRAC	calcium-release activated calcium
CsA	cyclosporin A
CSR	class switch recombination
DLBCL	diffuse large B cell lymphomas
EBV	Epstein-Barr-Virus
EGTA	ethylene glycol tetraacetic acid
GC	germinal center
GM-CSF	granulocyte-macrophage colony stimulating factor
GSK-3	glycogen synthase kinase 3
Ig	immunoglobulin
IL	interleukin
IP3	inositol trisphosphate
ITAM	immunoreceptor Tyrosine-based Activation Motifs
JAK3	Janus kinase 3
mTOR	mammalian Target of Rapamycin
NFAT	nuclear factor of activated T cells
NF- κ B	nuclear factor of κ B
NES	nuclear export signal
NLS	nuclear localization signal
PI3K	PI3 kinase
PIP2	phosphatidylinositol 4,5-bisphosphate
PKC/PKA	protein kinase C /Protein kinase A
PLC	phospholipase C
PI	propidium iodide
RSD	rel similarity domain
SCF	stem cell factor
SHM	somatic hyper-mutation
SRR	serine-rich regions
STAT	signal transduction and activators of transcription
SYK	spleen tyrosine kinase
TAD	transactivation domain
TAM	tumor associated macrophages
TGF- β	transforming growth factor- β
VCAM-1	vascular cellular adhesion molecule-1
VEGF	vascular endothelial growth factor

Table of Contents

1. Introduction	1
1.1. B cells: function, development, activation and receptor signaling	1
1.1.1. Development and differentiation of B cells	1
1.1.2. B cell signaling	2
1.1.3. Formation of the germinal center and the role of JAK3 and BCL6	4
1.2. Burkitt's lymphoma: a <i>MYC</i> -driven B-cell-derived tumor	6
1.2.1. Features of BL	7
1.2.2. Altered signaling pathways in BL	9
1.3. The proto-oncogene <i>MYC</i>	10
1.3.1. The <i>MYC</i> gene	10
1.3.2. <i>MYC</i> as transcription factor	11
1.3.3. Functions of <i>MYC</i> : survival, cell growth, differentiation and tumor genesis	12
1.4. NFAT - Nuclear factors of activated T cells	13
1.4.1. Protein structure of NFATs	14
1.4.2. DNA binding properties and target genes	15
1.4.3. Regulation and activation of NFAT	17
1.4.4. The inducible isoform of NFATc1: NFATc1/ α A	18
1.4.5. Oncogenic functions of NFAT proteins	20
1.5. Current approaches for the therapy of BL: advances and limitations	21
1.6. Gallium containing compounds in current clinical trials	21
1.7. Objectives	22
2. Material and Methods	23
2.1 Materials	23
2.1.1. Chemicals and reagents	23
2.1.2. Buffers	23
2.1.3. Antibodies and dyes	25
2.1.4. Inhibitors, antibiotics	26
2.1.5. Oligonucleotides	26
2.1.6. Enzymes	27
2.1.7. Stimulators	27
2.1.8. Size standards	27
2.1.9. Kits and systems	27
2.1.10. Cell lines	27
2.1.11. Experimental animals	27

2.1.12. Consumables	28
2.1.13. Instruments and accessories	28
2.2 Methods	29
2.2.1. Cellular technics	29
2.2.2. Flow cytometry (FACS)	30
2.2.3. CFSE: cell trace proliferation assay	31
2.2.4. ³ H-Thymidine incorporation assay	31
2.2.5. MTT cell proliferation assay	32
2.2.6. Generation of FITC labelled yeast	32
2.2.7. Working with proteins	32
2.2.8. Working with nucleic acids	34
2.2.9. Imaging	35
2.2.10 Electronic data processing and statistical analyses	37
3. Results	38
3.1. Nuclear location of NFATc1 is another hallmark of Burkitt's lymphoma	38
3.1.1. Nuclear location of NFATc1 in Burkitt's lymphoma cell lines	38
3.1.2. NFATc1 in E μ -myc mouse tumor cells	40
3.2. Molecular mechanisms of gallium in Burkitt's lymphoma	42
3.2.1. Gallium affects NFATc1 and MYC levels in Burkitt's lymphoma	44
3.2.2. Pancreatic cancer: NFATc1-overexpressing carcinomas are sensitive to gallium	48
3.3. Proliferation expansion of BL is not inhibited by calcineurin inhibition	50
3.3.1. Only atypical high concentrations of CN inhibitors affect proliferation of BL cells	50
3.3.2. CN inhibitors affect partly the translocation of NFATc1 in BL cells	52
3.3.3. NFATc1 is not largely regulated by PI3K pathway	55
3.3.4. JAK3 inhibition reduces proliferation of BL and translocates nuclear p65 but not NFATc1	57
3.4. MYC-overexpression contributes to the nuclear distribution of NFATc1 and regulates its expression on two different levels	59
3.4.1. CsA does not affect NFATc1 translocation in P493-6 cells	60
3.4.2. MYC repression releases partly NFATc1 into the cytosol and regulates NFATc2 and BCL-6 protein and NFATc1 mRNA expression	62
3.5. Plasticity of myc-driven tumor cells: the origin for "starry sky" –macrophages?	64
3.5.1. Expression of the myeloid markers	64

CD11b and F4/80 on E μ -myc mouse B cell lines	
3.5.2. Macrophage-like cells are inducible depending on calcium signaling	66
3.4.3. Transformed "M" Cells are competent for phagocytosis	69
4. Discussion	70
5. Summary	75
6. Table of Figures	76
7. Bibliography	78

1. Introduction

1.1. B cells: function, development, activation and receptor signaling

The most important function of B cells is the production of immunoglobulins (Igs). Together with T cells, they belong to the adaptive immune system. Originated from hematopoietic stem cells in the bone marrow, B cells migrate to peripheral lymphatic tissues after having passed series of differentiation and maturation steps. Whereas early steps are antigen-independent, specific receptors such as membranous IgM (mIgM) and IgD (mIgD) are crucial for further antigen-dependent differentiation (Fig.1.1). The individual maturation and differentiation steps are characterized by both Ig rearrangements and expression of specific surface markers.

1.1.1. Development and differentiation of B cells

All B cells are CD19 positive and derive from CD34 positive stem cells. Growth factors and receptors like vascular cellular adhesion molecule-1 (VCAM-1), stem cell factor (SCF), the tyrosine-kinase kit and interleukin-7 orchestrate the regulation of the first proliferation cycles in the bone marrow (Löffler 2007). Pu.1, Pax-5, E2A and EBF are key regulators in B cell lineage differentiation. The latter two regulate Ig gene rearrangements and Ig light chain expression. Pax-5 inhibits expression of the granulocyte-macrophage colony stimulating factor (GM-CSF) receptor, which otherwise would cause differentiation into myeloid precursors, and activates genes like *CD97A/MB-1* and *MYCN* (Yu, Allman et al. 2003).

Early pro-B cells carry germline configurations of the Ig genes. Intermediate pro-B cells and late pro-B cells initiate somatic rearrangement/recombination of the immunoglobulin heavy chain (IgH) locus on chromosome 14 that involve D_H and J_H segments and the V_H , D and J_H segments, respectively. Major recombination mediators are Rag1, Rag2 and TdT (Pillai 2005). At pro-B cell stage the B cell receptor (BCR) consists of $Ig\alpha/Ig\beta$ (also

named CD79a/b) heterodimers associated with calnexin (Kurosaki, Shinohara et al. 2010). However, the later pre-BCR is composed of $Ig\alpha/Ig\beta$ heterodimers, a transmembrane form of just rearranged heavy chains (mIg μ) and the invariant germ line light chains, called “surrogate light chains” (see Fig.1.1)

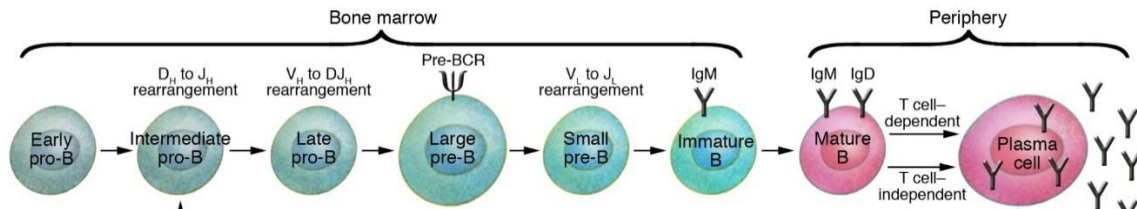


Fig. 1.1. B cell differentiation: First steps of B cell maturation occur antigen-independent in the bone marrow. In the pro-B cell stage, the Ig heavy chain locus is subjected to somatic recombination. This results in the pre-B cell receptor (pre-BCR). At the pre-B cell stage, the Ig light chain loci are rearranged, too, resulting in B cell receptor expression (also known as membranous IgM). After leaving the bone marrow, mature B cells detect antigens. Finally, they develop into plasma cells. Modified after (Pillai 2005)

After having performed rearrangements of the Ig light chains κ and λ on chromosome 2 and 22, respectively, surface expression of the IgM B cell receptor (BCR) takes place, and the immature B cell is born. These cells, which are typically IgM⁺ and IgD^{lo/-}, undergo a negative selection to exclude auto-reactive properties before being released into the blood stream (Kurosaki, Shinohara et al. 2010).

1.1.2. B cell signaling

Proliferation of mature B cells is commonly mediated through BCR signaling. However, albeit BCR signaling is critical for maturation and sustained generation of B cells, it also provides the potential to induce several B cell malignancies.

The BCR consists of two IgH and two IgL chains complexed with the $Ig\alpha/Ig\beta$ heterodimer (CD79A/B) (Niemann and Wiestner 2013). Upon antigen-binding, it activates multiple intracellular pathways such as MAP-kinase, NFAT, AKT and NF- κ B cascades (Fig.1.2). First, the Src-kinases (Lyn, Fyn, Blk, Hck) are activated and phosphorylate both Immunoreceptor Tyrosine-based Activation Motifs (ITAMs) of the receptor associated $Ig\alpha/Ig\beta$ heterodimers as well as the spleen tyrosine kinase (SYK). Together with PIP3, generated by PI3Kinase (PI3K), a hub for numerous proteins like SLP-65/BLNK (B cell linker Protein) is formed to activate subsequent proteins, e.g.

Bruton's tyrosine kinase (BTK), PLC γ 2 or AKT. Finally, the activation of Btk and PLC γ 2 leads to cytosolic increase of calcium and, thereby, to activation of the calcium-calmodulin-dependent phosphatase calcineurin (CN) that dephosphorylates NFAT, inducing its nuclear translocation (Mackay, Figgett et al. 2010). Especially Btk, which seems to be essential exclusively in B cells, mediates antigen processing, cell trafficking, receptor internalization and activation of NF- κ B via PKC β activation (Niemann and Wiestner 2013). Finally, AKT-Kinase activates mTOR (mammalian Target of Rapamycin). This ubiquitously expressed serine/threonine kinase acts as a cell cycle regulator at G1 to S phase transition. Rapamycin (first discovered as fungicide isolated from *Streptomyces hygroscopicus*), Everolimus or Temsirolimus can bind mTOR and, therefore, act as immunosuppressants or anti-tumor drugs in different types of lymphomas.

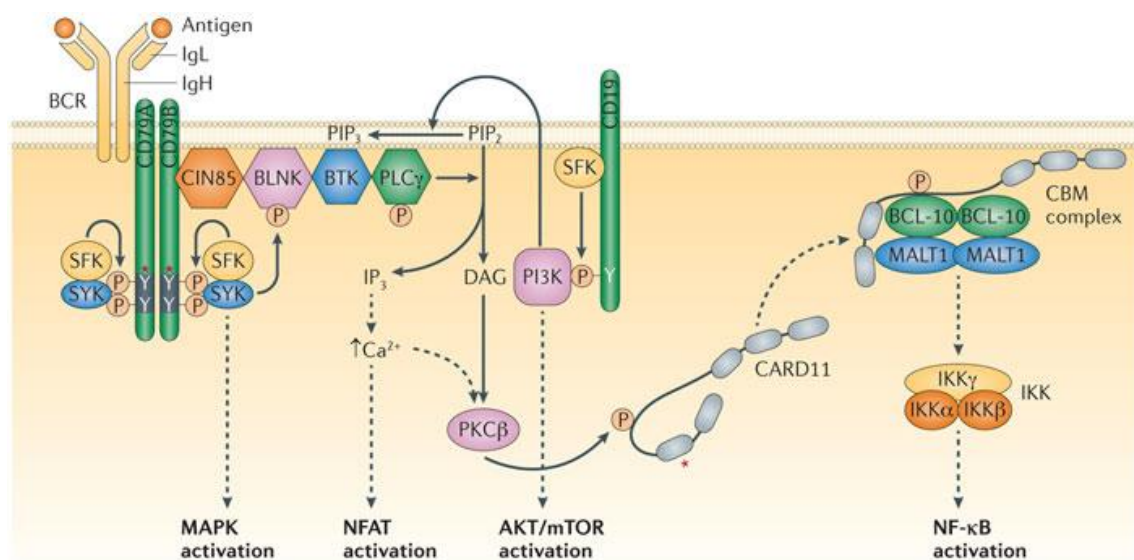


Fig. 1.2. The B cell receptor activates MAPK, NFAT, mTOR and NF- κ B pathways.

After antigen-binding, numerous intracellular proteins are activated through the BCR complex and its co-receptor CD19. The SYK Kinase triggers RAS-signaling and activates the MAPK. Due to PLC γ activation, NFAT activation is triggered by elevated calcium levels. The PI3K induces mTOR activation and supports activation of other enzymes, like the BTK. Finally, the canonical pathway of NF- κ B can be activated by induction of PKC β and the subsequent CBM complex. BLNK: B-cell linker protein, BTK: Bruton's tyrosine kinase, CARD11 (also known as CARMA1): caspase recruitment domain-containing protein 11, CBM: CARD11-BCL-10-MALT1, CIN85: Cbl-interacting protein of 85 kDa, DAG: diacylglycerol, IKK: inhibitor of NF- κ B kinase, IgH: immunoglobulin heavy chain, IgL: immunoglobulin light chain, IP3: inositol trisphosphate, MALT1: mucosa-associated lymphoid tissue lymphoma translocation protein 1, MAPK: mitogen-activated protein kinase, mTOR: mammalian target of rapamycin, NF- κ B: nuclear factor- κ B, PI3K: phosphoinositide 3-kinase, PIP2: phosphatidylinositol-4,5-bisphosphate, PIP3: phosphatidylinositol-3,4,5-trisphosphate, PKC β : protein kinase C β , PLC γ : phospholipase C γ , SFK: SRC family kinase: (Young and Staudt 2013)

Members of NF- κ B transcription factors, such as RelA/p65, RelB, c-Rel, kB1/p50/p105 or kB2/p52/p100, form dimers and regulate important genes that are involved in proliferation, intercellular signaling, immune answer and inflammation. There are two possibilities to activate them: first, via PKC and several intermediate steps, I κ B-kinase IKK degrades I κ B therefore liberating NF- κ B (see Fig.1.2). Second, the “B cell activation factor of the TNF family” (BAFF)-receptor mainly induces the non-canonical pathway of NF- κ B, thus activating NF- κ B2/p52/p100. Additionally, together with CD19, BAFF stimulates PI3K and AKT (Mackay, Figgett et al. 2010). If PIP2 is transformed to PIP3, proteins like BTK, PLC γ 2 or AKT can bind. The latter inhibits GSK-3 that, in turn, triggers NFAT activation. PI3K is known to support Myc via blocking its degradation and inducing degradation of MAD1, an antagonist of Myc (Sander, Calado et al. 2012).

1.1.3. Formation of the germinal center and the role of JAK 3 and BCL6

The production of high-affinity antibodies and the development of plasma and memory B cells results from the germinal center (GC) (see Fig.1.3). After antigen binding, follicular B cells (characterized by IgM^{low}, IgD^{high}, CD21⁺, CD23⁺, CD19⁺) move to the T cell zone of peripheral lymphoid tissues in lymph nodes, Peyer’s patches or spleen. Here, they interact with corresponding T helper cells via cytokines and binding of CD40 to CD40 ligand, CD86 to CD28 and the Fas ligand to its receptor.

One pro-survival cytokine is IL-21. It is expressed by T helper cells and follicular T cells. Bound to its receptor on B cells, it activates Janus kinase 3 (JAK3) through the common gamma chain (γ c). A subsequent phosphorylation of tyrosine residues leads to dimerization of STATs (signal transduction and activators of transcription), their nuclear translocation and finally the transcription of specific genes that are crucial for the immunoglobulin class switch and proliferation (O’Shea, Park et al. 2005). JAK3 is furthermore known to cooperate with STAT5 and NFATc1 in thymocyte development (Patra, Avots et al. 2013).

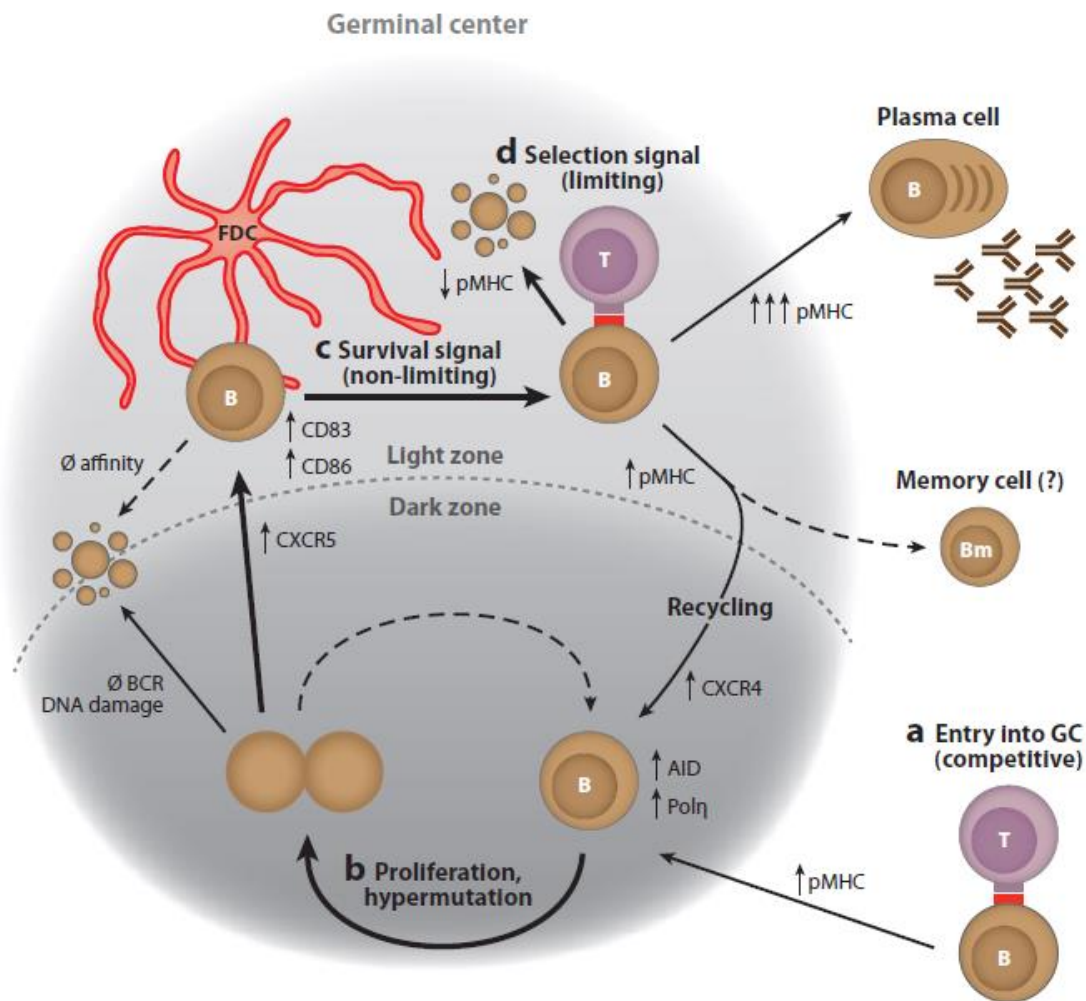


Fig. 1.3. The germinal center. a) B cells entering the germinal center (GC) have already detected an antigen and were activated and pre-selected with the help of T cells. b) As centroblasts, they proliferate in the dark zone (DZ) and upregulate the activation-induced deaminase (AID) to perform somatic hypermutation (SHM) (c) and d). Later, as centrocytes, their selection takes place in the light zone (LZ) with the help of follicular dendritic cells (FDC) and T follicular helper (T_{fh}) cells. This procedure is based on antigen-affinity: High affinity of the BCR results in higher production of peptide-MHC on cell's surface that for its part, increases T cell contacts in a competitive way. The base for continuous improvement of the B cell receptors (BCR) seems to be a “recycling” of created B cells, therefore passing multiple cycles between DZ and LZ. The chemokine receptors CXCR4 and CXCR5 regulate migration of centroblasts and centrocytes, respectively. (Victora and Nussenzweig 2012)

BCL6 acts as an administrator supporting high proliferation rates of centroblasts and inhibits their differentiation into plasma cells by silencing Blimp-1. Furthermore, it silences BCL2 and represses signals through the BCR and CD40 to ensure a constant pro-apoptotic state and the responsiveness to selective signals, respectively. Probably, this prevents development of auto reactive Igs and autoimmunity. However, with the repression of *TP53* and *ATR*, BCL6 helps the GC B cells to tolerate DNA damages due

to activation-induced deaminase (AID). Approximately 30-50% of Burkitt's lymphomas (BL) harbor *BCL6* mutations releasing its deregulation, probably preventing DNA damage responses.

Histologically, the proliferating centroblasts ($CXCR4^{\text{high}}$, $CD83^{\text{low}}$, $CD86^{\text{low}}$) are represented by the dark zone, where somatic hypermutation (SHM) takes place. Here, the already somatically recombined VJ and VDJ genes of both Ig light and heavy chains undergo a fine-tuning in their antigen binding region. Subsequently, their selection takes place in the light zone on centrocytes ($CXCR4^{\text{low}}$, $CD83^{\text{high}}$, $CD86^{\text{high}}$) with the help of T follicular helper cells and follicular dendritic cells (Victora and Nussenzweig 2012). AID, an enzyme that targets ssDNA in GC B cells, plays the major role in SHM and class switch recombination (CSR). Sometimes, its mutational properties incidentally affect other regions than Ig loci, thus producing oncogenes or chromosomal translocations resulting in GC lymphomas like BL (Victora and Nussenzweig 2012).

Selection into the plasma cell compartment is forced by T-dependent antigens: Through CD40 and CD40-ligand, NF- κ B and subsequent IRF4 activation suppress Bcl-6 activity. This releases Blimp-1 expression and permits the final plasma cell differentiation. Besides CD40, PD-1 and IL-21 influence plasma cell generation, too. Aside from germinal center derived plasma cells, there are marginal zone B cells or memory B cells that derive T cell independently from B1 B cells (Shapiro-Shelef and Calame 2005).

1.2. Burkitt's Lymphoma: a *MYC*-driven B cell-derived Tumor

In 1958, Denis Parsons Burkitt investigated tumors derived in children of equatorial Africa growing in their jaws. Later, this entity of Burkitt's lymphoma (BL) was named the "endemic type": its incidence correlates with malaria and Epstein-Barr-Virus (EBV). So, BL was the first tumor known to be associated with a virus. Also first in history is the discovery of the *c-MYC* oncogene that is deregulated in all entities of BL (Table 1.1.).

Endemic type	Diseased children are usually between 4 and 7 years old. Except from the jaws, the tumor often becomes manifested in bones, kidneys, breasts, ovaries or the gastrointestinal tract. Incidence correlates with malaria and Epstein-Barr-Virus (EBV).
Sporadic type	Only in 20% of all cases EBV+, accounts for 1-2% of the adult lymphomas, but 40% of lymphomas in childhood in Europe. It mostly occurs in the abdominal region, especially in the ileocecal area, or in peripheral lymph nodes, whereas the latter is more common in adults.
Immunodeficiency-associated	First non-Hodgkin's lymphoma that has been discovered to be associated with human immunodeficiency virus (HIV) infection. Nevertheless, it can also be seen in allograft recipients or patients with congenital immunodeficiency.

Table 1.1 Entities of BL (Hecht and Aster 2000, Ferry 2006). Three different clinical types of BL and their characteristics.

1.2.1. Features of BL

Morphologically, BL share the following histologic features: diffuse architecture (1), medium-sized lymphocytes with scant cytoplasm (2), round to irregular but not cleaved nuclei containing one to several peripheral nucleoli (3) and the “starry-sky” appearance: abundant large histiocytes that are phagocytizing apoptotic cell debris (4). Three tumor variants are discriminated: 1. Classical: medium-sized, round and uniform cells with frequent mitosis (Ki67 >95%) but also plenty apoptotic cells. It is often found in the endemic or in the sporadic type. 2. Plasmacytoid differentiation: In addition to the classical morphology, cells harbor monotypic cytoplasmic immunoglobulins. It is often found in immunodeficiency-associated types. 3. Atypical BL or BL-like variant: Frequently found in adult's sporadic type. Characteristics are larger and pleomorphic cells (Ferry 2006).

BL's typical marker expression is: IgM, Bcl-6, CD10, CD19, CD20, CD21, CD22, CD43, CD79a and p53, but not CD5, CD23, CD138, Bcl-2 and TdT. All BL are GC-derived, as there is evidence that IgH and IgL chain genes have performed SHM (Hecht and Aster 2000). Additionally, BCL-6 and CD10 expression is also common for GC B cells (see Fig. 1.4) (Blum, Lozanski et al. 2004, Ferry 2006).

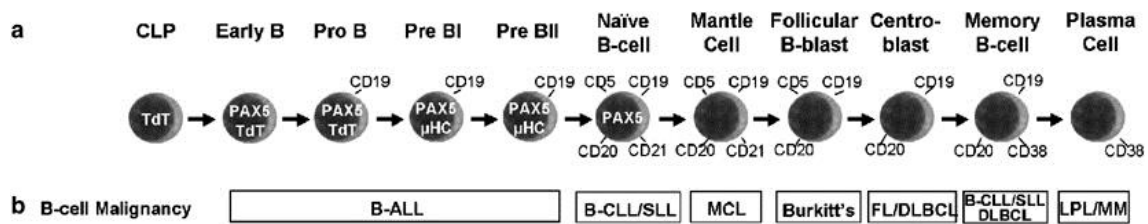


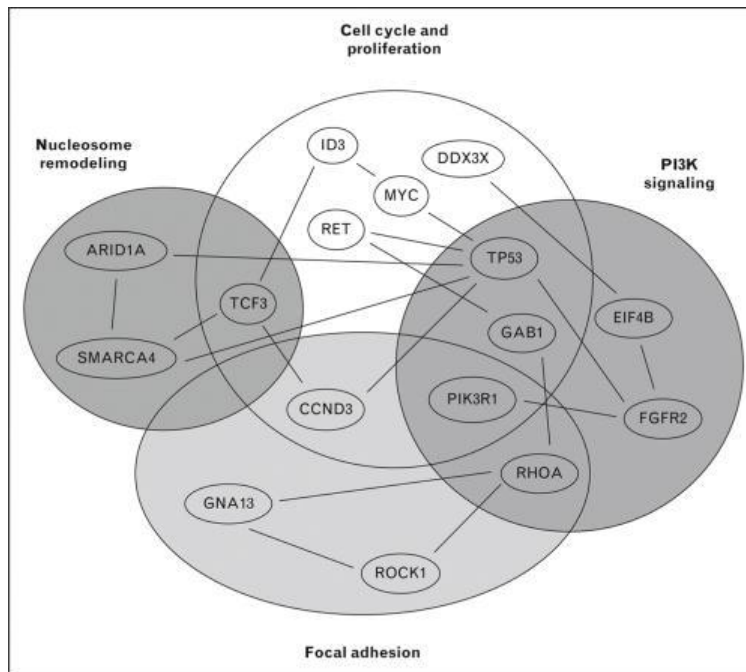
Fig. 1.4 B cell differentiation steps and their malignant counterparts. (a) Different B cell development stages, surface marker expression and selected cytoplasmic proteins. (b) Malignancies that derive from the associated developmental steps. B-ALL: precursor B-cell acute lymphoblastic leukemia; B-CLL/SLL: B-cell chronic lymphocytic leukemia/small lymphocytic lymphoma; MCL: mantle cell lymphoma; FL: follicular lymphoma; DLBCL: diffuse large B-cell lymphoma; LPL: lymphoplasmatic lymphoma; MM: multiple myeloma. (Taylor, Liu et al. 2006)

In BL, *MYC* is translocated and therefore under control of one of the three Ig enhancers¹. Most frequent translocations in BL take place between *MYC* and the *IgH* gene [t(8;14)] (80%). The remaining 20% are distributed to the two light chain genes (*IgL*) kappa (15%) and lambda (5%) [t(2;8) or t(8;22), respectively]. Typically for the endemic type is the configuration that unaltered *MYC* is juxtaposed to the joining segment of the *IgH* gene. Probably, translocation happens during V(D)J rearrangement. The two other types often exhibit a translocation to the switch region (S_{μ}) of *IgH*, whereas the break point in *MYC* is between its first and second exon. This translocation probably happens during Ig class switching (Hecht and Aster 2000).

¹It should be noted that *MYC* translocation is not specific for BL. There are many other tumor types such as large B cell lymphoma, follicular lymphoma, lymphoblastic lymphoma or multiple myelomas that occasionally exhibit a *MYC* translocation. Hecht, J. L. and J. C. Aster (2000). "Molecular biology of Burkitt's lymphoma." *J Clin Oncol* **18**(21): 3707-3721..

1.2.2. Altered signaling pathways in BL

Translocation and overexpression of *MYC* does not alone lead to tumor development. Cooperation between EBV, *BCL1*, *BCL2*, *N-ras* or most consistently, *TP53* mutations



(>30% of all BL) and alterations in its pathway, *TP53* mutations (30%) or *BCL6* mutations (30-50%) are frequently existing (Yu and Thomas-Tikhonenko 2002). Additionally, genes encoding proteins related to death-associated signals, like Fas, $\text{INF}\gamma$ or $\text{TNF}\alpha$, are often hypermethylated and transcriptionally inactive (Hecht and Aster 2000), also see Fig. 1.5.

Fig. 1.5. Frequently mutated genes and their context (Greenough and Dave 2014)

But what additional mutations are sufficient for tumorigenesis? In mice, p53 inactivation and *Myc* deregulation is sufficient for tumor formation (Yu and Thomas-Tikhonenko 2002), but these tumors do not resemble BL. *Myc* deregulation and constant PI3-kinase activation in mice B cells generates tumor cells resembling the phenotype of human BL (Sander, Calado et al. 2012). It is known that activating mutations in transcription factor *TCF3* (E2A) or inactivating mutations of its inhibitor ID3, often cause constitutively active PI3-kinase signaling, which is the case in 70% of sBL (Schmitz, Young et al. 2012). Another important role plays cyclin D3, whose transcription is promoted by E2A. Moreover, stabilizing mutations in *CCND3*, the cyclin D3 gene, are often selected by MYC-PI3-kinase coactivation and can be found in 38% of sBL cases (Schmitz, Young et al. 2012). All these findings implicate key roles of cyclin D3, PI3-kinase and MYC that orchestrate in the generation of BL. Toxicity of cyclin D3 inactivation or inhibiting of

PI3-kinase signaling underlined the hypothesis (Dominguez-Sola and Dalla-Favera 2012) (Niemann and Wiestner 2013). Intriguingly, contrary to many other B cell malignancies, the proliferation and survival of BL does not depend on NF- κ B activity which is low in BL cells. Moreover, a further decrease of NF- κ B activity has nearly no effect but increased NF- κ B activation kills BL cells (Klapproth, Sander et al. 2009, Niemann and Wiestner 2013).

1.3. The proto-oncogene *Myc*

To distinguish *Myc* from *N-myc*² and *L-myc*, the proto-oncogene is often termed as “c-myc”. However, *N-myc* and *L-myc* are two related but functionally different genes. One hypothesis about the function of the transcription factor is that *Myc* is able to increase the expression of nearly all active genes and therefore strongly supports all ongoing developmental stages of a cell (Nie, Hu et al. 2012). Up to 30% of all human cancers exhibit a deregulated *MYC* expression resulting in elevated protein levels of c-MYC (Weinberg 2007).

1.3.1. The *Myc* gene

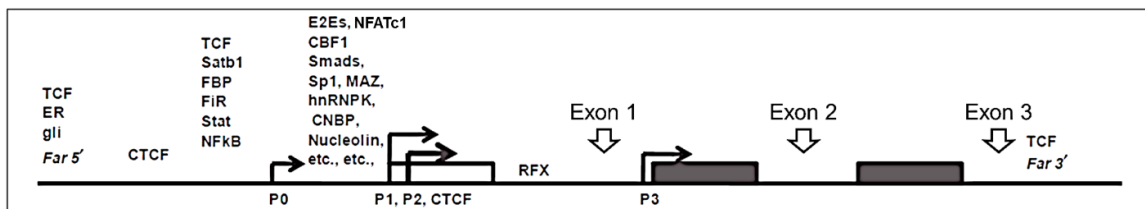


Fig. 1.6. Scheme of the *Myc* gene. The upper part shows a partial list of the numerous transcription factors that bind to different regions of *Myc*. The approximate locations of the promoters P0, P1, P2, and P3 are marked below. Black boxes represent introns. (Levens 2010)

Transcription of *MYC* is largely initiated through the two major promoters P1 and P2 (see Fig.1.6). Interestingly, NFATc1 binds to the so-called TGF- β Inhibitory Element within the P2 promoter, thereby increasing *MYC* transcription in pancreatic cancer cell lines (Buchholz, Schatz et al. 2006). Predominantly in the non-endemic types of BL, as a result

² The *N-myc* gene was first found to be amplified in 30% of childhood neuroblastomas and is responsible for the more aggressive type of this tumor. *N-myc* is also found to be amplified in tumors, like astrocytomas, retinoblastomas or small cell lung cancers. (Weinberg 2007)

of *MYC* translocation, promoter P3 initiates *MYC* expression. P0 is another minor promoter. *MYC* is located on chromosome 8 and consists of 2356 base pairs. Aside from its encoded protein, it is also the origin for several short RNAs having regulatory potentials *ex vivo* (Levens 2010). The *Myc* mRNA consists of 1365 bases encompassing 3 exons, whereas only 2 and 3 encode the *MYC* protein spanning 439 amino acids. There is also a minor *MYC* variant described that contains parts from the 3' end of exon 1. This rarely translated exon has negative regulatory properties: on the one hand, it suppresses transcription and, therefore, provides a negative feedback loop and on the other hand several sequences of exon 1 disturb the transcription machinery (Hecht and Aster 2000).

1.3.2. Myc as transcription factor

MYC belongs to the large family of basic helix-loop-helix (bHLH) leucine zipper transcription factors. All bHLH- transcription factors share the following three basic structures: a C-terminal DNA binding domain that binds to the 5'-CACGTG-3' sequence motifs that are called as E-boxes (1), the dimerization domain consisting of a loop, two α -helices and the leucine zipper (2), and an N-terminal transcription activation domain (3).

Enhancement or repression of target gene transcription is determined by *MYC* levels, its phosphorylation status and its association with bHLH partner proteins: e.g. *MYC/MAX* complexes act as transcriptional activators whereas *MYC/MAD* and *MYC/MIZ-1* complexes act as transcriptional repressors. Additionally, these partner proteins are able to form dimers among each other, thus competing for DNA binding. *MYC* does also interact with several other proteins that do not belong to the bHLH family. However, the function of these complexes remains largely unclear. For example, the C-terminal domain of *MYC* interacts with AP-2, YY-1, BRCA-1 and TFII-I, and the N-terminal domain of *MYC* with Bin1, MM-1, p107, Pam, and Amy-1 (Hecht and Aster 2000, Weinberg 2007).

1.3.3. Functions of Myc: survival, cell growth, differentiation and tumor genesis

In lymphocytes, Myc expression is highly induced 2-4 hours after activation (Nie, Hu et al. 2012). Analysis of approximately 8.000 binding sites revealed genes involved in RNA and protein biosynthesis, metabolism and cell cycle progression. These authors hypothesized that Myc-binding does not cause an “on” or “off” switching of target genes. Instead, it seems to function as a general amplifier for already activated genes that are pre-loaded with RNA polymerase II (Nie, Hu et al. 2012). However, Myc also acts as a transcriptional repressor: Approximately 30% of these target genes are transcriptionally down regulated. This might be caused by the expression of miRNAs that down regulate overall expression or the expression of transcriptional suppressors. (Nie, Hu et al. 2012).

Selected Myc targets are the genes encoding cyclin D2 and the CDK4. It sequesters the CDK inhibitor p27^{Kip1}, thereby orchestrating cell cycle progression. Growth inhibitory signals by TGF- β can be circumvented by Myc via suppression of cdc25A and the cell cycle inhibitors p15^{INK4B} and p21^{Cip1}. Hence, TGF- β and Myc act contrary by inducing or suppressing CDK inhibitors. Further features of Myc-actions are the induction of telomerase subunits (Weinberg 2007), regulation of the DNA replication machinery and recruitment of histone acetylases. Its overexpression results in toleration of DNA damages (Felsher and Bishop 1999), thus contributing to its oncogenic functions (Dominguez-Sola, Ying et al. 2007).

Myc prevents cell differentiation. Its complexes are displaced in differentiated or post-mitotic cells through other bHLH complexes. Proteins that direct differentiation, like CCAAT-enhancer-binding protein α (C/EBP α), are suppressed by MYC (Valledor, Borrás et al. 1998). Thus, in adult liver or intestine tissues that consist mainly of differentiated cells, a deletion of the *Myc* gene has only little effect (Levens 2010).

Myc provides strong pro-apoptotic signals leading to the induction of p53, alterations in death receptor signaling and *BCL2* expression. It is able to suppress *NF-kB* through impairment of RNA and protein synthesis (Keller, Huber et al. 2010). This is a highly important feature of BL, as NF-kB would otherwise exert its pro-apoptotic functions (Klapproth, Sander et al. 2009). Thus, anti-apoptotic signaling pathways are

necessary in BL to counterbalance MYC's pro-apoptotic features: Aside from PI3K signaling in BL, NFAT activity is known to be enhanced by MYC overexpression (Habib 2007).

1.4. NFAT - Nuclear factors of activated T cells

The family of the NFAT factors was first described in activated Jurkat T cells, acting as potent transcription factors for the induction of IL-2 promoter. Upon both B and T cell receptor activation, rising calcium levels lead to a CN dependent de-phosphorylation of NFAT that finally translocates into the nucleus. This takes only 5-10 minutes and is the requirement for its transcriptional function. Immunosuppressants like FK506/Tacrolimus or cyclosporin A (CsA) are potent inhibitors of CN. Thus, they are widely used reagents for the treatment of autoimmune disorders or transplant rejections. Nevertheless, apart from lymphocytes, many other tissues express NFAT proteins, e.g. cardiomyocytes, muscle, brain and bone cells.

There are five different NFAT proteins. Although their biological functions (Table 1.2) differ, their structure and intracellular activation have a lot in common. NFAT proteins, in particular NFATc1, NFATc2 and NFATc3, are present in different isoforms which differ in their N- or C- termini (see Fig.1.7). NFAT5/ Ton-EBP shares only around 45% of the characteristic Rel similarity domain (RSD) with other NFAT factors and does not contact AP-1 or CN (and is therefore not influenced by intracellular calcium levels). As it does not share any other NFAT family specific features, its "NFAT" membership remains debatable (Serfling, Berberich-Siebelt et al. 2000).

	Function
NFATc1 (Nfat2)	Heart valve development: NFATc1 deficient mice embryos die at day 14 of gestation. Especially, isoform α A supports proliferation of lymphocytes after immune cell receptor stimulation. Deficient lymphocytes have a reduction in proliferation upon stimulation; T and B cells produce less IL-2,-4 and other lymphokines.
NFATc2 (Nfat1)	Pro-apoptotic and suppressive role for lymphocyte proliferation: Mice lacking NFATc2 develop a hyper proliferative syndrome with two times

	more peripheral lymphocytes. Immune responses are increased, as well as T _h 2 cell cytokine expression.
NFATc3 (Nfat4)	Nfatc3 deficient mice show 50% less peripheral T lymphocytes. Mice lacking Nfatc2 and Nfatc3 suffer from splenomegaly and masses of peripheral lymphocytes (the result of apoptosis resistance due to decreased Fas ligand expression) with the tendency to produce T _h 2-type lymphokines and cells.
NFATc4 (Nfat3)	Playing a role in the inducible expression of cytokine genes in T cells, for example in the induction of IL-2 and IL-4.
NFAT5	Regulates the transcription of genes that are important to resist osmotic stress.

Table 1.2. Overview of the properties of NFAT factors (Serfling, Berberich-Siebelt et al. 2000)

1.4.1. Protein structure of NFATs

All four NFATc factors (NFATc1-4) contain a DNA binding domain, a regulatory domain and a N- or C-terminal transactivation domain (TAD) (see Fig.1.7).

Due to its sequence and particularly structural similarities to Rel/NF- κ B factors, the DNA binding domain is named RSD. It consists of approximately 300 amino acids forming two loops and 10 beta-strands. The first loop is responsible for DNA binding. In NFATc1, the amino acid residues Arg448 and Arg439 interact with the O6 and N7 atoms of guanosine nucleotides in the NFAT core motif, which is GGAAA. But also van der Waals contacts from Tyr442 to opposed thymidine nucleotides and several minor groove contacts support NFATc1 binding to DNA. Contacts to AP-1 proteins are provided by the second loop of the RSD.

The TAD of NFATc2 and NFATc1 provides contacts to nuclear proteins, like the transcriptional co-factors p300/CBP and AP-1. If bound, they act as transcription controllers. On the one hand, they regulate histone transacetylase activity, and on the other they can recruit further transcription factors.

The regulatory domain in NFATc1 harbors a bi-partite nuclear localization signal (NLS) and one nuclear export signal (NES). Relying on the phosphorylation status, they are alternately hidden or exposed. Therefore, numerous phosphorylation sites, organized in

serine-rich regions (SRR) and transactivation binding motifs for serin/threonine protein kinases (SP motifs), they are located in this region, too. Mutations or phosphorylations within the regulatory domain influence their nuclear or cytosolic appearance (Serfling, Berberich-Siebelt et al. 2000).

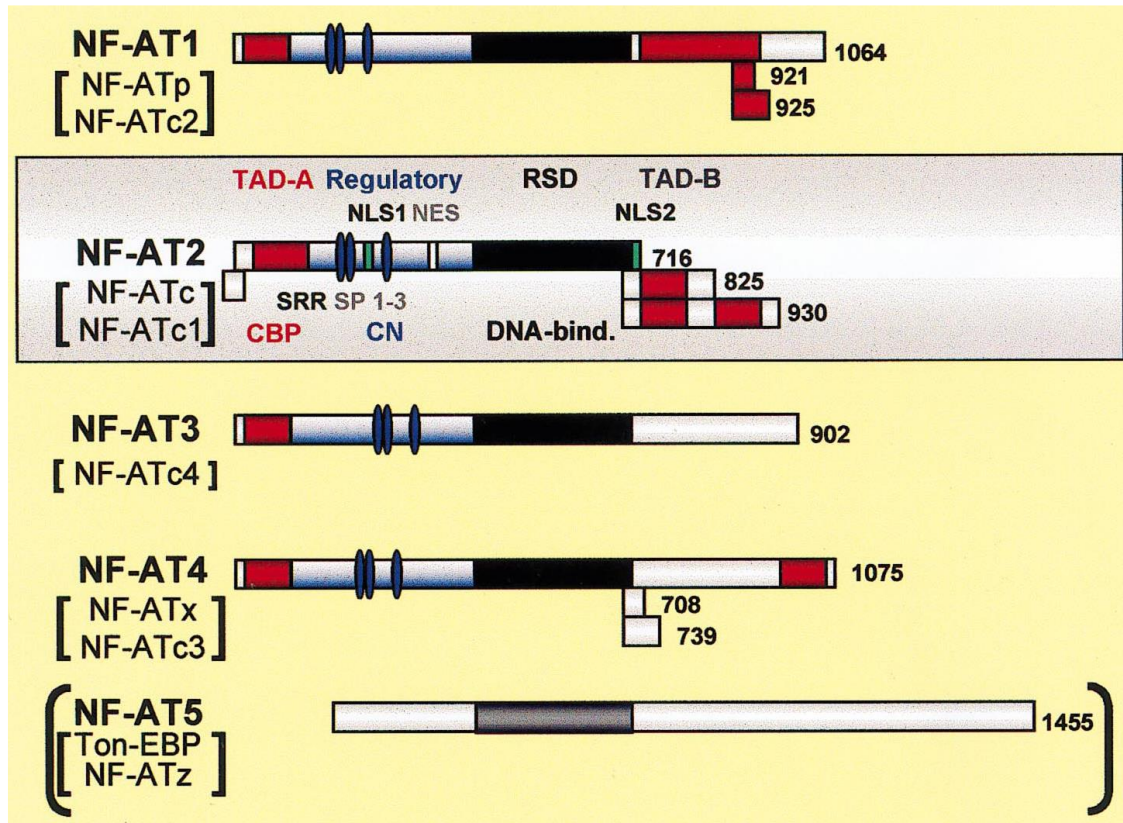


Fig. 1.7. Scheme of the five members of the NFAT family. The red boxes stand for the N- and C-terminal transactivation domains (TAD-A and TAD-B, respectively). Enframed by TAD-A and the DNA-binding Rel similarity domain (RSD), the regulatory domain is shown as black box. Within the latter, there are calcineurin (CN) binding sites, nuclear localization sequences (e.g. NLS1) and nuclear export signals (NES). Additionally, serine rich regions (SRR) and SP motifs are part of the regulatory region. (Serfling, Berberich-Siebelt et al. 2000)

1.4.2. DNA binding properties and target genes

Direct target genes for NFAT factors contain mostly the core binding motif GGAAA, which is embedded in the larger NFAT binding site. Frequently, target genes in T cells have a composite NFAT and AP-1 binding site of structure 5'-caxwGGAAAawxxxg/aTGAC/GTCAg/tc-3' (capital letters: highly conserved nucleotides; lower case letters: poorly conserved nucleotides; w=A or T; x=any nucleotide). NF- κ B core motifs are partly similar to the core motif of NFAT factors

resulting in a competitive binding mechanism. Target genes of NFATs are summarized in Fig.1.8.

GENE	CELL TYPE
Endothelin	Endothelium
Cox2	"
Glucagon	Pancreatic islet
BNP	Heart
IL-2; IL-3; IL-4; IL-5; GM-CSF; IFN- γ ; FasL.	Lymphocyte
Carabin	
Myf-5; MYC I; SERCA2a; TRPC3.	Skeletal muscle
aP2	Adipocyte
IP ₃ receptor 1	Hippocampal neuron
Calcitonin receptor	Osteoclasts

Fig. 1.8. Overview: Target genes of NFAT factors. (Berridge 2011)

The IL-2 promoter contains two high affinity and three low affinity binding sites (around the positions -145, -285 and -45, -90,-160 respectively). In this case, the transcriptional activity seems to be controlled by the sum of NFAT factors, as inactivation of either NFATc2 or NFATc1 alone does mildly affect IL-2

RNA or protein levels. The activity of the IL-4 promoter is also positively regulated by NFATc1, whereas NFATc2 seems to act as a negative regulator. Therefore, *Nfatc1*-deficient T cells show a defect in the production of IL-4 and other T helper 2 (Th2) -type lymphokines. The NFATc1 promoter itself contains several NFAT core motifs, suggesting the existence of a regulatory feedback loop.

NFATc1 is the “master regulator” of osteoclast development. Upon RANK ligand activation and several intermediate steps, NFATc1 is upregulated promoting osteoclast differentiation. Intriguingly, gallium blocks this differentiation by impairing the transcription of NFATc1 without affecting viability (Verron, Masson et al. 2010). Here, several molecular mechanisms orchestrate NFATc1 levels: e.g. calcium release by TRAPV channels is decreased, *c-Fos* gene expression is inhibited, whereas *Traf6*, *p62* and *Cyld* expressions are increased. The latter three inhibit the nuclear translocation of NF-kB factors which support to induce NFATc1 transcription. Therefore, gallium is used to therapy bone disorders, like Paget’s disease of bone or tumor hypercalcemia (Verron, Loubat et al. 2012).

1.4.3. Regulation and activation of NFAT

In B and T cells, activation of NFAT factors is mainly the result of B or T cell receptor signaling. On the one hand, rising calcium levels cause their nuclear translocation and on the other, numerous protein kinases, p56lck and p21ras induce their transcription.

Increasing levels of free calcium are the result of an influx through calcium-release activated calcium (CRAC) channels and the release of Ca^{2+} from endoplasmic reticulum stores. When calcium binds calmodulin, this complex activates CN that is composed of one regulatory and one catalytic subunit. The latter dephosphorylates phosphorylated SRR motifs in NFAT proteins, thereby inducing structural changes and triggering the subsequent nuclear translocation of NFATs by unmasking their NLS. In addition to NFATs, CN binds also other proteins, like transforming growth factor- β (TGF- β) receptor, IP3, PKA, NMDA receptor, transcription factors, NO synthase (Medyouf and Ghysdael 2008) or immunophilins, like cyclophilin A or FKBP12. The latter two acts as very potent CN inhibitors if bound to CsA or FK506, respectively (see Fig.1.9)(Liu, Farmer et al. 1991). There is also a highly specific peptide that binds to CN with high affinity to inhibit CN activity and NFAT dephosphorylation, called VIVIT (Yu, van Berkel et al. 2007).

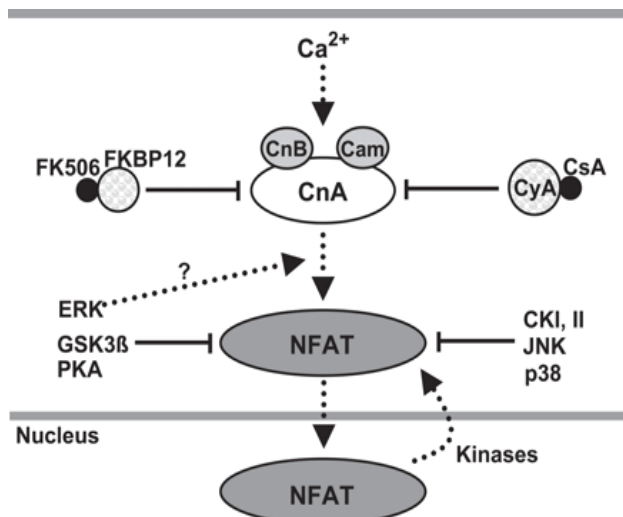


Fig. 1.9. Regulation of NFAT (Molkentin 2004). Elevated calcium levels lead to CN-activity. After dephosphorylation, NFAT is able to pass the nuclear membrane. Several regulatory networks inhibit its translocation: FK506 and CsA can bind to FKBP12 and cyclophilin A, respectively. Additionally, numerous proteins directly act on NFAT: GSK3 β , protein kinase A (PKA), casein kinase I and II (CKI and CKII), JNK and p38. CnA: calcineurin A; CnB: calcineurin B, Cam: calmodulin; CsA: cyclosporine; CyA: cyclophilin A; FKBP12: FK506 binding protein 12.

The contact between CN and NFAT is mediated through two docking motifs consisting of seven amino acids with the sequence P_xI_xIT, whereas the best connection is provided by SPRIEIT (Gachet and Ghysdael 2009). They are located in the regulatory domain of NFAT. Many serine/threonine kinases like GSK-3, casein kinase 1 α (CK1 α), PKA, JUN kinase 1 (JNK1) and DYRK are known to counteract CN function and, therefore, phosphorylate NFAT proteins. However, the stability, activity and location of NFATs is also modulated by other events, like sumoylation or ubiquitinylation (Nayak, Glockner-Pagel et al. 2009).

Representing a regulatory circuit, genes like *Ppp3cb* and *Rcan1* are targeted and controlled by NFATc1. These two genes encode one of three catalytic subunits of CN and its inhibitory protein, RCAN, respectively (Bhattacharyya, Deb et al. 2011).

1.4.4. The inducible isoform of Nfatc1: Nfatc1/ α A

Upon T and B cell receptor activation, the inducible isoform NFATc1/ α A is generated within 24 hours. When the appendant Nfatc1-P1 promoter becomes active, this results in both the expression of the inducible N-terminal α -peptide encoded by exon 1, and the use of proximal poly A site pA1. This leads to short Nfatc1 transcription products, indicated by the letter “A” on protein level (see Fig. 1.10). Contrariwise, the constitutively active promoter P2 collaborates with the stronger poly(A) site pA2, therefore expressing the longer isoforms NFATc1/ β B and NFATc1/ β C. The differences between the α A isoform and the β B or β C concern the N-termini (α - versus β -peptide) and, in particular, the missing C-terminal peptide of approximately 250 aa in NFATc1/ α A. This C-terminal peptide harbors two sumoylation motifs (Nayak, Glockner-Pagel et al. 2009).

As P1 represents the gateway to NFATc1/ α A expression, it has numerous important properties. Just right in front of exon 1, there are several binding sites for NFAT, NFAT/NF- κ B and CRE-like sequence motifs. Furthermore, P1 (and P2) harbor numerous epigenetic chromatin marks and CpG methylation islands that control its activity. The methylation pattern of P1 promoter correlates to the expression or suppression of NFATc1 in different cancer cell lines (Akimzhanov, Krenacs et al. 2008), suggesting a crucial role for NFATc1 in cancer growth.

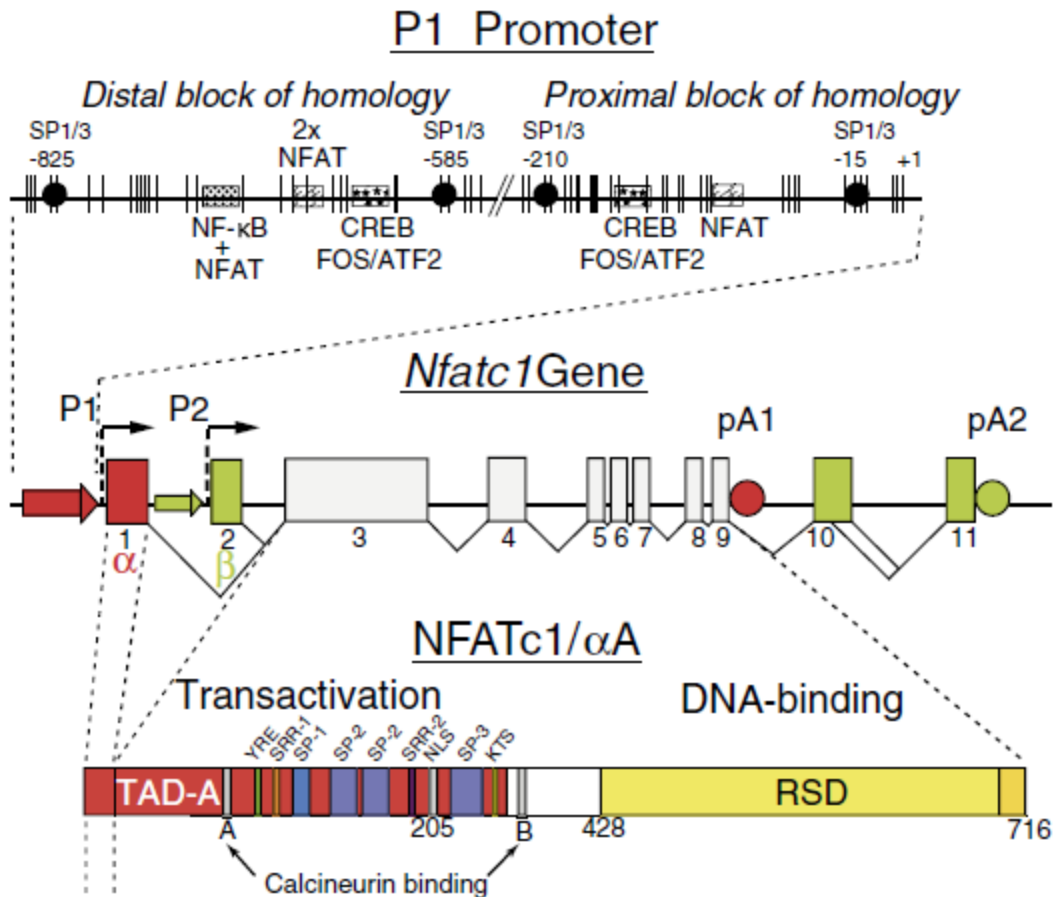


Fig. 1.10. Scheme of the murine P1 promoter, the *Nfatc1* gene and NFATc1/αA (modified) (Serfling, Avots et al. 2012). The P1 promoter consists of the distal and proximal block of homology. Within them, indicated binding motifs are spread. Vertical dashes stand for CpG residues. The gene has a length of approximately 11kbp and is controlled by two promoters, P1 and P2, and two polyadenylation sites, pA1 and pA2, respectively. Moreover, *Nfatc1* contains eleven exons but in NFATc1/αA only the α-peptide and the peptides encoded in exons 3-9 are present. Similar to Fig. 1.7, the protein can be subdivided into a TAD, a regulatory domain with its SP-motifs, SRR, NLS, NES and its CN binding sites, and the DNA-binding RSD.

A negative regulation of NFATc1/αA is mediated through proteins like Foxp3 in regulatory T cells, or the inducible cAMP early repressor ICER³. In regulatory T cells, Foxp3 and NFATc1 compete binding sites in the P1 promoter (Torgerson, Genin et al. 2009).

³ short isoform of the cAMP Response Modulator gene CREM

1.4.5. Oncogenic Functions of NFAT Proteins

Immunohistochemical analyses of NFATc1 expression revealed high levels and the nuclear appearance in many of aggressive B cell lymphomas, including diffuse large B cell lymphomas (DLBCL) or BL. However, due to silencing of the P1 promoter, both in Hodgkin lymphoma and plasma cell proliferations, its expression was very low (Akimzhanov, Krenacs et al. 2008). In DLBCL and pancreatic cancer cell lines, NFATc1 up-regulates *MYC* expression (Buchholz, Schatz et al. 2006, Buchholz and Ellenrieder 2007). First, NFATc1 recruits histone acetylases to the *MYC* promoter. Second, it binds to the TGF- β inhibitory element on the proximal promoter of the *MYC* gene. Third, together with p300, both NFATc2 and NFATc1 up-regulate its expression by directly binding to proximal and distal sites (Mognol, de Araujo-Souza et al. 2012).

By controlling the expression of cyclooxygenase (Cox)-2, NFAT plays a pivotal role in the migration of endothelial cells induced by vascular endothelial growth factor (VEGF) (Hernandez, Volpert et al. 2001). Additionally, the ability of cancer cells to seed metastasis or invade other tissues is partly regulated by NFAT. In human breast and colon carcinoma cell lines protein levels of $\alpha 6\beta 4$ integrin correlate with NFATc2 and 5 levels (Jauliac, Lopez-Rodriguez et al. 2002). Furthermore, NFATc1 down regulates the expression of E-cadherin in tumor cell lines supporting their progression in vivo (Oikawa, Nakamura et al. 2013).

In preadipocyte NIH 3 T3 cells, constitutively active NFATc1 led to resistance against reduced serum growth requirements, growth autonomy and the ability to form tumors in athymic nude mice (Neal and Clipstone 2003, Robbs, Cruz et al. 2008). Whereas NFATc1 acted as oncogene, NFATc2 was found to suppress tumors, especially in chondrocytic malignancies (Akimzhanov, Krenacs et al. 2008) and BL cell lines (Kondo, Harashima et al. 2003). This might be caused by repression of cyclin-dependent kinase 4 (CDK4) expression (Baksh, Widlund et al. 2002) or the negative regulation of cyclin B, A2 and E (Viola, Carvalho et al. 2005). But also the genes encoding short isoform of caspase 8-inhibitor c-Flip, the CD40 ligand, programmed cell death-1 (PD-1) protein and TNF- α or Fas-Ligand expression are controlled by NFATc1. Moreover, *Nfatc2* knockout mice are less resistant to carcinogen-induced tumorigenesis (Robbs, Cruz et al. 2008).

1.5. Current approaches for the therapy of BL: advances and limitations

Clinically, BL is an aggressive malignancy with a very high proliferation rate. Even with high-dose chemotherapy regimens, like R-CODOX-M/IVAC⁴ or EPOCH-R⁵, 2 year survival rates vary from 60-90%, whereas age and tumor stage influence the outcome (e.g. nervous system or bone marrow is infiltrated in 10% up to 30%) (Hecht and Aster 2000, Ferry 2006, Wilson, Dunleavy et al. 2008, Hoelzer, Walewski et al. 2014). More precisely, in a large multicenter trial from 2002-2011, the actual therapeutic standard is a 5-day chemotherapy for 6 cycles (Dexamethasone, Vincristine, Ifosfamide, Methotrexate, Cytarabine, Vindesine, Teniposide, Etoposide) including a triple intrathecal therapy (Cytarabine, Methotrexate, Dexamethasone) and a radiotherapy (24 Gray) if central nervous system is infiltrated (Hoelzer, Walewski et al. 2014). After a prophylactic treatment (by cyclophosphamide and prednisone), the first cycle starts at day 7, whereas 16 days are between each cycle. Rituximab, a CD20 antibody, is given before each cycle and as maintenance, for a total of 8 doses. The most pronounced toxicity was a neutropenia, affecting 58% of patients. Severe infections occurred in 38% of all cases.

1.6. Gallium containing compounds in current clinical trials

Gallium nitrate, a metal salt, was shown to have anti-neoplastic effects in animal tumor models, non-Hodgkin lymphomas and lymphoma cell lines, including BL (Chitambar, Wereley et al. 2006). Therefore, it was further evaluated for its anticancer activity in phase I and II clinical trials in various cancer treatments (Chitambar 2012). However, predominantly patients with advanced bladder cancer and non-Hodgkin's lymphomas appeared to benefit from it. Moreover, gallium nitrate is suitable for a combination with

⁴ Rituximab, cyclophosphamide, vincristine, doxorubicin, methotrexate; intrathecal therapy with ifosfamide, etoposide, cytarabine (also known as cytosin-arabinoside)

⁵ Etoposide, prednisone, vincristine, cyclophosphamide, doxorubicin and rituximab

the conventional chemotherapy, especially because it does not exert myelosuppressive effects (Chitambar 2012). On the molecular level, it binds to transferrin and enters the cell through the transferrin receptor. On the one hand, gallium affects the iron-uptake therefore inhibiting various iron-dependent enzymes, such as ribonucleotide reductase. On the other hand, numerous intracellular processes are affected leading to apoptosis. Gallium inhibits magnesium-dependent ATPases, tubulin-formation, proteasome function, CDP and ADP reductase and DNA polymerase activity and induces the translocation of inositol phosphatidylserine to the cell surface. However, probably the most important cellular response to gallium is the loss of mitochondrial membrane potential that induces Bax activity, thereby releasing cytochrome c from mitochondria and activating Caspase 3 (Chitambar 2012). Additionally, gallium maltolate induces reactive oxygen species from mitochondria and induces apoptosis in a p53-independent manner (Chitambar, Purpi et al. 2007).

1.7. Objectives

Burkitt's lymphoma is a highly aggressive lymphoma derived from germinal center B cells. Although it is well-known for his *MYC* translocation, several other factors and intracellular pathways contribute to its genesis: apart from constitutive active PI3-kinase signaling, p53, TCF3 or cyclin D3 mutations, NFAT factors are virtually always present and, furthermore, appear in the nucleus. Together with NF- κ B factors, which are typically down regulated in BL, they represent the most important transcription factors in lymphocyte activation. Moreover, they were recently discovered as oncogenes in different types of tumors. As gallium components were successfully used for BL treatment and are known to influence NFATc1 expression in osteoclast differentiation, I hypothesized that (1) NFATc1 represents a major survival signal for BL and that (2) NFATc1 is specifically targeted by gallium. The aim of this thesis was to evaluate the potential of NFAT factors as therapeutic targets and to investigate the effect of both "classical" CN inhibition and gallium in BL, *Myc*-driven B cell tumors and NFAT expressing tumors.

2. Material and Methods

2.1 Materials

2.1.1. Chemicals and Reagents

Acrylamide/Bisacrylamide 29:1	Liquid Nitrogen
Ammonium peroxodisulfate (APS)	Kalium chloride
Antibody diluent (DAKO Real)	Magnesium chloride
Agarose	Methanol
Acetic acid	Midori green (Nippon Genetic Europe GmbH)
Bradford reagent	MTT (Thiazolyl Blue Tetrazolium Bromide)
Bromophenol blue	Sodium chloride (NaCl)
β -Mercaptoethanol	Sodium hydrogenphosphate buffer
Bovine Serum Albumin (BSA)	Sodium hydroxide
DAPI (4',6-diamidino-2-phenylindole)	Sodium pyruvate
Dimethyl-sulfoxide (DMSO)	Sodium fluoride
Distilled water (dH ₂ O)	Paraformaldehyde
Ethylenediaminetetraacetic acid (EDTA)	Poinceau Red
Ethylene glycol tetraacetic acid (EGTA)	Sodium dodecyl sulfate (SDS)
Ethanol	TEMED (Tetramethylendiamine)
Fetal calf serum (FCS)	Tris(hydroxymethyl)aminomethane
Fluoroshield	Triton-X-100
Glycerol	Trypan Blue Solution
Glycin	Trypsin/EDTA
Hydrochloric acid	Tween 20
³ H-Thymidine (by Hartmann Analytics)	

Materials were used from the following manufactories: AppliChem GmbH, Calbiochem, Carl Roth GmbH, Fluka, GE Healthcare Life Sciences, Gibco BRL/Life Technologies, Merck, Roche Diagnostics and Roche Molecular Biochemicals, Serva, Biocel MilliQ system (Millipore), Sigma-Aldrich.

2.1.2. Buffers

Distilled water was used to dilute the buffers.

Annexin-Binding Buffer	HEPES (pH 7.4)	10 mM
	NaCl	149 mM
	CaCl ₂	2.5 mM
Buffer-A	HEPES (pH 7.9)	10 mM
	KCl	10mM
	EDTA	0.1 mM
	EGTA	0.1 mM

Buffer-B	HEPES (pH 7.9)	20 mM
	NaCl	0.4 M
	EDTA	1 mM
	EGTA	1 mM
FACS buffer	Na ₂ HPO ₄ (pH 7.4)	10 mM
	NaCl	137 mM
	KCl	2.6 mM
	KH ₂ PO ₄	1.8 mM
	BSA	0.1% (w/v)
	(NaN ₃)	0.1% (w/v)
Genomic lysis buffer	Tris (pH 8.0)	50 mM
	NaCl	300 mM
	SDS	0.2% (w/v)
	EDTA	25 mM
	Proteinase K	1000 U/ml
Laemmli buffer (5x)	Tris (pH 6.8)	0.3M
	β-Mercapthoethanol	0.5M
	SDS	10%
	Glycerol	50%
	Bromophenol blue	0,25%
PBS	NaCl (pH 7.4)	137 mM
	Na ₂ HPO ₄	10 mM
	KCl	2.6 mM
	KH ₂ PO ₄	1.8 mM
RIPA buffer (100mL)	Tris-HCl 1M (pH 7.8)	5ml
	NaCl 5M	0,87g
	TritonX-100	1ml
	Na-deoxycholol	0,25g
	EDTA 0.5M pH 8	200μl
	EGTA 0.1M	1ml
	β-Glycerophosphat	0,216g
	NaF 0.2M	25ml
SDS running buffer	Tris-HCl (pH 8.4)	25 mM
	Glycin	192 mM
	SDS	0.1% (w/v)
TBS (1x)	Tris-HCl (pH 7.5)	25 mM
	Glycin	150 mM
	(NaN ₃)	0.1% (w/v)

TBS-Tween	Tris-HCl (pH 7.5) Glycin Tween 20	25 mM 150 mM 0.2% (v/v)
Transfer buffer	Tris-HCl (pH 8.4) Glycin SDS Methanol	48 mM 40 mM 14 mM 20% (v/v)
10% Resolving gel (10 ml)	H ₂ O 30% Polyacrylamide 1.5 M Tris (pH 8.8) 10% APS 10% SDS TEMED	4.0 ml 3.3 ml 2.5 ml 0.1 ml 0.1 ml 0.004 ml
Stacking gel (3 ml)	H ₂ O 30% Polyacrylamide 1.5 M Tris (pH 6.8) 10% APS 10% SDS TEMED	2.1 ml 0.5 ml 0.25 ml 0.03 ml 0.03 ml 0.003 ml

2.1.3. Antibodies and Dyes

Annexin V APC	BD Pharmingen
Antibody Diluent	Dako
B220 FITC (RA3-6B2)	eBiosciences
B220 Biotin (RA3-6B2)	BD Pharmingen
CD19 Biotin (eBio1D3/1D3)	BD Pharmingen
CD19 PE (1D3)	BD Pharmingen
CD3 ϵ APC (145-2C11)	eBiosciences
CD11b FITC (M1/70)	eBiosciences
Fc block (93)	BD Pharmingen
CD69 Biotin (H1.2F3)	BD Pharmingen
CD3 APC (45-2C11)	eBiosciences
CD3 Brilliant violet (145-2C11)	eBiosciences
F4/80-eFluor 450 (BM8)	eBiosciences
Ki-67 Alexa Fluor 647 (Sol A 15)	eBiosciences
Streptavidin APC	eBiosciences
Streptavidin eFluor 450	eBiosciences
Streptavidin PerCP.Cy5.5	BD Pharmingen
Mouse anti NFATc1 (7A6)	BD Pharmingen
Mouse anti- β Actin (C4)	Santa Cruz Biotechnology
Mouse anti NFATc3	Santa Cruz Biotechnology
Goat anti CD20 (M-20, polyclonal)	Santa Cruz Biotechnology

Goat Akt1 Antibody (C-20): sc-1618	Santa Cruz Biotechnology
Mouse anti-c-Myc (9E10)	Santa Cruz Biotechnology
Rabbit anti-c-Myc antibody [Y69] (ab32072)	abcam
Rabbit anti NFATc2 (M-300, polyclonal)	Cell Signaling
Rabbit anti BCL6 (D65C10)	Cell Signaling
Rabbit anti p65	Cell Signaling
Rabbit anti p100/p52	abcam
Rabbit anti Caspase 7	Cell Signaling
Rabbit anti phospho-AKT SC-7985	Santa Cruz Biotechnology
Rabbit anti NFATc2	Immunoglobe
Goat- anti-Mouse Alexa Fluor 555	eBiosciences
Goat- anti-Mouse Alexa Fluor 488	eBiosciences
Goat- anti-Rabbit Alexa Fluor 555	eBiosciences
Goat- anti-Rabbit Alexa Fluor 488	eBiosciences
Streptavidin Alexa Fluor 488	eBiosciences
Goat-anti-Mouse Alexa Fluor 647	Dianova
Donkey anti-Goat Alexa Fluor 488	Invitrogen
FITC protein labeling kit	Thermo Scientific Kit Pierce

2.1.4. Inhibitors, Antibiotics

Cyclosporin A (CsA)	Calbiochem
Estrogen (β -estradiol)	Sigma
FK506	Sigma
HALT Protease inhibitor cocktail	Thermo scientific
Jak3 inhibitor	Calbiochem
Penicillin/Streptomycin	Gibco
Doxycycline	Sigma
Wortmannin	Sigma
Idelalisib	Medchemexpress
JNK-Inhibitor SP600125	MedChemtronica

2.1.5. Oligonucleotides

Primers were dissolved in water at a final concentration of 100pmol/ μ L. They were synthesized by Eurofins/MWG/operon or Sigma-Aldrich.

Primers

<i>Eμ-myc for</i>	<i>Eμ-myctransgene</i>	cagctggcgtaatagcgaagag
<i>Eμ-myc rev</i>		ctgtgactggtgagtactcaacc
qRT-NFATc1-U	<i>Nfatc1</i>	ccctgtcccctacgtcctac
qRT-NFATc1-L	<i>Nfatc1</i>	cacctcaatccgaagctcat
qRT_hP1-U	<i>P1 Promoter</i>	cttcgggagaggagaaactttg
qRT_hP1/P2-L	<i>P1/P2 Promoter</i>	gtggaggctgaagggttg
qRT_hP2-U	<i>P2 Promoter</i>	tgcactcgagttcctctcg
qRT_hP1-2U	<i>P1 Promoter</i>	catgaagtcagcggaggaag
hL32 L1	<i>RPL32</i>	agcactccagctccttgac
hL32 U1	<i>RPL32</i>	tgtgaagcccaagatcgtc

2.1.6. Enzymes

Proteinase K (822U/ml) Fermentas

2.1.7. Stimulators

anti-IgM Dianova
anti-CD40 R&D
TPA #
Ionomycin Life Technologies

5.1.8 Size standards

DNA-Marker Gene Ruler 1 kb Thermo Scientific
DNA-Marker Gene Ruler 100 bp Thermo Scientific
PageRuler™ Prestained Protein Ladder Thermo Scientific

2.1.9. Kits and systems

anti-mouse B cell-isolation kits Miltenyi Biotec
PCR Master Mix (2x) Fermentas
CFSE Celltrace: Cell proliferation kit Invitrogen

2.1.10. Cell lines

The following human Burkitt's lymphoma cell lines were used (ATCC):

Ramos, Namalwa, Balm 9k, Balm14, Daudi, DND-39

Pre-B Philadelphia chromosome-positive cell line BV-137

Pancreatic cancer cell lines: Panc-1, IMIM-PC2, ASPC-1, PC-1, PC-2

Medium: RPMI, 10% FCS, 0.1% β-Mercapthoethanol

M29 cells were cultured on Lab-Tek II Chamber slides with Cover RS Glass, Nalgene Nunc #154534 slides

A special human lymphoblastoid B cell line, whereas EBNA-2 can be controlled by estrogen and c-myc is under the control of a tetracycline regulated promoter: P-493-6

Cultured in tetracycline free RPMI medium (also containing 10% FCS, 2% glutamine, 1% streptomycin, 50μM β-Mercaptoethanol)

2.1.11. Experimental Animals

The mice that were used for the experiments were kept at a twelve hour circadian rhythm at 22°C in the Institut für Mikrobiologie und Hygiene of the University of Würzburg. They were fed with a special dry animal pellet and water ad libitum. Genotyping was

performed at the age of 4 weeks. The mouse used for the experiments were 8-20 weeks old. Their genetic background was C57BL/6. The reference of the B6.*Eμ-myc* mouse is Adam et al. (1985).

2.1.12. Consumables

Cell culture plates (96 well)	Greiner, Nunc
Cell culture plates (6, 12, 24, 48 well)	Greiner, Nunc
Cell culture plates (6cm, 10cm)	Greiner, Nunc
Cell culture flasks (75cm flask)	Greiner
Cell separation columns (LS)	Milteny Biotech
Cell strainer (70μm)	BD Bioscience
Cover slips	Paul Marienfeld GmbH
Cryo tube (2ml)	Greiner
Cuvettes (plastic)	Braun
FACS tubes	Greiner
Microcentrifuge tubes (1.5ml, 2ml)	Eppendorf
Object glass slides	Hartenstein
PCR plates, white (96 well)	Thermo Fisher
Pipette tips (1000μl, 100μl, 10)	Sarstedt
Sterile filters (0.2μm, 0.45μm)	Sartorius stedim
Whatman 3MM filter paper	Hartenstein
Lab-Tek II Chamber slides with Cover RS Glass slides	Nalgene Nunc #154534

2.1.13. Instruments and Accessories

Autoclave	Systec Dx45
Centrifuge	Eppendorf
Cold centrifuge	Heraeus
Confocal microscope TCS SP5 II	Leica Microsystems
Heating blocks	Hartenstein
Light microscope (dual head)	Olympus
Microcentrifuge	Eppendorf
Microwave	Privileg
Neubauer counting chamber	Brand
PCR machine	Primus 96
pH meter	WTW
SDS-PAGE apparatus	Hofer
Vortexer	Eppendorf
Waterbath	Heidolph
Western blot apparatus	Hofer
FACS Canto II	BD Bioscience
CO2 Incubator	Heraeus Instruments

2.2 Methods

2.2.1. Cellular Technics

2.2.1.1. Cell Culturing

Cells were grown in a humified incubator at 5% CO₂ and 37 °C in the following Gibco media:

RPMI supplemented with 10% FCS, 2 mM L-Glutamin; 1 mM sodium pyruvat; 100 U/ml Penicillin/Streptomycin and 50 μM β-Mercaptoethanol

X-Vivo 15 supplemented with 10% FCS, 2 mM L-Glutamin; 100 μM Non-Essential Amino Acid (NEAA); 1mM sodium pyruvat; 100 U/ml Penicillin/Streptomycin and 50 μM β-Mercaptoethanol

2.2.1.2. Centrifugation of cells

Centrifugation was performed in a Rotina 420R from Hettich for 3 min at 1400 rpm in 4° C.

2.2.1.3. Counting of cells

After mixing the cells with a trypan blue solution, living cells were counted in a Neubauer chamber. According to the dilution factor, the counted cells reflected 1×10^4 cells/ml.

2.2.1.4. Freezing and thawing of cells

Approximately 2×10^7 cells were resuspended in freezing medium cotaining 90% FCS and 10% DMSO. Cell suspensions were transferred in cryo tubes that were stored in a isopropanol freezing container for 24 hours at -70°C. For long-term storage, they were finally stored at -150 °C in liquid nitrogen.

The cells were fastly thawn in a 37°C waterbath and transferred into a 50 mL tube of corresponding growth medium. They were washed twice and resuspended in growth medium and placed in the incubator.

2.2.1.5. Cell isolation and culture

2.2.1.5.1. Isolation of mouse B lymphocytes

B cells were isolated with Miltenyi's B cell isolation kit according to the manufacturer's instruction. Afterwards they were resuspended in X-vivo medium at a concentration of $2-5 \times 10^6$ /mL.

2.2.1.5.3. Culture of E μ -myc mouse tumor cells

Mouse B cell lines were held at a concentration of 5×10^6 cells/mL. Every day, 50% of the medium was replaced by fresh one.

2.2.2. Flow cytometry (FACS)

With the flow cytometry, one can differentiate the cells according to their size, granularity and – if stained before – their surface markers or intracellular proteins. Finally, fresh living cells must be washed two times in PBS, blocked, permeabilized for intracellular staining and incubated with first and secondary antibodies. In the end, they are sorted by forward and sideward scatter and their fluorescence by the FACS machine.

2.2.2.1. Surface marker staining

Approximately 10^6 cells were washed twice in ice cold FACS buffer. Then they were resuspended in 100 μ l of blocking solution (Fc block, 1:300). Within this solution, the primary antibody was present at a concentration of 1:300. The incubation time was 20 minutes at room temperature in the dark. After washing the cells twice with FACS buffer, the secondary antibody was put in the cell suspension (1:300) for 20 minutes. Finally, after two more washing steps, the labeled cells were transferred into FACS for measurement.

2.2.2.2. Intracellular Staining for Ki67

Intracellular stainings were performed with the Foxp3 staining kit (eBioscience). After having stained the surface markers, cells were fixed with eBioscience Fixation/Permeabilization buffer for 20 minutes at 4°C. Subsequently, the cells were permeabilized with eBioscience permeabilization buffer. The antibody was added for 20 minutes at room temperature (for example anti-Ki-67 1:400 in 1x Perm buffer). Finally, they were washed three times with Perm buffer and resuspended in FACS buffer for measurement.

2.2.2.3. Annexin V/PI-staining

After washing the cells twice with FACS buffer, they are resuspended in 100 µL of annexin binding buffer (includes 1µL of Annexin-APC) and stored at room temperature for 15 min. Then, the binding reaction is stopped by adding 100µl of annexin binding buffer. Before measurement, 1µL of PI (1mg/ml) is added to the cell suspension.

2.2.3. CFSE Cell Trace

To study proliferation, the “Cell Trace CFSE proliferation Assay” is one possibility. Cellular proteins are labelled with a fluorescent dye and are detected by flow cytometry. Each cell division leads to fluorescence reduction by half, hence the abatement of fluorescence correlates to cell proliferation. Of particular importance are cytometer recordings directly after the labelling (equates time point zero) and, of course, recordings of non-treated cells. First, cells are washed twice with FACS buffer and resuspended in 6ml. 4 µl of fresh prepared CFSE (diluted in DMSO) is given to the cell suspension that is maintained 3 min at 37°. Then, cells are washed twice with medium. For controlling the maximum staining at time point zero with CFSE, it is likely to take one sample of the cells and store them in 2% formaldehyde/PBS at 4°C. The rest of the CFSE stained cells can be used for experiments. All other samples were taken at the time points indicated, washed twice with PBS/BSA0.1% and either stored in 2% formaldehyde/PBS or directly measured by flow cytometry.

2.2.4 ³H-Thymidine Incorporation Assay

When radioactive ³H-Thymidine is given to proliferating cells, they incorporate it depending on their proliferation and growth properties. The radioactivity can be measured afterwards. Therefore, radioactive counts reflect proliferation properties. Equal numbers of cells are seeded under experimental conditions in a 96 well plate. Usually, we use 2×10^5 cells in 200 μ l of medium. Inhibitions or stimulations are performed for a certain time (usually 48 h). After 24 h, 25 μ l of thymidine (0.05 μ Ci/ μ l ³H-Thymidine) is given to each sample and incubated for the last 24 h. A washing machine (Tomtec industries) cleans intact DNA from cell debris and removes the liquid supernatant. The DNA is collected on a filter membrane, a solution (Betaplate Scint by Perkin Elmer) is given to the membrane, and the radioactivity is counted in a beta-counter (1450 Microbeta Wallac Trilux). The software “microbeta windows” collects the data.

2.2.5 MTT Cell Proliferation Assay

Cell proliferation was also assessed by monitoring the conversion of MTT to formazan. The reduction of MTT by mitochondrial dehydrogenase enzymes can be used as a measure of cell viability. 100 μ l of adherent cells are seeded as triplets into a 96 well plate at densities of 1×10^4 cells /ml. For 90 minutes of incubation, 25 μ l of 10 mg/ml MTT (in PBS) is given to the cells. Afterwards, medium was removed with a needle and the blue formazan crystals trapped in cells are dissolved in 100 μ l of DMSO. The absorbance at 550 nm was measured with a plate reader.

2.2.6 Generation of FITC labelled yeast

Fluorescent yeast are useful to measure ingestion and phagocytosis with the flow cytometer. First, yeast were heated for 30 min at 75 °C to inactivate them. Cultivation was performed to guarantee it. We used the manufacturer’s instruction of the FITC protein labeling kit to stain the yeast. For 2×10^5 cells, we gave 5×10^5 yeast to them and harvested the suspension after indicated time points and fixed them with by adding 4% formaldehyde in a 1:1 ratio. Finally, flow cytometry was performed with all collected samples.

2.2.7. Working with proteins

2.2.7.1. Preparation of protein extracts

All steps are done in the cold room.

Whole cell protein extracts: The cells were washed twice with ice cold PBS. The supernatant is removed after the last washing step. The cell pellet is dissolved in 100 μ L of RIPA buffer supplemented with protease inhibitor cocktail. The suspension is incubated on ice for 15 minutes. For storage, one can freeze them in liquid nitrogen and store them at -70°C. For proceeding, suspensions are frozen multiple times in liquid nitrogen and re-thawed, followed by vortexing for 30 minutes at 4°C. A final centrifugation at 13.200 rpm for 15 min separates the upper whole cell protein extract from the pellet.

For nuclear and cytosolic extracts: Cells were washed twice in ice cold PBS. The cell pellet is re-suspended in 120 μ l of hypotonic buffer A (1 mL of buffer A include 5 μ l of 0.1 M protease inhibitor and 1 μ l of 1M DTT) for 15 min on ice in Eppendorf tubes. Then, 25 μ l of 10% NP-40 is added and the suspension is vortexed for 10 seconds and the tubes are sat on ice for 30 seconds. After centrifugation for 3 min at 8000 rpm, the supernatant is transferred into new freshly labelled tubes. This is the cytosolic extract. Then, the pellet is resuspended in Buffer B/C and vortexed for 30 min followed by a centrifugation for 5 min at 13.200 rpm. The supernatant is the nuclear extract and is transferred into new tubes.

2.2.7.2 Protein concentration measurement (Bradford assay)

Protein concentrations are determined by the Bradford assay. Bradford reagent “Protein Assay Dye Reagent Concentrate” (BioRad) is diluted 1:4 with water. 1 ml of this dilution is added to each plastic cuvette. 2 μ l of protein extracts are given to it and mixed. At 595 nm its absorption is measured and compared to reference concentrations of BSA solutions.

2.2.7.3 Sample preparation and separation by SDS-PAGE

Protein extracts were mixed at a 1:4 ratio with 5x Laemmli buffer and heated for 5 minutes at 95°C. This step is necessary to reduce disulfide bridges in proteins and to denature and

unfold protein structures. Especially, the negatively charged SDS allows a separation in an electric field according to protein size. Therefore, small proteins migrate faster through the polyacrylamide gel. The gel itself consists of a stacking gel (5%, pH 6.8) and a separation gel (10%, pH 8.9). After loading the gel with equal amounts of proteins (usually 40µg), electrophoresis was carried out in running buffer at 25 mA per gel.

2.2.6.4 Immunological detection of proteins (Western Blotting)

The separated proteins are transferred onto a nitrocellulose membrane: In transfer buffer, sponges, the nitrocellulose membrane, the gel and some wet filter papers are put together in the transfer chamber. The transfer process is performed at 300 mA for 90 min at 4 °C. To verify a successful transfer, the membrane was stained with acidic 1% Ponceau red solution. After washing, the membrane is blocked for 30 minutes with 5% milk in TBS/0.05% tween at room temperature. All further washing steps are done with TBS/0.05% tween. For primary antibody incubation, membranes were incubated overnight with in TBS/0.05% Tween and the antibody concentrations indicated (usually 1:500). The next day, three washing steps for 15 min each were followed by the incubation of the secondary antibody. The membranes are incubated for 1 hour at room temperature with a 1:5000 dilution in 5% milk in TBS/0.05% tween. After six more washing steps, “Super Signal West Pico chemiluminescence substrates” are added to the membranes to visualize the proteins. Following two minutes of incubation, the signal was detected with the Fusion SL (Vilbert) camera.

2.2.8. Working with Nucleic Acids

2.2.8.1 Isolation of Genomic DNA from Cells or Mouse Tail Biopsies

For genotyping, the tip of a tail of the mouse was placed in an Eppendorf tube. 20 µl genomic lysis buffer (containing Proteinase K) was added to it and incubated at 56 °C overnight. Then, 480 µl of water were added and incubated for 10 min at 95°C. 3µL were used for subsequent PCR reactions.

2.2.8.2 Isolation of total RNA with Trizol

1x10⁶ cells were centrifuged, washed twice and cell pellet is diluted in 1ml of Trizol reagent.

2.2.8.3 RNA Purification and Reverse Transcription

Cells were washed twice with PBS. After having removed the supernatant after the second centrifugation, cell pellet is dissolved in 1ml of Trizol reagent, transferred into a fresh Eppendorf tube and vortexed for 10 sec. 1. Phase separation. 200µl of chloroform is added to the tube and vortexed every min for 15 min. Centrifugation for 15 min at 12.000 rpm separates the RNA (upper phase) from DNA (interphase) and Trizol. 2. RNA precipitation. The RNA containing upper layer is transferred into a new Eppendorf tube. 500µl of isopropanol is added, vortexed every min for 15 min and finally centrifuged for 15 min at 12.000 rpm. 3. RNA wash. The supernatant is removed from the RNA pellet. Then 75% ethanol is added to the pellet. Vortexing and centrifugation re-precipitates the RNA pellet. Finally, the RNA is dissolved in 20µl of DEPC-treated water. Synthesis of cDNA was performed with the cDNA synthesis kit by “Thermo Scientific”. I followed the instructions of the given protocol and used random hexamer primer.

2.2.8.4 Measurement of RNA

RNA concentrations were measured with a photometer and a 1:50 dilution.

2.2.8.5 Polymerase Chain Reaction (PCR)

The PCR amplifies DNA through a three-step-cycle. First, denaturation, second, annealing of primers, third, elongation of DNA. We used a PCR master mix (Fermentas) consisting of 0.05 U/µl Taq DNA Polymerase, 4 mM MgCl₂, 0.4 mM dNTPs (dATP, dCTP, dGTP, dTTP) and an optimal reaction buffer. MgCl₂ could be included. The PCR conditions were the following:

2' 95°C (opening denaturation) > 20'' 95°C (denaturation) > 20'' 58°C (annealing) > 30'' 72°C (elongation) 35-40x > 5' 72°C (final elongation).

PCR reaction	cDNA	5 µl
	2x PCR Master-Mix	10 µl
	Primer for (100 nM)	0.2 µl
	Primer rev (100 nM)	0.2 µl
	H ₂ O	4.6 µl

2.2.8.6 Gel electrophoresis

Amplified DNA was separated in an agarose gel at a constant voltage of 150V. Depending on the DNA fragments, we used agarose gels from 1% to 2.5%. Midori green was added to the gel solution to visualize DNA under UV-light by excitation at 254 nm. 1 kB GeneRuler was added during electrophoresis to identify the size of the separated fragments.

2.2.9. Imaging

2.2.9.1 Confocal fluorescence microscopy

Proteins can be visualized by immunochemistry. Fluorochrome coupled antibodies are able to stain proteins of interest on fixed and permeabilized cells. The confocal microscope detects emitted light of fluorochromes after excitation of laser lights. Additionally, different colors can be differentiated in the same cell. Moreover, the microscope is able to scan through the cell providing higher resolution and eliminates out-of-focus lights. It is controlled by a computer and coupled to a photomultiplier detection system.

2.2.9.2 Preparation of histological and immuno-histochemical samples

The tissues were fixed with 4% formaldehyde for 24 h room temperature. Water was removed from the tissues by an automatic tissue processing machine (Tissue-Tek VIP-Sakura) through ascending alcohol concentrations ending with 100% xylene. Then, they were prepared for embedding in hot paraffin. With a sliding microtome (Leica), slides were prepared (thickness: 1 micron). The section was mounted on a slide and dried. H&E staining was kindly provided by the staff members of the hematology, histology laboratory of the Institute of Pathology or ZOM (central for operation medicine), University of Würzburg.

2.2.9.3 Immunocytochemistry

10^4 cells were washed twice with PBS and resuspended in 100 μ L. Centrifugation in a cytospin centrifuge was performed at 300 rpm for 3 min to spin the cells onto silanized slides. The slides were stored in the fridge overnight to dry. The next day, they were fixed for 20 min with 4% formaldehyde in PBS and subsequently washed three times with PBS

in a staining jar. Permeabilization was done with 0.2% Triton for 5 min at room temperature. Slides were again washed three times. Then the slides were blocked with 1% BSA in PBS for 20 min. Incubation of the primary antibody (usual concentration 1:100 in antibody diluent) was performed in a humid and dark chamber for 1 h and followed by three washing steps. The secondary antibody (1:400) was also added for 1 h, and slides were put in the humid and dark chamber. The last washing steps were followed by adding one drop of mounting medium with DAPI (Fluoroshield) and covering the cells with a cover slip. For storage, slides were put in the fridge at 4°C.

The pictures were taken with a Leica Confocal Laser Scanning Microscope (TCS SP5 II), analyzed with the Leica Software Image Pro Plus. For further demonstration, the digital images were processed using Paint.net or Microsoft Office Power Point 2010.

Fixation solution (pH 7.4)	NaCl	137 mM
	Na ₂ HPO ₄	10 mM
	KCl	2.6 mM
	KH ₂ PO ₄	1.8 mM
	(Para-)Formaldehyd	4% volume
Permeabilization solution	NaCl	137 mM
	Na ₂ HPO ₄	10 mM
	KCl	2.6 mM
	KH ₂ PO ₄	1.8 mM
	Triton X-100	0.2% volume

2.2.10 Electronic data processing and statistical analysis

Collection and analyses of the data was performed on a Hewlett Packard EliteBook 8440p laptop. The following programs were used: BD FACS Diva 5.0; FlowJo Software (Tree Star); FUSION CAPT; FusionCapt Advance of Fusion Vilber Lourmat program; GraphPad Prism 5; Leica Software ImagePro Plus; paint.net; Microsoft Office Excel 2010; Microsoft Office PowerPoint 2010; Microsoft Office Word 2010; Thomson EndNote X7 0.2.

Statistical analyses were done with GraphPad Prism version 5 and the student t test. P values under 0.05 were considered as significant.

3. Results

3.1. Nuclear location of NFATc1 is another hallmark of Burkitt's lymphoma

NFAT-activation as well as NF- κ B, PI3K and RAS-signaling belong to the most important pathways in B cell activation. Hence, aside from constitutive low NF- κ B activity (Klapproth, Sander et al. 2009) and high PI3K activity (Schmitz, Ceribelli et al. 2014), I hypothesized that the NFAT cascade is strongly activated in both BL cell lines and tumor cells derived from *E μ -myc* mice. Upon IgM stimulation of naive B cells, NFAT activation is characterized by nuclear translocation (Fig.3.2 A).

3.1.1. Nuclear location of NFATc1 in Burkitt's lymphoma cell lines

Confocal microscopy of different BL cell lines indicates all over a predominant nuclear location of all NFATc1 isoforms (including α A, α B, α C and β A, β B, β C), whereas Daudi cells show both a nuclear and cytoplasmic staining (see Fig.3.1).

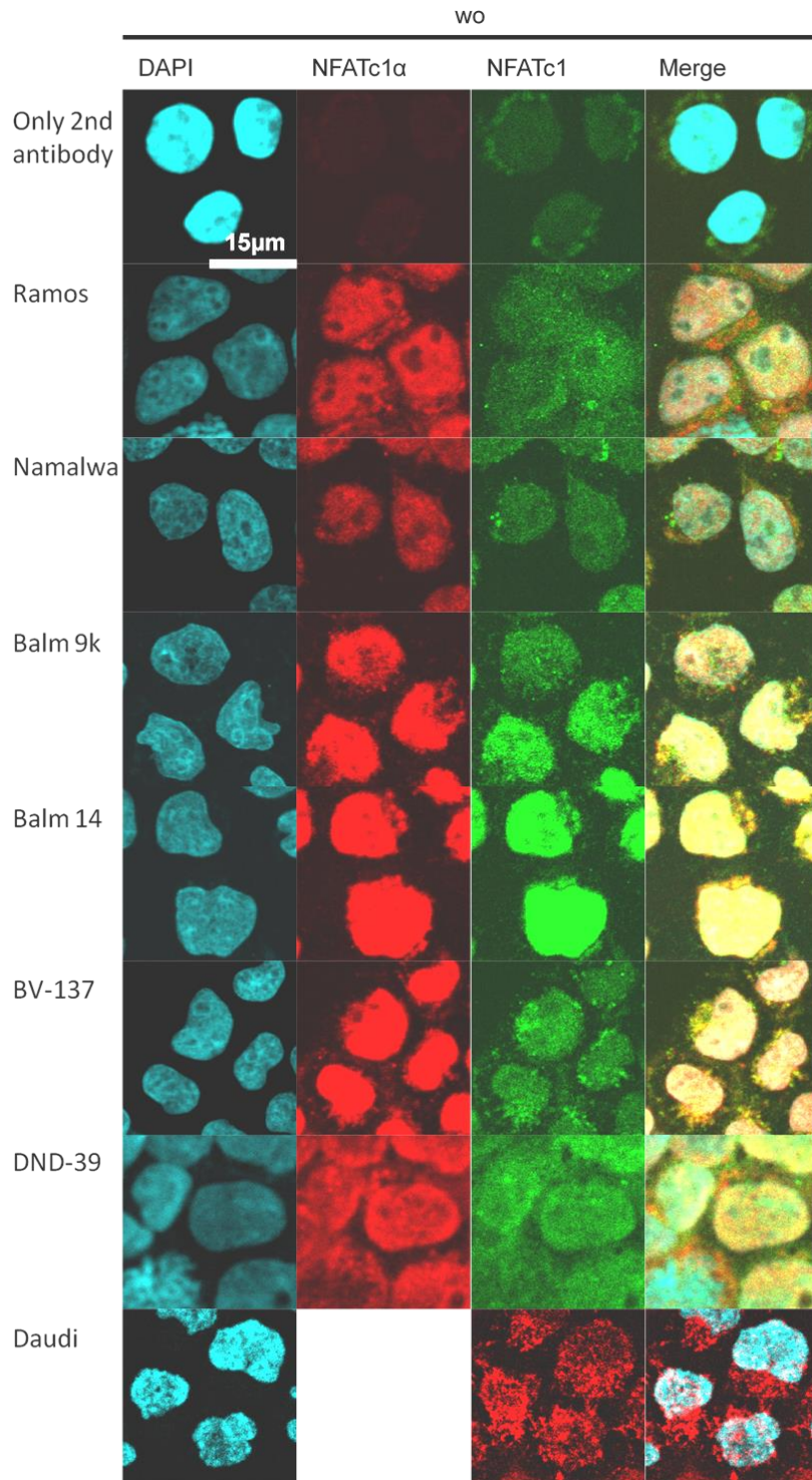


Fig. 3.1. Nuclear location of NFATc1 proteins, and of its inducible isoforms NFATc1 α , in Burkitt's lymphoma cell lines. Confocal microscopy. The BL cell lines indicated (and BV-173 cells) were maintained in the absence of any additional stimuli, fixed and stained with antibodies directed against all NFATc1 isoforms, or with an NFATc1 α -specific antibody. In the uppermost row, Ramos cells were stained with secondary antibodies only for specificity control.

3.1.2. NFATc1 in *E μ -myc* mouse tumor cells

The *E μ -myc* mouse bears a *Myc* transgene that is driven by the *E μ* -enhancer in B cells. This line is commonly used as a model for human BL. After several weeks, *E μ -myc* mice develop massive tumors in lymph nodes, spleen, thymus and bowel or suffer from leukemia (Adams, Harris et al. 1985). Fig. 3.2 (B) reflects the typical appearance of tumor growth: swelling of the cervical lymph nodes and prominent clumps on both shoulders and the neck. In hematoxylin and eosin (HE) stained sections, the “starry sky” appearance in tumors, a typical morphologic feature of BL, can be recognized. As expected, immunocytochemistry uncovers a predominant nuclear location of NFATc1 in *E μ -myc* induced tumors, like in human BL cell lines. One of the paraffin embedded cervical lymph nodes was stained against B220⁶ and NFATc1 α for confocal microscopy (Fig. 3.2 C), and the tumor cells are B220+ and show NFATc1 α , in their nuclei.

Tumor B cells, purified from the spleen, show a nuclear distribution of NFATc1 α , too, accompanied by high Ki-67 signals, indicating proliferation (Fig. 3.2 C). Although we conjectured that tumor cells isolated from *E μ -myc* mouse #2229 are under constant intracellular activation, they were CD69⁷ negative: signal intensities remain the same like in the control picture (not shown).

⁶ B220/CD45R is an isoform of CD45, a tyrosine phosphatase playing an essential role in B cells for antigen receptor-mediated signaling. It is known to be expressed in human B lymphocytes throughout their development from early pro-B stages onwards. It is finally down-regulated in differentiated plasma cells, additionally often expressed in lymphoproliferative disorders, but acts as a pan B cell marker in mice. Rodig, S. J., A. Shahsafaei, B. Li and D. M. Dorfman (2005). "The CD45 isoform B220 identifies select subsets of human B cells and B-cell lymphoproliferative disorders." *Hum Pathol* **36**(1): 51-57.

⁷ CD69 or activation inducer molecule (AIM) is one of the earliest cell surface antigens indicating activation in both T, B cells and also other leucocytes. Moreover, it is involved in lymphocyte migration and cytokine secretion. Vazquez, B. N., T. Laguna, J. Carabana, M. S. Krangel and P. Lauzurica (2009). "CD69 gene is differentially regulated in T and B cells by evolutionarily conserved promoter-distal elements." *J Immunol* **183**(10): 6513-6521..

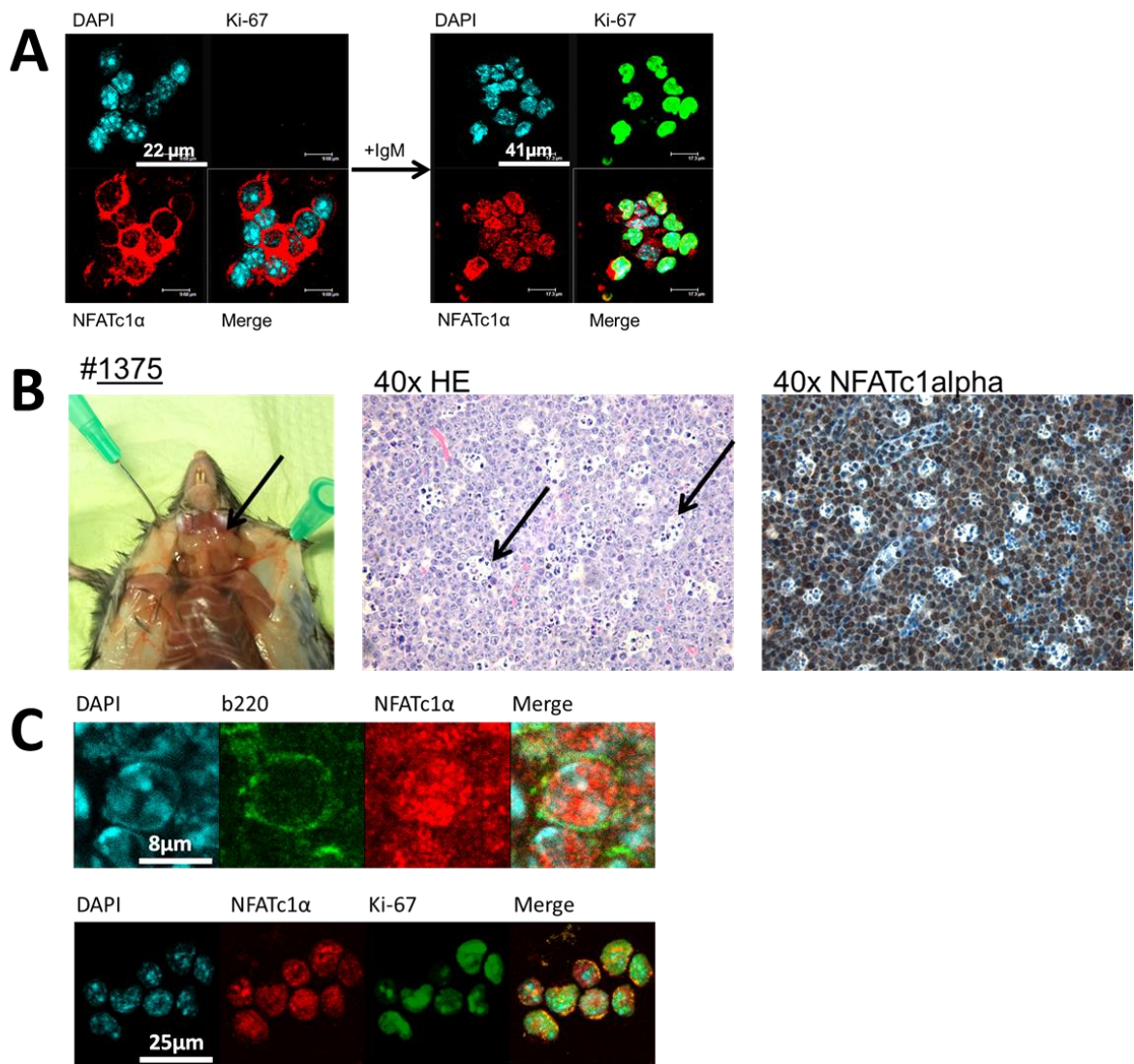


Fig. 3.2. Nuclear location of NFATc1 α in tumors derived from *E μ -myc* mice. (A) Confocal microscopy of wild type mouse B-cells. They were either directly harvested or stimulated and subsequently cytopspinned and stained against Ki-67 and NFATc1 α . (10 μ g/ml anti-IgM-antibody pulsed for 30 min, subsequently 5 μ g/ml anti-CD-40-antibody for 43 hours) (B) Macroscopic and microscopic pictures of a lymph node tumor derived from *E μ -myc* mouse #1375. Arrows: “starry-sky” histiocytes. (C) Confocal microscopy of a paraffin embedded lymph node (mouse #1375, upper pictures) and purified tumor cells (mouse #2229, lower pictures), stained against B220, NFATc1 α and Ki-67, as indicated. Staining and capture of pictures were done in cooperation with Krisna Murti.

3.2. Molecular mechanisms of gallium in Burkitt's lymphoma

Gallium nitrate, a metal salt, was shown to have anti-neoplastic effects in animal tumor models and on lymphoma cell lines (Chitambar, Wereley et al. 2006). After binding to transferrin, it enters the cell through the transferrin receptor. On the one hand, gallium affects the iron-uptake and inhibits iron-dependent enzymes, such as ribonucleotide reductase, and on the other, it induces apoptosis via releasing cytochrome c from mitochondria. Additionally, gallium blocks osteoclastic differentiation of RAW cells and human osteoclast precursors through RANKL by impairing NFATc1 levels (Verron, Masson et al. 2010). Here, several molecular mechanisms orchestrate to inhibit both the initial induction and the auto-amplification of *NFATC1* gene: e.g. the release of calcium by TRAPV channels is decreased, *c-Fos* gene expression is inhibited, whereas *Traf6*, *p62* and *Cyld* expressions are increased (Verron, Loubat et al. 2012). The latter three inhibit the nuclear translocation of NF- κ B factors, which probably affects *NFATC1* gene expression subsequently.

First, to investigate the extent of inhibitory properties on proliferation by gallium nitrate, I incubated both the BL cell lines Ramos and Namalwa, and the human T cell line Jurkat with different concentrations for several days. In all cell lines, high concentrations of gallium nitrate inhibited their proliferation (Fig.3.3 A) as shown by the decrease of ^3H thymidine incorporation (B), and induced apoptosis (C).

BL cell lines, especially Ramos cells, appeared to be more sensitive against gallium than Jurkat cells. This finding is in line with the IC_{50} concentrations of 50 μM for Raji cells and 125 μM for Jurkat cells (Chitambar, Wereley et al. 2006).

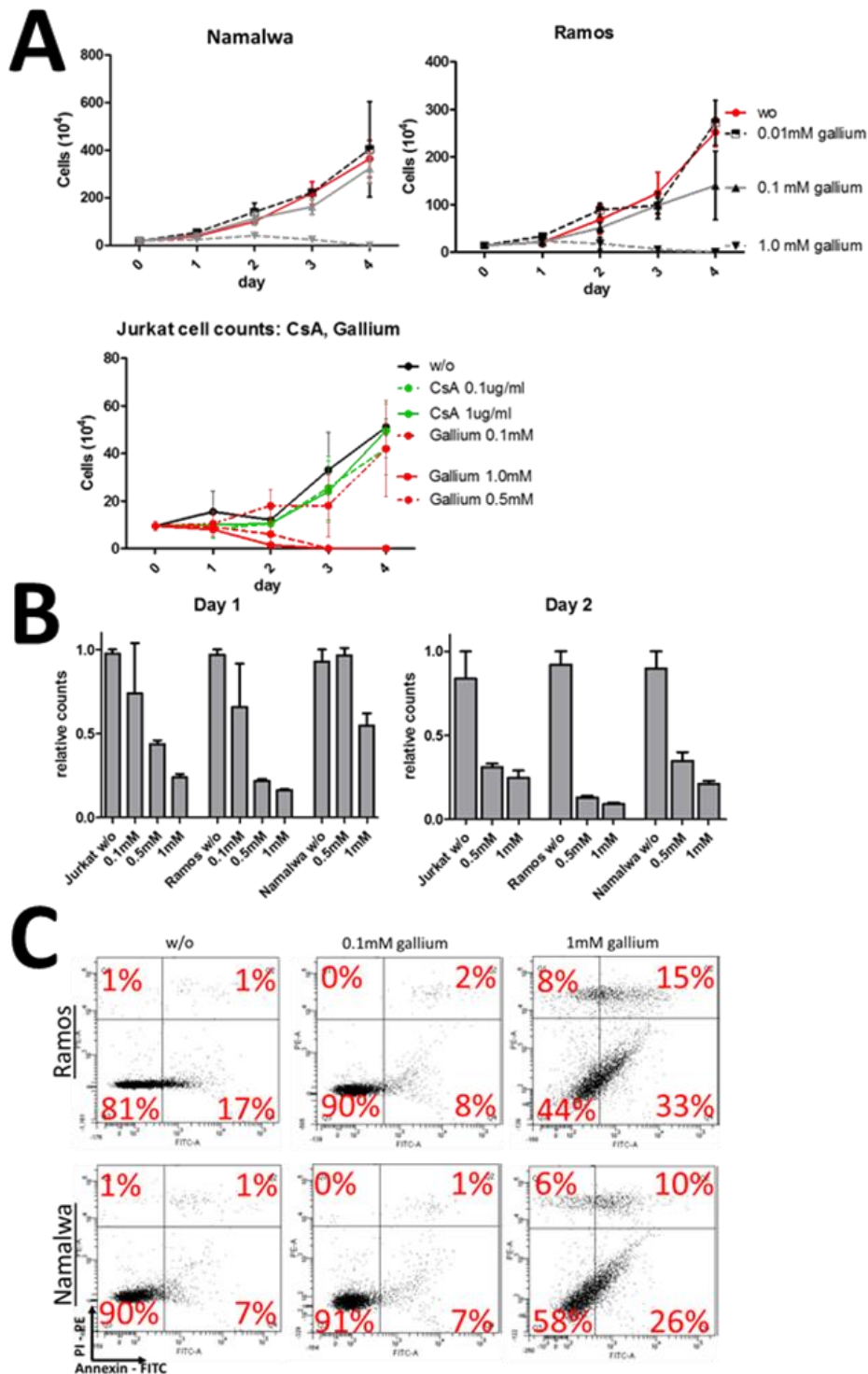


Fig. 3.3. Gallium inhibits the proliferation and induces the cell death of cell lines Ramos, Namalwa and Jurkat. (A) Cell counts for 4 d with indicated concentrations of gallium (and CsA for Jurkat cells). The proliferation inhibition is clearly seen with 1 mM of gallium, but a reduction of ³H-thymidin incorporation is also detectable with lower concentrations and at earlier time points (B). Cells were cultured for either 24 h or 48 h. ³H-thymidin was given to the cells the last 12 h of culturing. Each bar represents 3 cell colonies. (C) Flow cytometric analysis of annexin/PI staining of Ramos and Namalwa cells after 3 d of incubation with gallium.

3.2.1. Gallium affects NFATc1 and MYC levels in Burkitt's lymphoma

As NFATc1 was shown to play a crucial role in Burkitt's lymphoma (BL), I ascertained whether gallium affects NFATc1 distribution and protein levels, like in RAW and osteoclast progenitor cells, as described before.

Western blotting, but not confocal microscopy, revealed a slight re-translocation of NFATc1 protein into the cytosol of Ramos and Namalwa cells (Fig. 3.4. A,B). Although Jurkat cells are sensitive to gallium, too, they do not express NFATc1 and MYC as high as BL cell lines. Thus, the translocation or down-regulation of these proteins was less visible. As gallium nitrate was shown to block NF- κ B translocation into the nucleus upon RANKL stimulation in RAW cells (Verron, Loubat et al. 2012), I checked also p65 distribution in BL cell lines. However, in my assay p65 remained nuclear (A, B).

Like MYC or NFATc1 levels, the nuclear levels of p65 decreased in Ramos cells after 2 d of incubation with gallium, and a second band of higher molecular weight appeared (B, C). The loss of non-cleaved Caspase 7 indicates apoptosis induction that obviously takes place after 2 d of incubation, with 1 mM gallium.

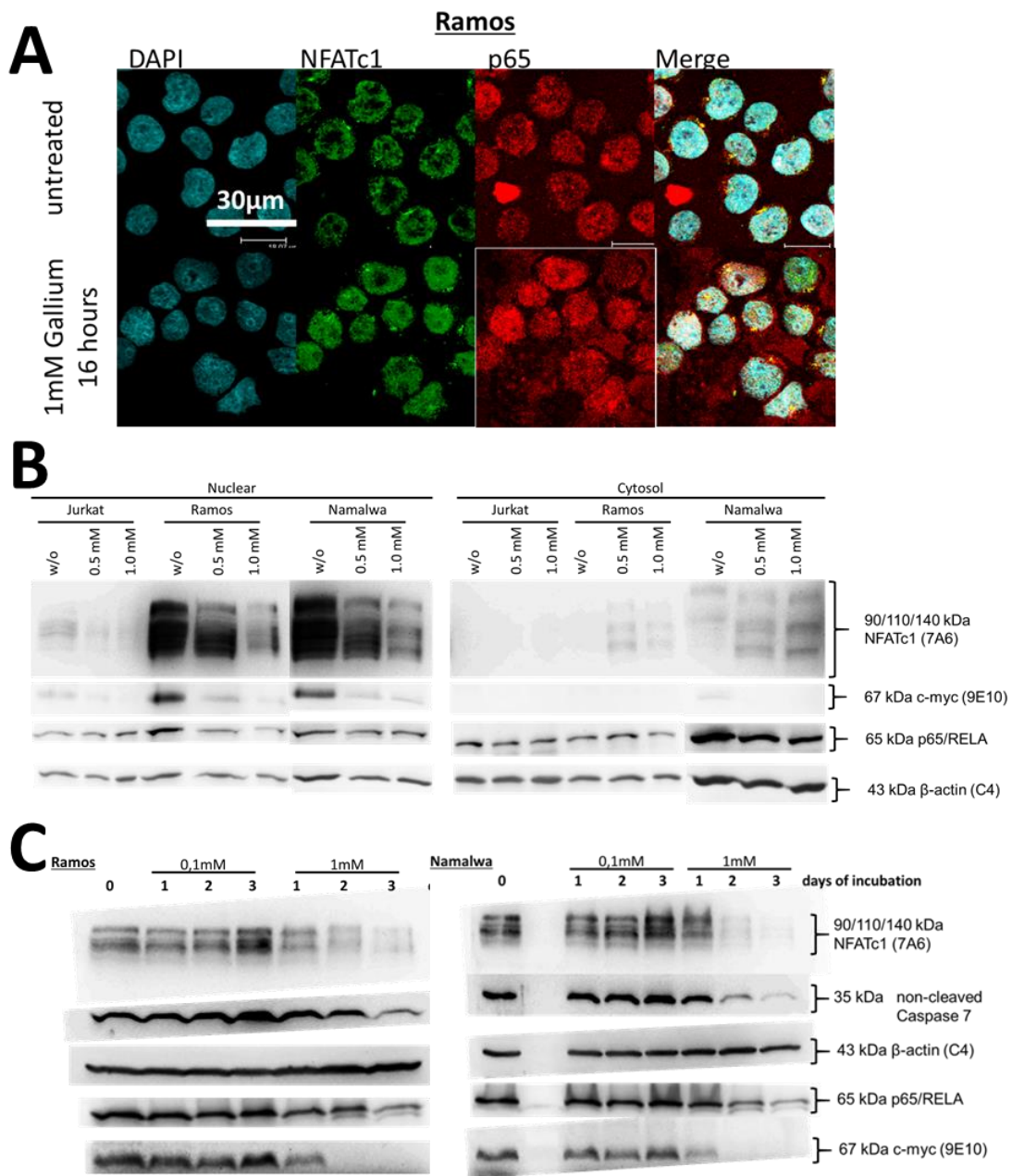


Fig. 3.4. Gallium treatment leads to a reduction in protein levels of NFATc1, MYC and slightly p65 in BL cell lines Ramos and Namalwa. Moreover, a cytosolic translocation of NFATc1 is detectable. (A) Confocal microscopy of both untreated Ramos cells treated for 16 h with gallium. Cells were stained with antibodies against NFATc1 and p65. (B) Western blot of nuclear and cytosolic protein extracts from Ramos, Namalwa and Jurkat cells. Cells were treated with indicated concentrations of gallium for 2 d, and blots were stained with antibodies against NFATc1, c-myc, p65 and beta-actin as loading control. (C) Western blot of Ramos and Namalwa cell protein extracts, treated for several days with either 0.1mM or 1mM gallium. Blotting was done with antibodies against NFATc1, non-cleaved Caspase 7, p65, c-myc and beta-actin as loading control.

To find out the reason for lower NFATc1 levels in gallium-treated Ramos cells, I compared NFATc1 degradation by additional treatment of cells with cycloheximide (Fig. 3.5. A). Additionally, to check the impacts of transcription, I compared mRNA levels of both transcripts from the P1 and P2 promoter (B), too. Finally, degradation of MYC, NFATc1 or its α A proteins remained unaffected by gallium. But, the mRNA levels decreased upon gallium treatment – both transcripts from the P1 and P2 promoter. Hence, the reduction of NFATc1 protein levels in gallium treated Ramos cells is due to the inhibition of *NFATC1* transcription.

Gallium - strictly speaking gallium molybdate - was shown to increase the level of mitochondrial reactive oxygen species (ROS) in CCRF-CEM cells (Chitambar, Purpi et al. 2007). ROS increases JNK-kinase activity with subsequent p53 activation and apoptosis induction in the colon and breast carcinoma cell lines HCT116 and MCF7, respectively (Shi, Nikulenkov et al. 2014). Therefore, I checked the activation of JNK upon gallium nitrate treatment in Ramos cells (Fig. 3.5. D), and whether JNK inhibition might rescue the growth inhibitory effect of gallium nitrate (Fig.3.5. C). However, I detected that JNK was not induced, and the expected effect of JNK inhibition was the contrary – ^3H -thymidin incorporation was even found to be reduced.

JNK is known to mediate NFAT phosphorylation and its subsequent proteasomal degradation, I first wanted to quantify protein levels of NFATc1 in Ramos cells with both gallium and JNK-inhibitor treatment. However, the data from Fig. 3.5. (C) excludes a JNK activation or increase in NFATc1 degradation in gallium treated Ramos cells. Therefore, an effect on NFATc1 through JNK can be excluded.

To exclude that gallium acts on proliferation and survival through the PI3K pathway, I performed Western blotting of the activated and, therefore, phosphorylated isoform of AKT (Fig.3.5. D). However, the AKT levels remained constant, which means that the PI3K pathway is not disturbed. Nevertheless, gallium does not only affect protein levels of NFATc1 alone – NFATc2 levels decreased, too.

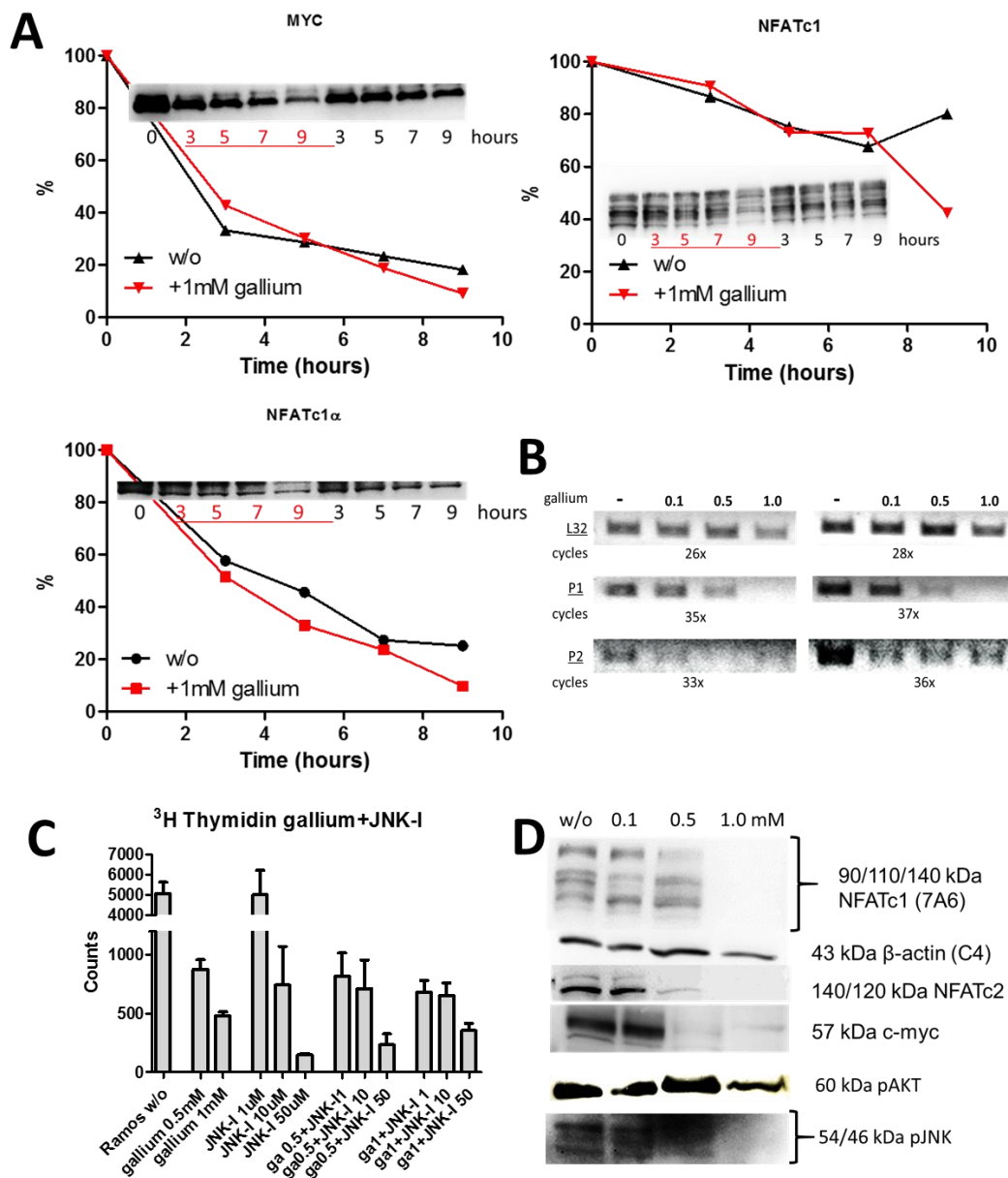


Fig. 3.5. Gallium treatment of Ramos cells does not significantly reduce protein stability of NFATc1, NFATc1 α or MYC, but mRNA levels directed by the the inducible promoter P1 are decreased. (A) Western blots of Myc, NFATc1 and NFATc1 α . Ramos cells were treated for 3, 5, 7 and 9 h with 100 μM cycloheximide to stop protein synthesis. In four samples, 1 mM gallium was added (in red). (B) PCR amplified cDNA samples out of 4 indicated gallium treated RNA probes. (C) ^3H -thymidine incorporation in Ramos cells treated by inhibition of JNK increases the growth inhibitory effect of gallium. (D) Activity of JNK Ramos cells decreased after 3 d of treatment with the gallium concentrations, indicated.

3.2.2. Pancreatic cancer: *NFATC1*-overexpressing carcinomas are sensitive to gallium

Another, so far not tested cancer type for gallium treatment is pancreatic cancer. Generally, pancreatic cancer tissues are known to overexpress *NFATC1* (Buchholz, Schatz et al. 2006). Thus, they represent a model for anti-cancer therapy with gallium.

Among various cell lines, especially Panc-1 cells are known to show *NFATC1* overexpression that, if blocked by CsA or siRNA, result in proliferation inhibition. In this context, I tested five different pancreas carcinoma cell lines whether or not they are sensitive to gallium nitrate. With an MTT proliferation assay, I confirmed that even 0.1 mM gallium is sufficient to inhibit their proliferation (Fig. 3.6. A). Moreover, gallium induced apoptosis in all cell lines tested (Fig. 3.6. B). In order to prove an effect on NFATc1, Western blotting with protein extracts from Panc-1 and PC-1 cells was performed (Fig. 3.6. C). Indeed, NFATc1 levels were found to decrease. To find out whether this effect is caused at the level of mRNA transcripts, I investigated by RT-PCR transcripts from both the P1 and P2 *NFATC1* promoters. Surprisingly, *NFATC1* mRNA levels of Panc-1 cells were mainly down-regulated through the P2 promoter, whereas transcript levels from the P1 promoter remained almost unaffected (Fig. 3.6. D)

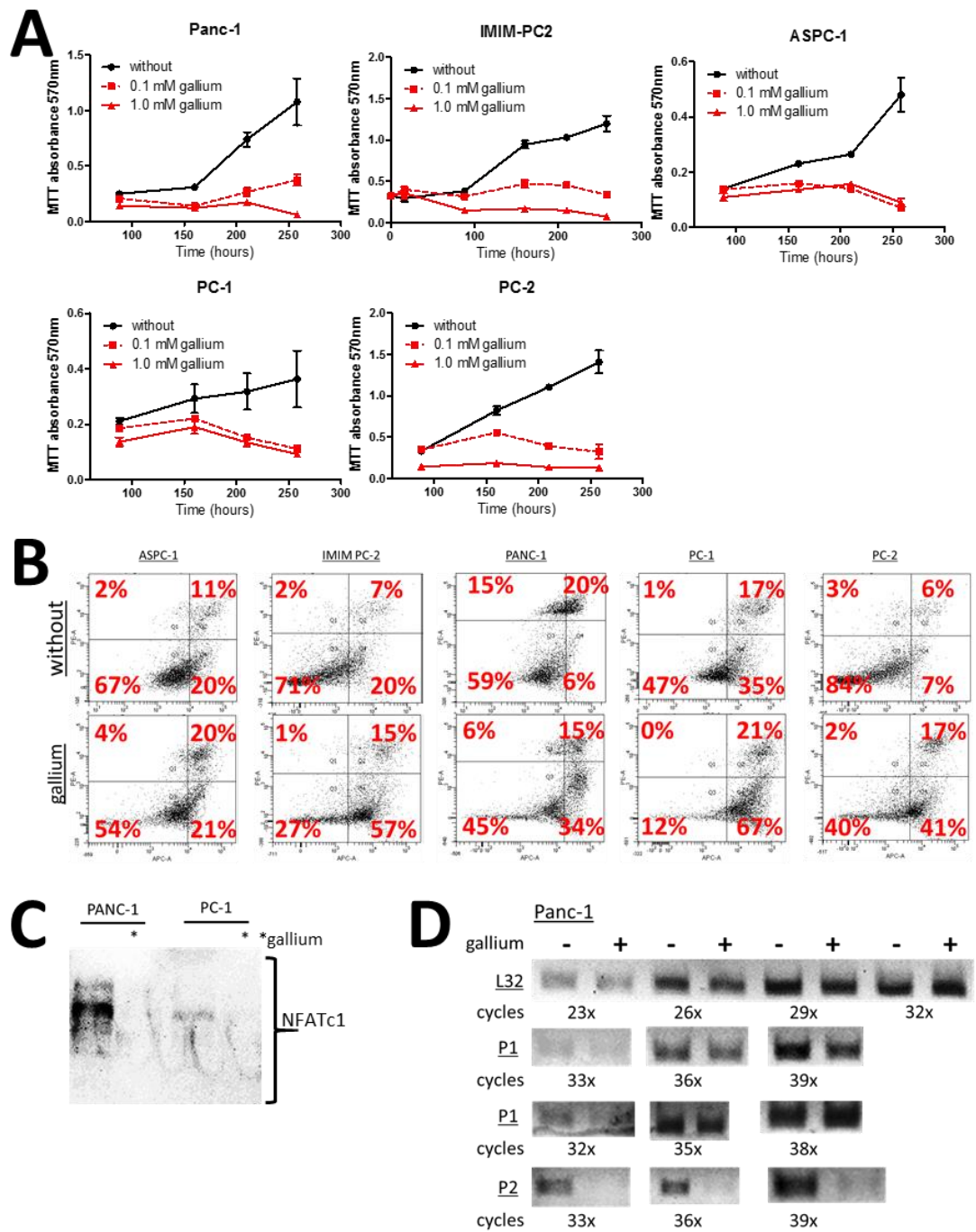


Fig. 3.6. Pancreas carcinoma cell lines are sensitive to gallium. Their proliferation rate is diminished, apoptosis is induced and *NFATc1* expression is down-regulated. (A) MTT proliferation assay of indicated cell lines with both 0.1 and 1.0mM gallium. (B) Flow cytometry of annexin/PI stainings of gallium treated pancreas carcinoma cell lines. (C) Western blot of cell lines Panc-1 and PC-1, stained with an antibody against *NFATc1*. (D) RT-PCR assays of gallium-treated Panc-1 cells. Gallium affects predominantly *NFATc1* transcripts of the P2 promoter. Cells were treated with 1 mM gallium for 3 d. L32 transcript analysis is included as loading control.

3.3. Proliferation expansion of BL is not inhibited by calcineurin inhibition

To investigate the impact on proliferation inhibition and cytosolic translocation of NFAT by CN inhibitors⁸, BL cell lines were incubated with the CN inhibitors CsA and FK506 and the VIVIT peptide that blocks the interaction of CN with NFAT proteins. (Fig. 3.7.).

3.3.1. Only atypical high concentrations of CN inhibitors affect proliferation of BL cells

To investigate the effect of CN inhibitors on the proliferation of BL cells, I used the CFSE-Proliferation-Assay or counted cell numbers after in vitro culturing (Fig. 3.7.).

After 4 days treatment with 0.1 or 1 µg/ml of CsA, the numbers of BL cells were only slightly reduced (Fig.3.7. A). This effect is strengthened by the use of 10 µg/ml CsA. In case of FK506, an effect was achieved with a minimum concentration of 10 µg/ml. At lower concentrations, cell numbers were similar to untreated or DMSO-treated cells.

Already with 0.2 µg/ml CsA, a slight difference in proliferation is observable by CFSE staining. Especially for BV-173 and Ramos cells (Fig. 3.7. B). Red curves shift to the right in comparison to the black ones, indicating proliferation inhibition. For quantification, areas under the curves of low-fluorescent populations were compared, giving a hint for CsA sensitivity/inhibition. Whereas 55% of the entire population of untreated DND-39 cells was low fluorescent, hence proliferated frequently, only 25% of CsA-treated cells were located in the same intensity range, reflecting a diminished proliferation rate. For “Ramos” cells, only 8% of the CsA-treated population is low fluorescent, related to 50% in the control group.

⁸ Inhibition of T cell proliferation can be found with CsA dilutions up to 0.01 µg/ml. In our lab we commonly use 0.1 µg/mL as standard T cell inhibiting concentration. On a molar basis FK506 is 10- to 100-fold more potent than CsA. As FK506 is more effective than CsA, it can be used at lower concentrations in transplant recipients for anti-rejection therapy. VIVIT peptide is a high-affinity and specific peptide binding to the NFAT side of calcineurin phosphatase. It acts as a very potent inhibitor of NFAT binding and downstream NFAT signaling. Furthermore, it does not interfere with other de-phosphorylations carried out by calcineurin Aramburu, J., M. B. Yaffe, C. Lopez-Rodriguez, L. C. Cantley, P. G. Hogan and A. Rao (1999). "Affinity-driven peptide selection of an NFAT inhibitor more selective than cyclosporin A." *Science* **285**(5436): 2129-2133.

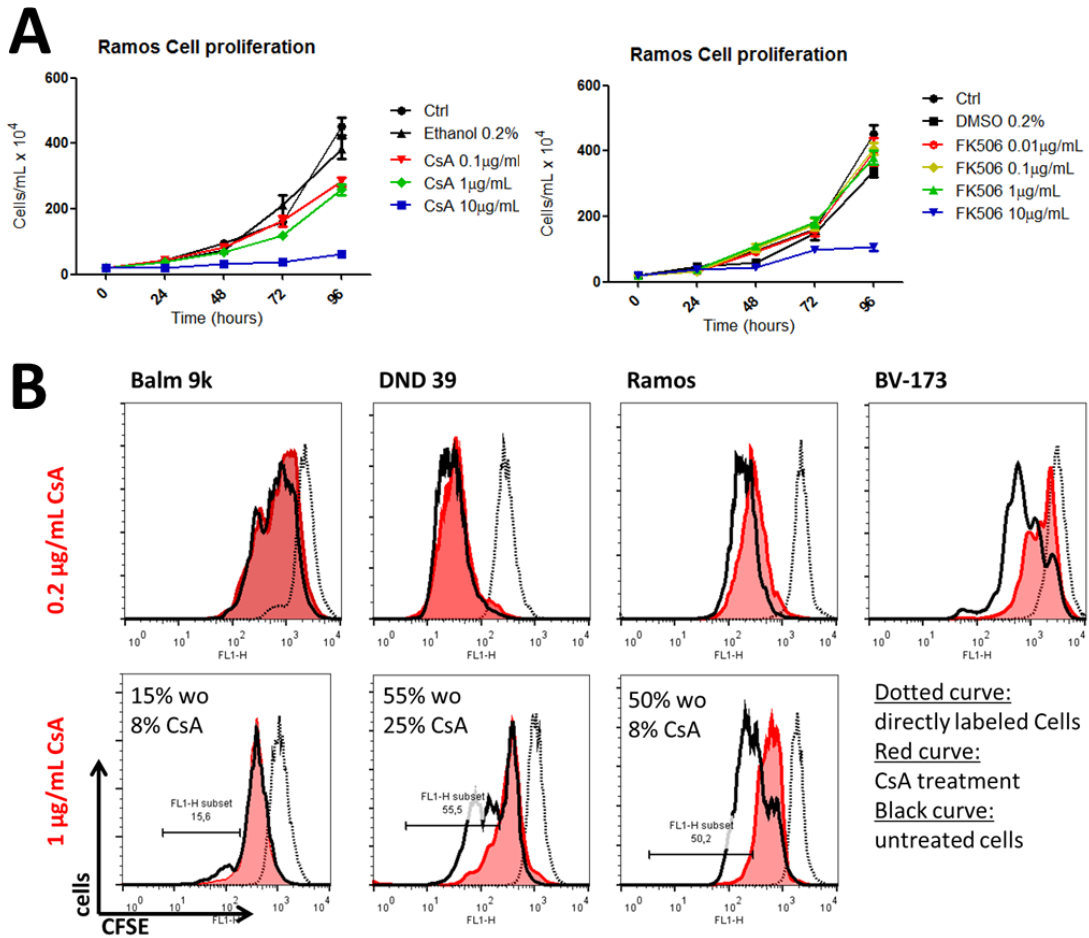


Fig. 3.7. Only atypical high concentrations of CN-inhibitors affect the proliferation of BL cells. (A) Proliferation curves of Ramos cells, either treated with CsA or FK506. (B) CFSE proliferation assay of different cell lines for 3 d under indicated concentrations of CsA. Labeled cells are measured directly = 0 hours (dotted curve) and 72 h later, whereas the red and black curves reflect CsA treated and untreated cells, respectively. Vertical bars represent median range. Ethanol and DMSO act as negative controls for CsA and FK506, respectively.

3.3.2. CN inhibitors affect partly the translocation of NFATc1 in BL cells

Although I used ascending concentrations of CsA, only a partial cytosolic translocation of NFATc1 was detectable. BL cell lines were treated and either stained for confocal microscopy or lysed to prepare Western blots (Fig. 3.8., 3.9.). Confocal microscopy pictures showed a slight translocation of NFATc1 from nucleus to cytosol after CsA treatment, as small circles of stained NFATc1 around their nuclei were detectable. This is most clearly seen in the BL cell lines Ramos, Namalwa, Balm 9k and Balm-14. BV-173 and DND39 cells (Fig. 3.8 A), however, showed a predominant nuclear distribution of NFATc1 or its “ α ”-isoforms. Hence, the effect of CN inhibition does only mildly influence NFAT distribution. Surprisingly, this effect is even lower with the CN inhibitors FK506 and VIVIT (Fig.3.3 B,D), although they are known to be more potent.

Confocal microscopy software enables to portray the individual channel intensities in a graph (Fig.3.8 C), displaying a translocation of NFATc1 in CsA-treated Ramos cells more precisely.

At a concentration of 0.1 $\mu\text{g/ml}$, CsA is able to trigger NFAT-translocation out of the nucleus into the cytosol significantly: The mean ratio of “nuclear to whole cell” changes from approx. 82% to 68% if Ramos cells are stained with anti-NFATc1 (7A6)-antibody. Also significant (according to Ttest $p < 0.005^{***}$), but with lower extend, a translocation for its α -isoforms is detectable: mean ratios change from approx. 75% to 65% ($p < 0.05^*$). FK506 does not trigger translocation of NFATc1 α , but surprisingly a slight translocation of NFATc1 was observed (Fig.3.3 D). However, Western blotting indicated no translocation after treatment with FK506 (Krisna Murti, not shown).

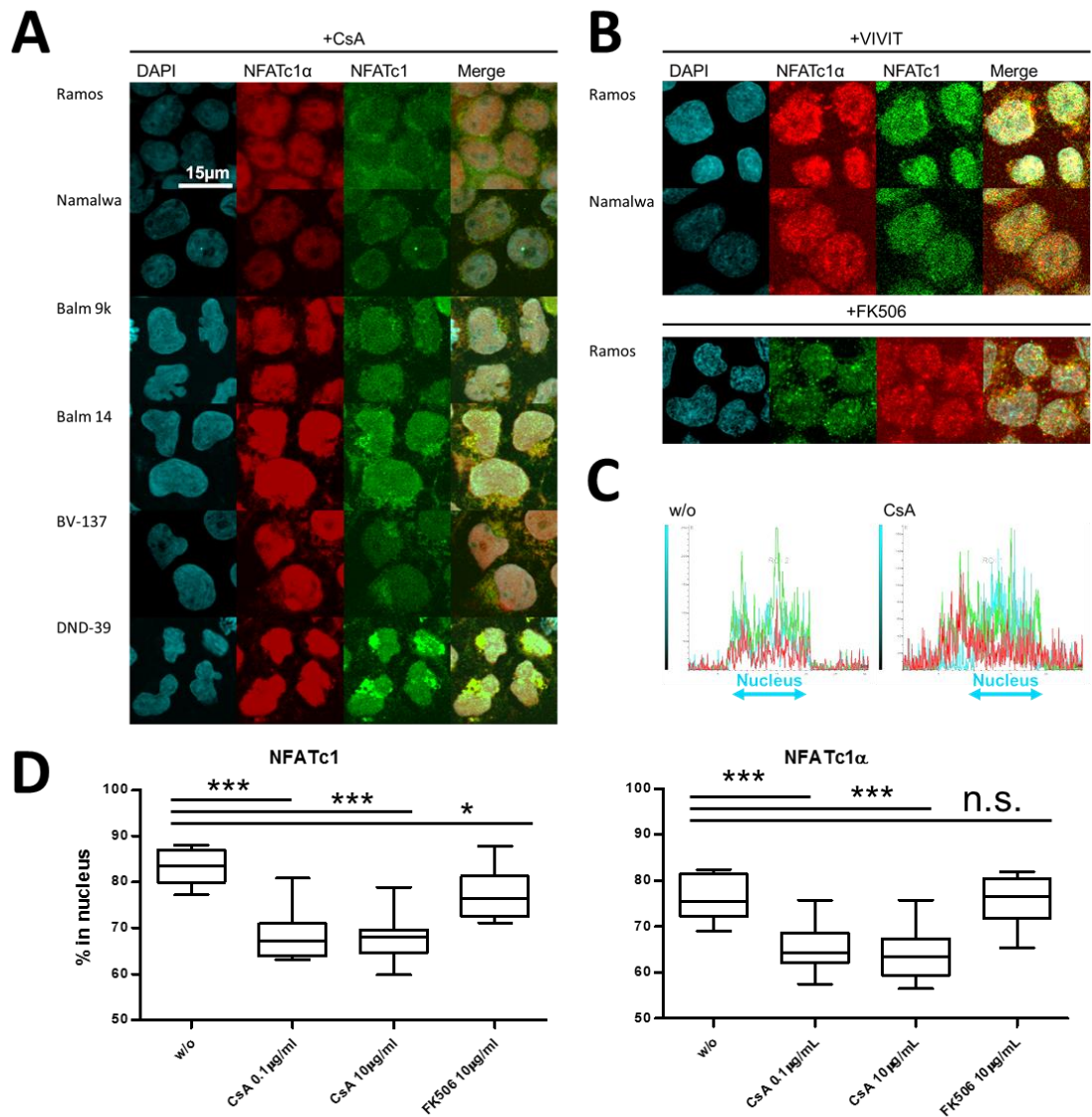


Fig. 3.8. The calcineurin inhibitor CsA, but not FK506 or VIVIT peptide, leads to a slight cytosolic translocation of NFATc1 and NFATc1 α in Burkitt's lymphoma cell lines. Confocal microscopy of indicated Burkitt's lymphoma cell lines after (A) 14 h of 1 μ g/ml Cyclosporin A (CsA), (B) 12 h of 10 μ M VIVIT peptide or 24 h of 10 μ g/ml FK506 treatment. (C) Cross-section of two typical Ramos cells without or with CsA treatment. Signal intensities of the different channels are portrayed on a graph (blue=DAPI, red=NFATc1 α , green=NFATc1). (D) Confocal microscopy analysis of nuclear to whole cell ratios for both NFATc1 and NFATc1 α levels in Ramos cells after treatment with indicated reagents. For each treatment, a minimum of 10 cells were analyzed. Bars represent the standard deviation, whiskers the minimum and maximum of nuclear to cell ratios.

Western blotting of proteins from Ramos and Namalwa cells (Fig. 3.9.) illustrates the CsA-mediated translocation more precisely. A part of NFATc1 was observed in the cytosolic fraction. Moreover, even lowest concentrations are causative (providing that more than 0.1 $\mu\text{g/ml}$ were used). Comparing the intensities of untreated nuclear bands with those of treated ones, a slight shift to higher molecular weights is visible. Assuming changes of phosphorylation levels, it represents a successful CN inhibition. Unexpectedly, these phosphorylations do not lead to its cytosolic export. This phenomenon was also detected in the *E μ -myc* mouse tumor cell line B1542 (data not shown, done in cooperation with Krisna Murti).

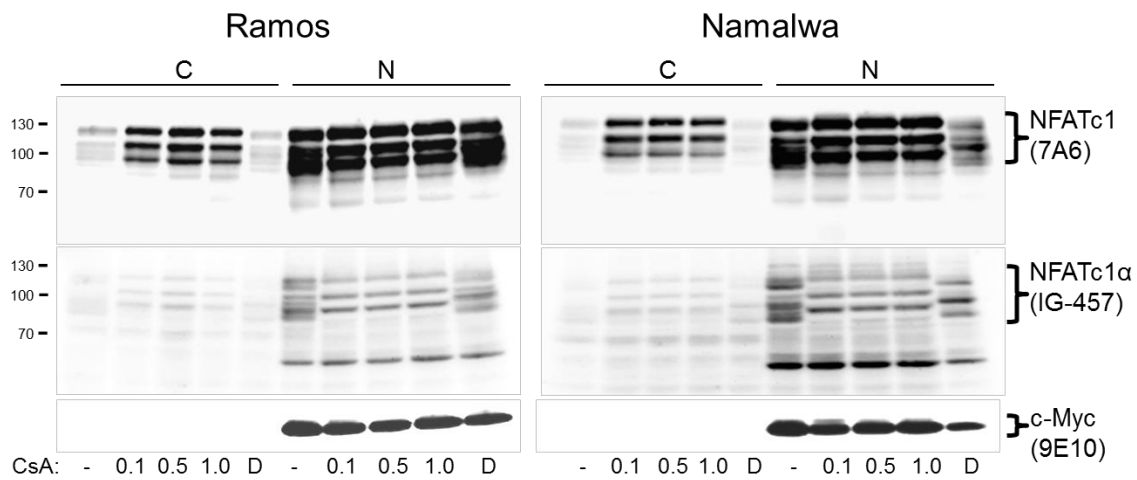


Fig. 3.9. CsA treatment induces translocation of NFATc1 isoforms from nucleus to cytosol and increases their molecular weights. The cell lines indicated were cultured for 5 d at indicated concentrations of CsA (0.1 $\mu\text{g/ml}$, 0.5 $\mu\text{g/ml}$ and 1 $\mu\text{g/ml}$) or DMSO (D). Three different antibodies were used, as indicated on the right side. C, N: cytosolic and nuclear extracts, respectively. Western blot was done in cooperation with Krisna Murti.

Summed up, NFATc1 is nuclear and, probably, active in BL cells (Fig. 3.1). Already with quite low concentrations (0.1 $\mu\text{g/ml}$ of CsA) of CN-inhibitors, CN-activity is blocked. This is shown both in Fig. 3.9., as the molecular weights of NFATc1 shifted indicating alterations in the phosphorylation status of NFATc1, and in Fig. 3.11. C, D, as p65 is relocated into the cytosol. The latter effect on NF- κ B caused by CN-inhibition was shown before in our lab (personal communication with Andris Avots). Hence, as CN-inhibitors are even active at low concentrations, whereas proliferation inhibiting effects need atypical high CN-inhibitor concentrations, I assume that this is due to unspecific, toxic effects that has nothing to do with specific CN-inhibition.

3.3.3. NFATc1 is not largely regulated by PI3K pathway

PI3K pathway activating mutations are frequently found in BL. PI3K and MYC are inducing themselves via several intermediate steps and cooperate in tumorigenesis, but activation of either one of these pathways does not lead to malignant transformation. In Ramos and Namalwa cells, a constant PI3K activation was already demonstrated (Sander, Calado et al. 2012). Therefore, PI3K inhibitor treatment induces dephosphorylation of subsequent enzymes, e.g. AKT and p70S6. The effect of PI3K inhibitors on proliferation is shown Fig.3.10. A. Both 1 μ M and 10 μ M Wortmannin affect Ramos cells strongly, whereas Idelalisib is less potent. However, after shorter treatment for 3 H-thymidine incorporation, the effects are similar (Fig.3.10. B).

Moreover, Wortmannin treatment for 3 d induces apoptosis (Fig.3.10. C). In synopsis with a successful pAKT down-regulation in Western blot (Fig. 3.10. D), PI3K inhibition by Wortmannin represents a powerful weapon against BL cells.

To uncover a putative connection between PI3K signaling and NFAT, we treated BL cell lines with 10 μ M Wortmannin for 4 h (a treatment that has already been shown to inhibit thymidine incorporation (Padmore, Radda et al. 1996)). However, the distribution of NFATc1 remained unaffected (see Fig. 3.10. G). Nevertheless, Western blotting revealed a slight increase of NFATc1 in the cytosolic fraction after incubation with 1 μ M or 10 μ M, especially in Ramos cells (Fig. 3.10. E, F). This effect strengthens by stimulation of BL cells.

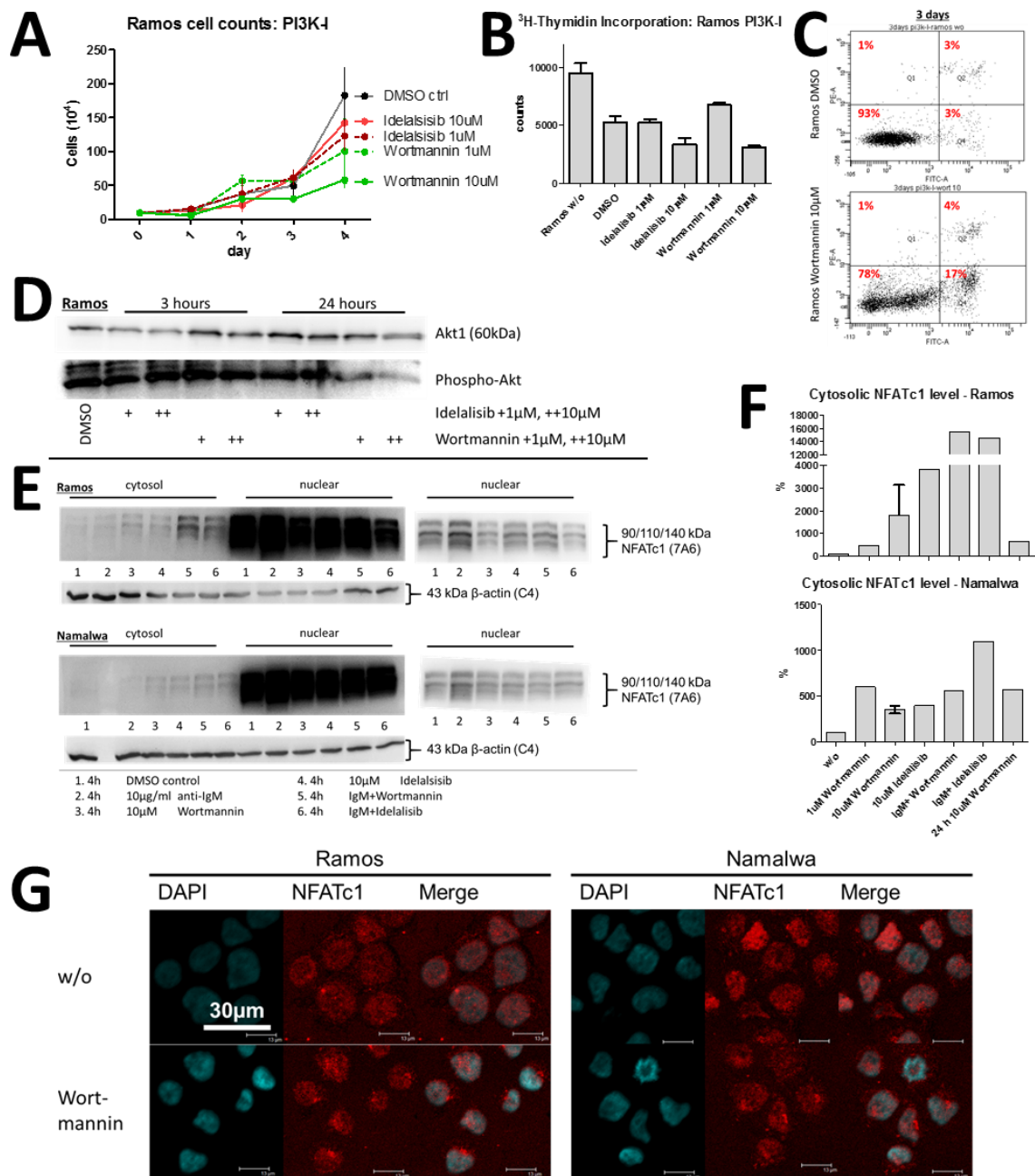


Fig. 3.10. Inhibition of PI3K in BL cell line cells leads to proliferation inhibition, cell death and slight cytosolic translocation of NFATc1. (A) Proliferation curve of Ramos cells under the conditions indicated. (B) ³H-thymidine incorporation into Ramos cells within 24 h of incubation. (C) Annexin/PI staining of Ramos cells after 3 d in culture. (D) Western blot of Ramos cells under indicated conditions. Phospho-Akt impairment implicates successful PI3K inhibition. (E) Western blot of cytosolic and nuclear protein extracts of Ramos and Namalwa cells under PI3K inhibition. (F) Analyses of cytosolic NFATc1 levels in Ramos and Namalwa extracts resulting of 2 Western blots are shown. (G) Confocal microscopy of NFATc1 distribution in Ramos and Namalwa cells upon PI3K inhibition by Wortmannin (4 h, 10 μ M).

3.3.4. JAK3 Inhibition reduces proliferation of BL and translocates nuclear p65 but not NFATc1

In Ramos cells, I found a predominant but not exclusive nuclear distribution of RelA/p65 (Fig. 3.11. D). This discovery is quite interesting, because NF- κ B is actually known to suppress *myc*-induced lymphoma genesis (Klapproth, Sander et al. 2009) - therefore it should have a low activity in BL and I did not expect its nuclear presence. However, aside from CsA treatment, the JAK3 inhibitor WHI-P131 induces its strong cytosolic translocation that simultaneously resulted in a 50% reduction in proliferation (Fig. 3.11. A, C, D).

As the JAK3 pathway is known to activate NFATc1 in thymocytes during their development, I investigated the impact of WHI-P131 on NFATc1 in BL cells. On the contrary to p65, distribution of NFATc1 is not significantly influenced by JAK3 inhibitor treatment (Fig. 3.11. B and D, Western blot analyses from Krisna Murti).

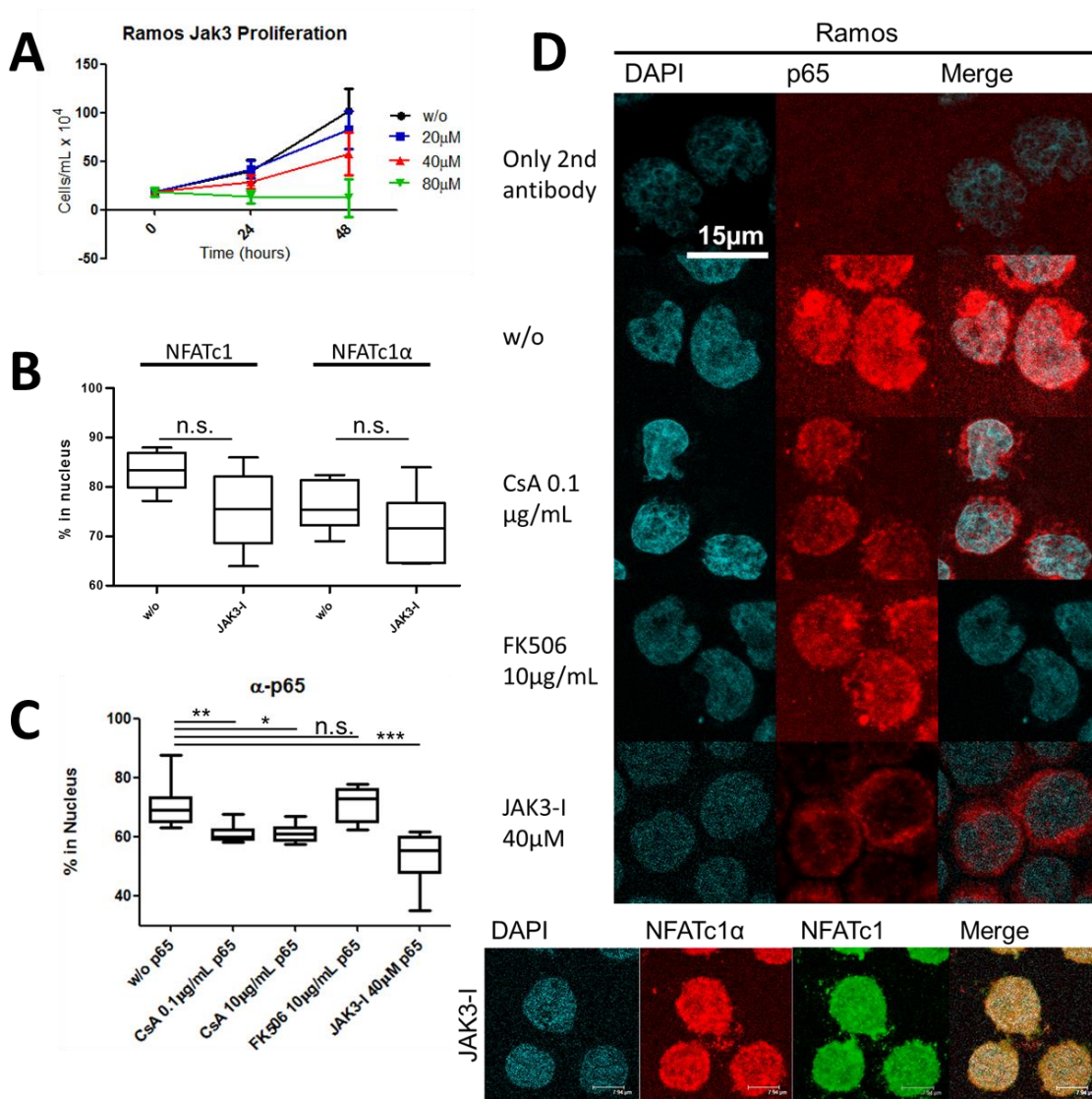


Fig. 3.11. JAK3 Inhibition reduces proliferation of Ramos cells without affecting NFATc1 distribution but leading to a translocation of the NF- κ B protein family member RelA/p65 from nucleus to cytosol in Ramos cells. (A) Cell numbers are counted at indicated time points. The inhibition concentration of JAK3-I is approximately 40 μ M. Confocal microscopy analyses of nuclear to whole cell ratios of (B) both NFATc1 and NFATc1 α levels after JAK3 inhibition and (C) p65 after treatment in Ramos cells with the reagents indicated. (D) Confocal microscopy of distribution of p65 and NFATc1 in Ramos cells after 4 h of treatments indicated.

3.4. MYC-overexpression contributes to the nuclear distribution of NFATc1 and regulates its expression on two different levels

To evaluate the impact of MYC on NFAT distribution and expression, I used the cell line P493-6. It is originally derived from the human lymphoblastoid B-cell line EREB2-5. In this EBV-EBNA-I positive cell line, the viral protein EBNA2 is expressed as a fusion protein with the ligand binding domain of the estrogen receptor. Hence, activation of EBNA2 is dependent on the presence of estrogen leading to proliferation. However, in P493-6 cells, *c-myc* is under the control of a tetracycline regulated repressor (Pajic, Spitkovsky et al. 2000). As a result of these two constructs, one can induce MYC-driven and/or EBV-driven proliferation, or contrariwise cell cycle arrest (see Fig.3.12. A).

First, I investigated the proliferation behavior and sensibility of P493-6 cells to CsA, doxycycline and estrogen. Therefore, cell number was counted each day (Fig 3.12. E). As expected, P493-6 cells do not grow with doxycycline because *c-myc* is repressed: In order to estimate *myc* repression in the presence of doxycycline, Western blots were performed and Myc was detected immunologically. Surprisingly, even 1ng/ml of doxycycline leads to a complete Myc down-regulation (Fig. 3.12. B). Proliferation is released with (1) estrogen, (2) estrogen plus doxycycline or (3) without any treatment (Fig. 3.12. F).

3.4.1 CsA does not affect NFATc1 translocation in P493-6 cells

To evaluate P493-6 cell viability under experimental conditions, cells were stained for annexin and propidium iodide (PI) for apoptosis and necrosis. It turned out that after 2 d of incubation none of the used CsA concentrations (or of the reagents mentioned above) increased cell death. Just a minimal effect of CsA with a 2% reduction of living cell population was observed (Fig. 3.12. G).

CsA inhibits proliferation of P493-6 cells dependent on the concentrations used. At least 0.5 $\mu\text{g/ml}$ is required for inhibition. After 4 d of incubation, proliferation was strongly inhibited (Fig. 3.12. E, F). However, an MTT proliferation assay revealed that the cells continue to grow even in the presence of 0.4 $\mu\text{g/ml}$ of CsA (not shown). A CFSE proliferation assay demonstrated that proliferation was completely blocked with 1.0 $\mu\text{g/ml}$ of CsA or doxycycline, whereas 0.5 $\mu\text{g/ml}$ CsA blocked it partially - detectable by the lower FITC intensities after 7 d (Fig. 3.12. F). Estrogen-treated or non-treated cells continued to proliferate.

Confocal pictures of P493-6 cells revealed a predominant nuclear location of NFATc1 or NFATc1 α and show that neither CsA nor VIVIT lead to an increase of cytosolic translocation (Fig. 3.12. C). A predominant nuclear distribution of NFATc1 is even present under doxycycline treatment (when the *MYC* promoter is repressed), as seen in Western blot (Fig. 3.12. D).

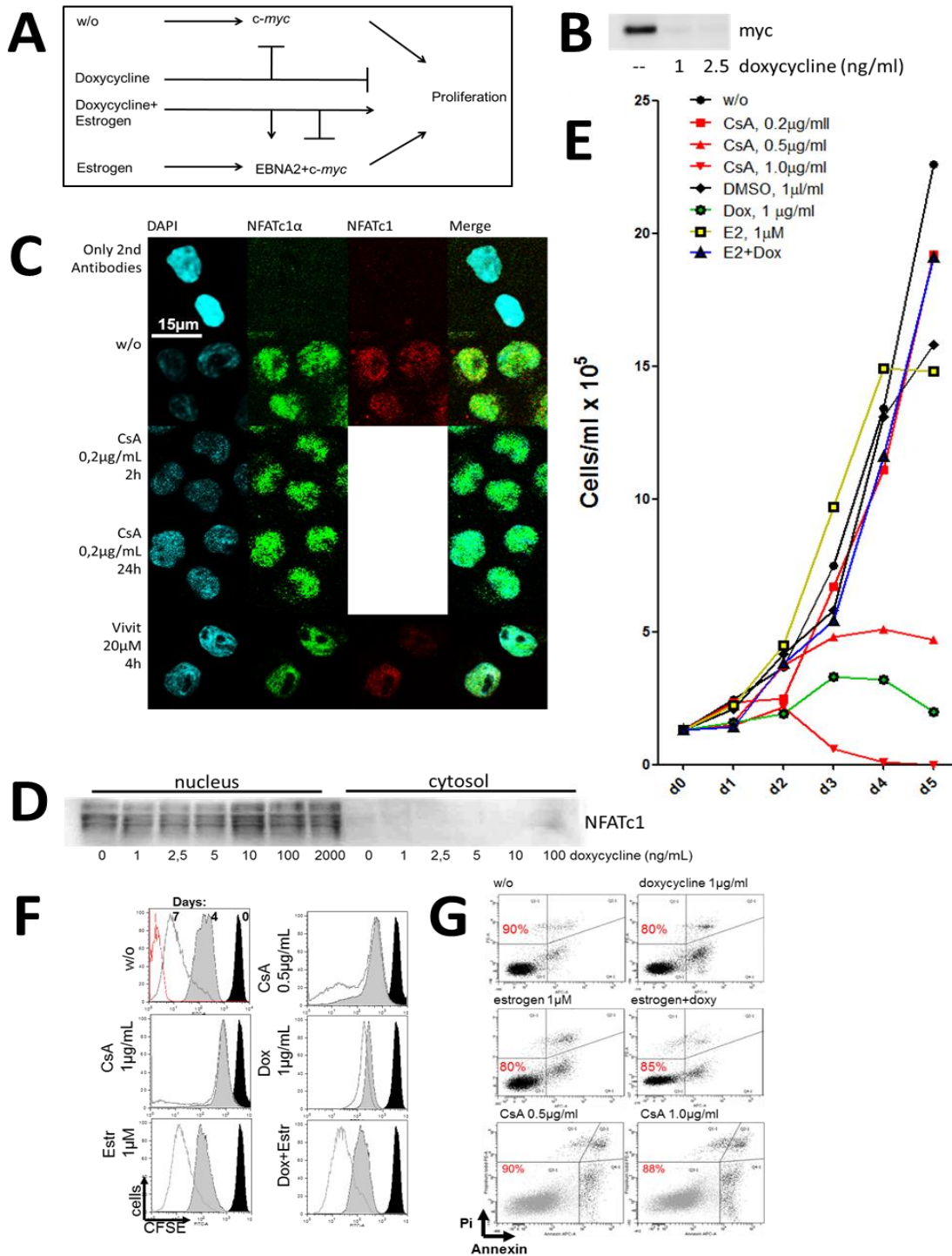


Fig. 3.12. CsA does not induce the cytosolic translocation of NFATc1 in P493-6 cells, but high concentrations inhibit their proliferation. (A) Scheme of tetracycline regulated *c-myc* and estrogen dependent EBNA2 function. (B) Western blot of nuclear extracts from P493-6 cells upon 3 d doxycycline treatment. Stained against MYC. (C) Confocal microscopy of P493-6 cells treated as indicated. (D) Western blot of NFATc1 in doxycycline treated P493-6 cells. (E) Proliferation curves of P493-6 cells under the conditions indicated. (F) CFSE proliferation assay of 4 and 7 d culturing under indicated conditions. Black curve: 0 days, grey curve: 4 d, empty curve: 7 d, red curve: unstained control. (G) Annexin/PI staining after different treatments (4 d culturing, CsA treated cells: 2 d)

3.4.2 MYC repression releases partly NFATc1 into the cytosol and regulates NFATc2 and BCL-6 protein and NFATc1 mRNA expression

If MYC levels are low, a part of NFATc1 was found to be translocated into the cytosol (Fig. 3.13. A). Therefore, the cytosolic appearance is exclusively dependent on the absence of MYC – thereby it is of no importance if the cells are in cell cycle arrest or proliferating, since proliferation induction can be provided by estrogen alone. (Fig 3.13 A, Lane 3). The effect of MYC on NFATc1 distribution is in line with the fact that MYC positively regulates Ca^{2+} levels (Habib, Park et al. 2007).

Additionally, molecular weights of NFATc1 in the cytosol are shifting. This might indicate a MYC-dependent dephosphorylation. Moreover, protein levels of NFATc1 remains unaffected, whereas both BCL6 and NFATc2 expression is repressed by Myc. However, both proteins remained largely nuclear.

A comparison of transcription data of (Biegling, Fish et al. 2011) (GSE26918) between primary mouse B cells and *Myc*-overexpressing B cells ruled out, that Myc causes a decrease of *Nfatc1* expression (both in tumor cells and in cells that were extracted before tumor development) (Fig.3.13 B). This goes in line with RNA data from Murti, K (not shown) and published data (Dave, Fu et al. 2006). Surprisingly, these data show no (!) decrease in *NFATC1* expression levels between primary B cells and tumor cells in the human system. As NFATc1 protein levels are higher in tumor cells, both from mouse and human, compared to resting B cells, somehow MYC positively influences the translation of NFATc1.

Taken together, NFATc1 protein expression in human BL or *Myc*-induced tumors does not correlate with mRNA levels. Consequently, NFATc1 expression must be up-regulated by MYC in a post-transcriptional and/or -translational way.

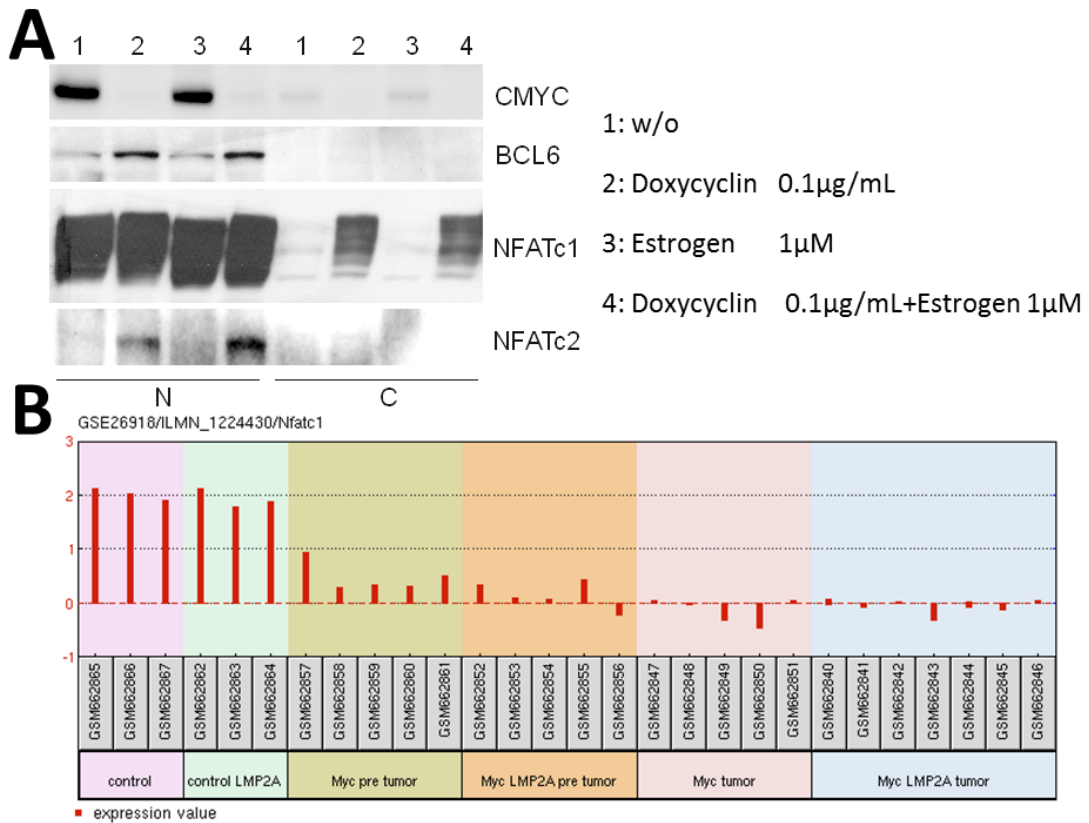


Fig. 3.13. Overexpression of MYC induces nuclear location of NFATc1 in P49-6 cells and down-regulates NFATc1 mRNA levels in tumors derived from $E\mu$ -myc mice. (A) Western blot of nuclear and cytosolic extracts of P493-6 cells upon incubation for 4 d with the treatments indicated. (*MYC* “on”: Number 1 and 3). (B) Analysis from transcription data GSE26918 (Biegling, Fish et al. 2011). Red columns represent RNA transcripts of NFATc1 in B cells derived from different mice: control mice, LMP2A transgenic mice, $E\mu$ -myc mice. B cells were taken from the latter two either before or after tumor development.

3.5. Plasticity of *myc*-driven tumor cells: the origin for “starry sky” –macrophages?

3.5.1. Expression of the myeloid markers CD11b and F4/80 on E μ -*myc* mouse B cell lines

Approximately four weeks after establishing the E μ -*myc* mouse cell lines #2229 and #1542, they changed in many manners. They became granular and some of the cells were attached to the tissue culture plate (Fig. 3.14. A). Moreover, they lost their round appearance and developed pseudopodia. Because of their macrophage resemblance, we called these attached cells “M29” and “M1542” cells, respectively. Separation of the floating cells from attached cells revealed novel aspects in flow cytometry. Attached cells expressed higher levels of CD11b⁹ and F4/80¹⁰ but lower levels of B220 or CD19. These findings resemble a switch to macrophage-lineage (Fig. 3.14. B, D). The same results were shown by flow cytometry after subcloning of M29 cells (data not shown). Intriguingly, M29 cells are also positively stained against MAC387 (L1/calprotectin¹¹), suggesting that these cells belong to the macrophage lineage (Fig. 3.14. C).

Aside from F4/80 and high Ki-67 expression under the confocal microscope, M29 cells show a mixed distribution of NFATc1 and NFATc1 α (Fig. 3.14. C), in contrast to the primary mouse tumor cells: now, small rings around the nuclei are detectable.

⁹ CD11b, also known as „Integrin alpha M” forms a heterodimer with CD18. It is expressed on macrophages, granulocytes and other cells from the innate immune system. It mediates adhesion, cellular activation and phagocytosis. Solovjov, D. A., E. Pluskota and E. F. Plow (2005). "Distinct roles for the alpha and beta subunits in the functions of integrin alphaMbeta2." *J Biol Chem* **280**(2): 1336-1345.

¹⁰ F4/80 is expressed on the surface of various macrophages. Its human analog is EMR1. It supports adhesion, signaling and cooperation between macrophages and natural killer cells. Austyn, J. M. and S. Gordon (1981). "F4/80, a monoclonal antibody directed specifically against the mouse macrophage." *Eur J Immunol* **11**(10): 805-815.

¹¹ Expressed on macrophages and granulocytes. Promotes anti-microbial properties. Especially in non-Hodgkins B cell lymphomas, L1+ and CD86+ macrophages are present. Bjerke, K., T. S. Halstensen, F. Jahnsen, K. Pulford and P. Brandtzaeg (1993). "Distribution of macrophages and granulocytes expressing L1 protein (calprotectin) in human Peyer's patches compared with normal ileal lamina propria and mesenteric lymph nodes." *Gut* **34**(10): 1357-1363.

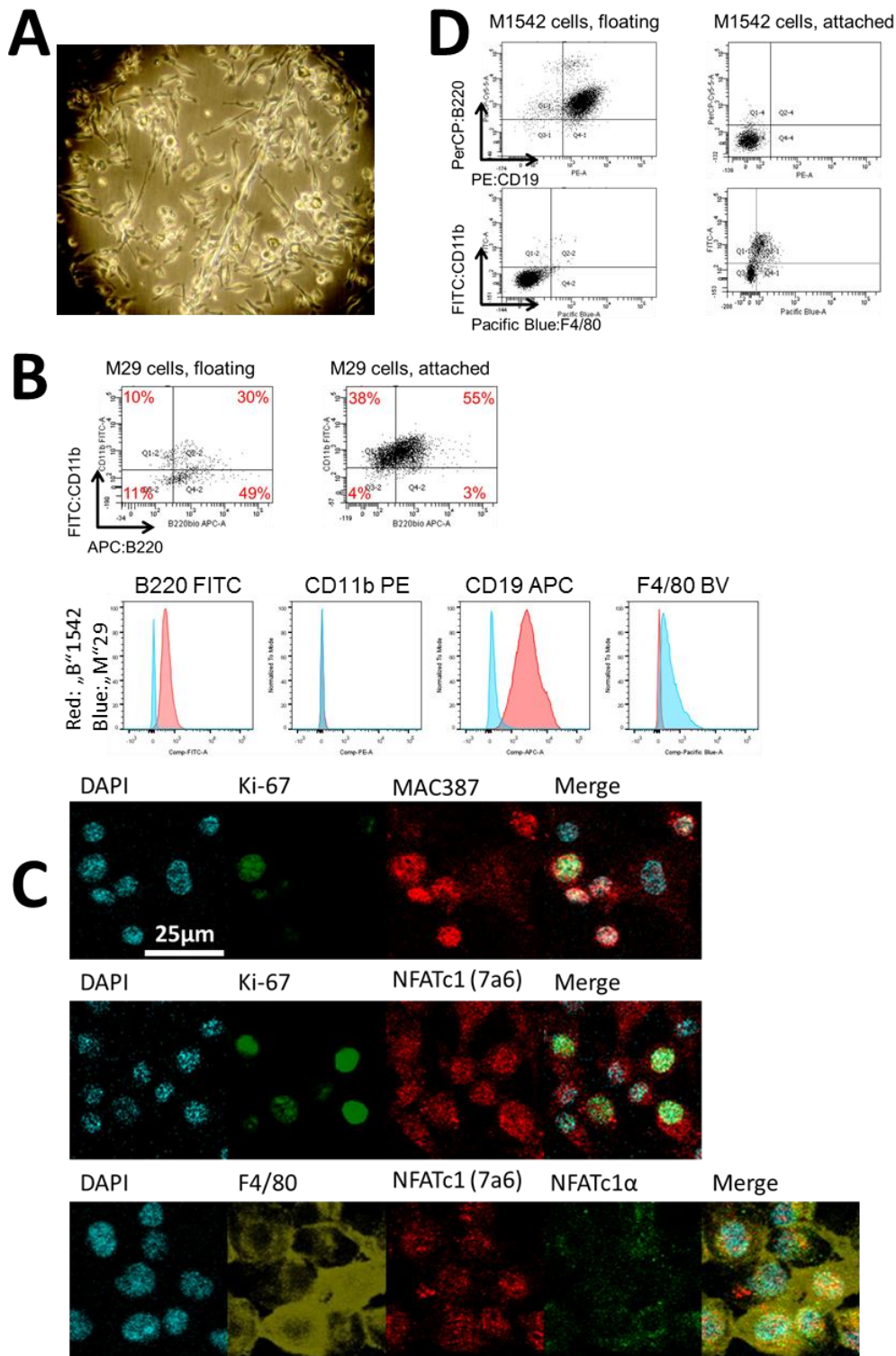


Fig. 3.14. Appearance, surface marker expression and nuclear NFATc1 distribution of macrophage-like tumor cells from the *Eμ-myc* mice 2229 and 1542 (M29 and M1542, respectively). (A) Cell culture of M29 cells. (B) Flow cytometry of surface expression of CD11b, B220, CD19, F4/80 on M29 cells. Comparison between attached and floating M29 cells (above), and between M29 and B1542 cells (below). (C) Confocal microscopy of M29 cells. NFATc1 and α are present in nuclear and cytosolic fraction. (D) Flow cytometry of M1542 cells: comparison between floating and attached cells.

3.5.2. Macrophage-like cells are inducible depending on calcium signaling

As NFATc1 distribution was different in M29 cells from primary tumor B cells, I tested the correlation between calcium signaling and macrophage oscillation of these cells. I treated the “M” cells with different reagents and, intriguingly, CD11b and B220 markers changed their presence contrarily. High calcium concentrations obtained by TPA plus ionomycin or calcium chloride treatment impaired CD11b expression. When EGTA¹² or CsA was used, CD11b expression slightly increased, and, in parallel, B220 expression decreased. This was even more distinct with all-trans retinoic acid (ATRA)¹³ that induced highest CD11b expression (Fig. 3.15.).

Counting of CD11b positive cells by confocal microscopy underlined this significant difference: untreated M29 cells were 70% (92/132 cells counted) positive, whereas T/I treated cells were 19% (38/198) positive for CD11b.

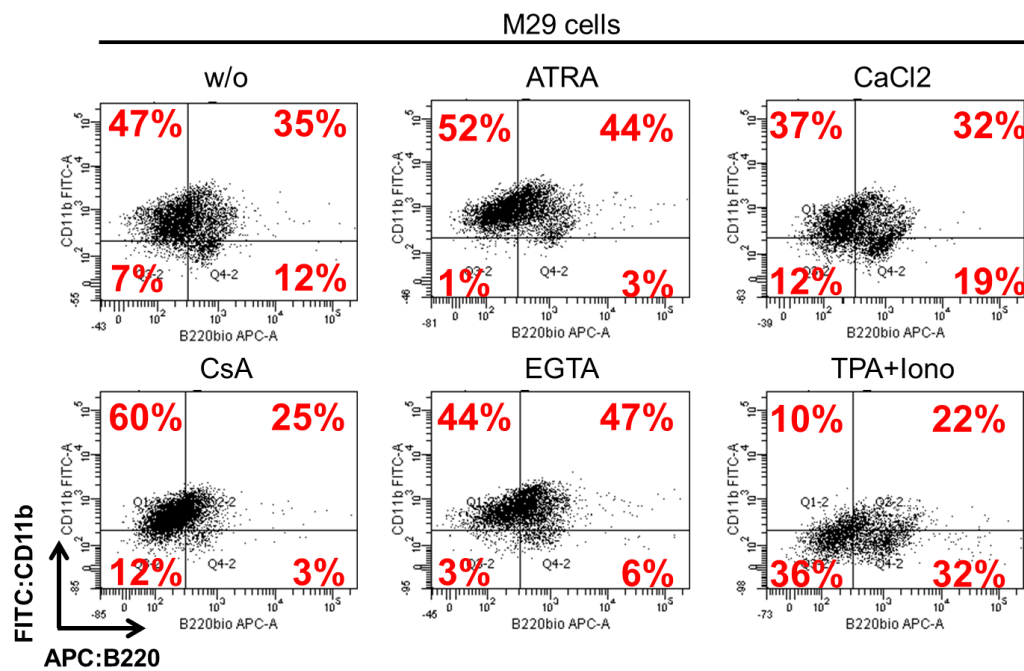


Fig. 3.15. Different treatments modulate surface marker expression of M29 cells. Flow cytometry of M29 cells. Cells were cultured in X-VIVO medium for 24 h with different reagents: 1 μ M all-trans retinoic acid, 4mM Calcium chloride, 2 μ g/mL CsA, 3 mM EGTA (ethylene glycol tetraacetic acid), 0.5 μ l/ml TPA (tetradecanoyl phorbol acetate) and 0.5 μ l/ml Iono (ionomycin). Cells were stained with biotinylated B220-antibody and FITC-labeled CD11b-antibody.

¹² ethylene glycol tetraacetic acid, a calcium specific chelating agent

¹³ all-trans retinoic acid, used for the induction of differentiation of myeloid cells.

The distribution of NFATc1, as observed by confocal microscopy, after treatment with various reagents is shown Fig. 3.16. Reagents that support calcium signaling impaired CD11b surface marker expression, which may be caused by increased NFAT activity. Hence, reagents that increase intracellular Ca^{2+} levels, like T/I or CaCl_2 , support the nuclear appearance of NFATc1 or NFATc1 α . This finding is accompanied by a low CD11b signal. However, a pronounced converse effect of its cytosolic translocation was only observed with ATRA.

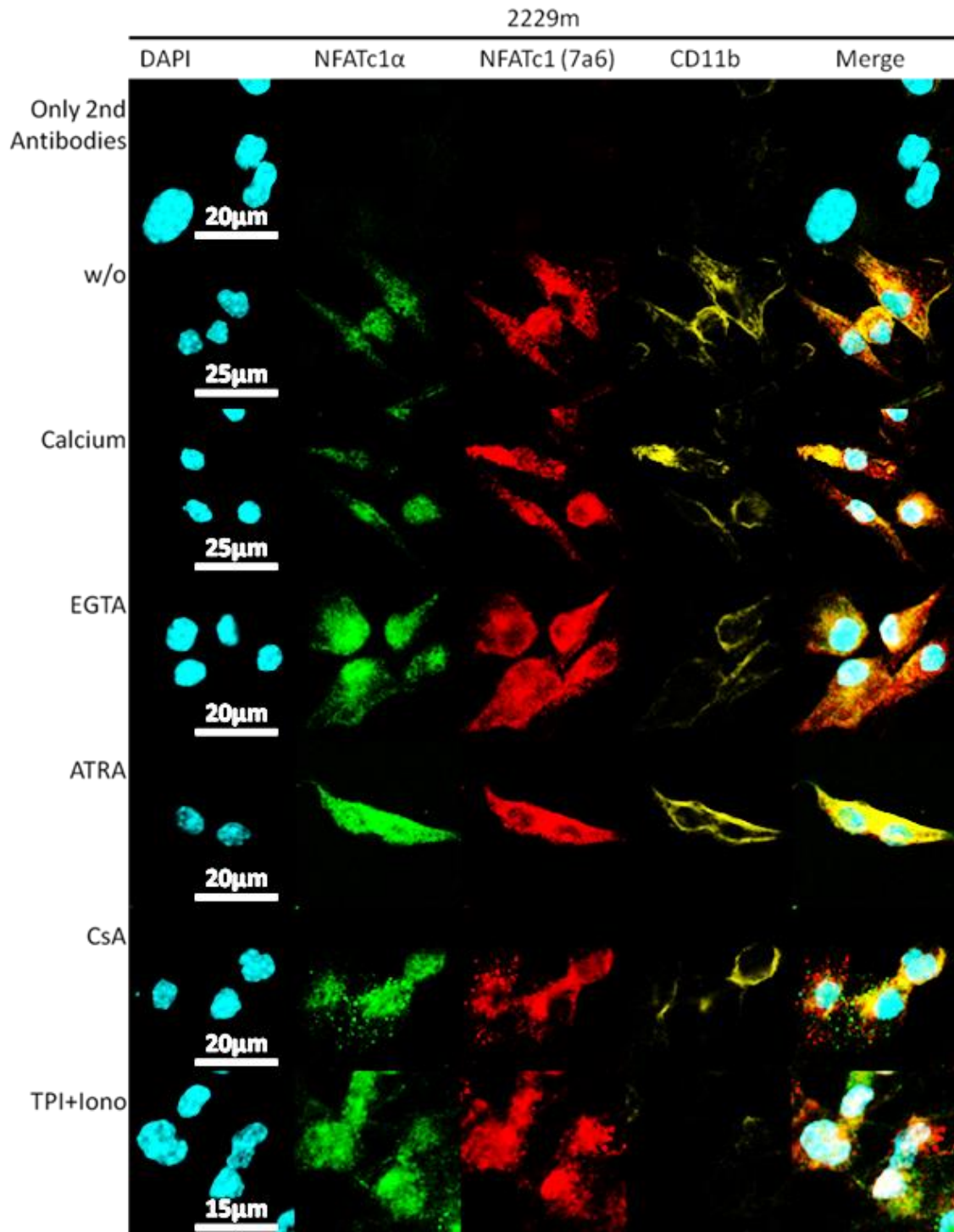


Fig. 3.16. CD11b down regulation correlates with high calcium signaling and nuclear translocation of NFATc1 or NFATc1 α in M29 cells. Confocal microscopy of M29 cells, treated for 24 h with: 8 mM calcium chloride, 6 mM EGTA, 1 μ M ATRA, 0,5 μ l/ml TPA, 0,5 μ l/ml ionomycin or 2 μ L/mL cyclosporin A. Cells were stained with antibodies for NFATc1, NFATc1 α or CD11b.

3.5.3. Transformed “M” Cells are competent for phagocytosis

To answer the question, whether transformed “M” cells have the ability for phagocytosis, like macrophages have, I took dead yeast, labeled them with FITC and incubated them together with M cells. Both subclones from M29 cells and M1542 cells were able to ingest and digest yeast, whereas P493-6 cells, used as negative control, were unable to digest yeast (Fig. 3.17).

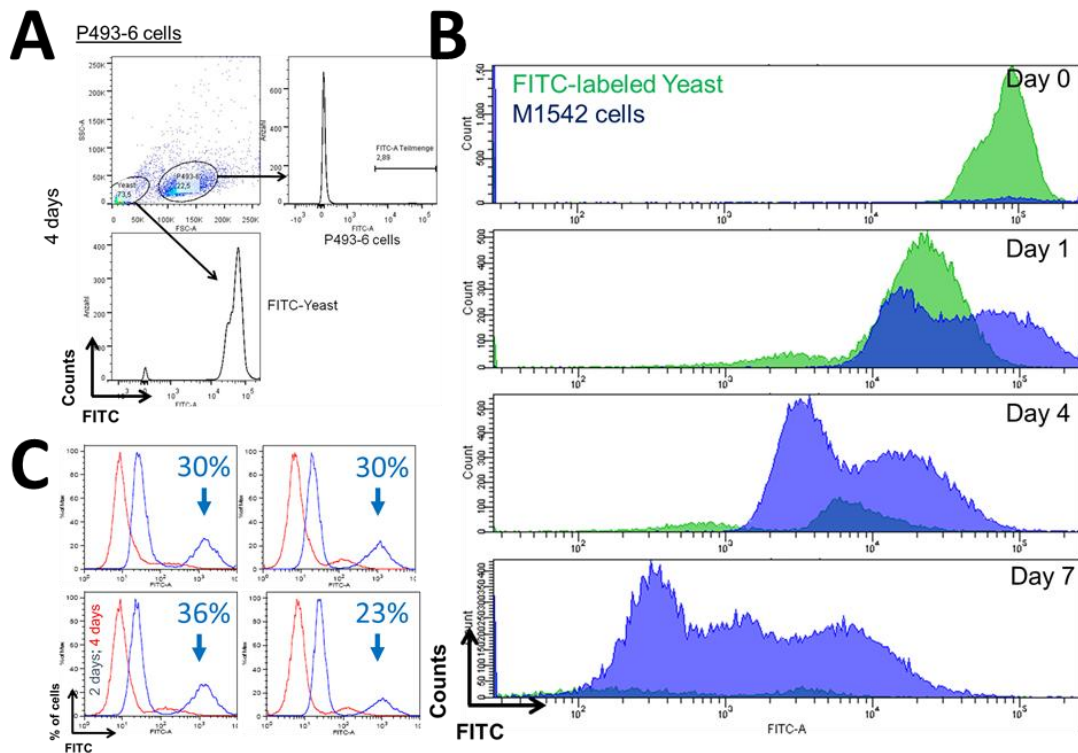


Fig 3.17. „M“ cells are competent for phagocytosis. (A) P493-6 cells do not ingest yeast. After 4 days, they are negatively stained for FITC. (B) Subclones of M29 cells digest yeast (extract of 10 subclones – phagocytosis after 2 days varies between 14% and 70%). Flow cytometry was done after 2 (blue curve) and 4 d (red curve) of incubation. (C) M1542 cells: phagocytosis of FITC labelled yeast after the days indicated.

Taken together, under certain conditions *Myc*-driven tumor B cells are capable to re-differentiate into macrophage-like cells. Both their outward appearance, surface marker expression and phagocytic feature confirm this conclusion. Hence, it is very likely that changes in environmental conditions within the tumor mass generate the “starry sky” macrophages. Being one hallmark in the diagnosis of BL, these typical macrophage clusters might improve homeostasis, thereby supporting overall proliferation properties.

4. Discussion

To drive proliferation and counteract pro-apoptotic signals, tumor cells are hi-jacking cellular signal activation pathways. In case of BL, together with *MYC*-overexpression, the AKT/PI3K pathway is active and important for the survival of cells (Schmitz, Young et al. 2012). However, the effect of PI3K inhibitors was only moderate (see Fig. 3.10 A). The fact that gallium was used widely in cancer and non-Hodgkin lymphoma treatments (Adamson, Canellos et al. 1975, Chitambar, Wereley et al. 2006), but does not interfere with PI3K signaling (constant pAKT levels in Fig. 3.5. D), led me conclude that another major survival pathway acts in BL.

Gallium's strong effects on BL cell lines guided me to study NFAT factors (Fig. 3.4.). This is supported by the fact that gallium blocks *NFATC1* expression in RAW cells upon RANKL activation (Verron, Loubat et al. 2012). In addition, I also investigated pancreatic cancer cell lines which are known to overexpress *NFATC1* (Buchholz, Schatz et al. 2006). Finally, I confirmed that gallium impairs NFATc1 mRNA and protein expression in BL and pancreatic cancer cell lines, inducing apoptosis and inhibiting proliferation (see Fig. 3.4., 3.5., 3.6.). By which mechanism gallium affects Jurkat cells that do not depend on NFATc1 or MYC, remains unclear (see Fig. 3.4. B). Most probably, aside from its iron-dependending effect, gallium influences NF- κ B activity as well, as it was already shown in RAW cells (Verron, Loubat et al. 2012). A possible way how gallium acts through NFATc1 is shown in Fig. 4.1.

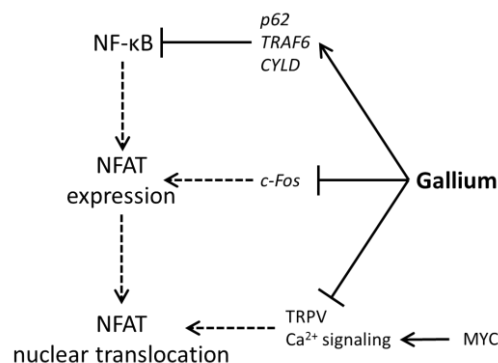


Fig. 4.1. Putative molecular ways of gallium to suppress NF- κ B and NFAT dependent cancer types. Arrows indicate positive regulation, dotted lines indicate blocked pathways.

NFAT factors are known to contribute to lymphoma genesis (Viola, Carvalho et al. 2005, Buchholz and Ellenrieder 2007, Gachet and Ghysdael 2009). They are expressed in most BL cases. NFATc1 is predominantly localized in the nuclei of numerous BL (Marafioti, Pozzobon et al. 2005, Akimzhanov, Krenacs et al. 2008). These features predestinate NFAT factors as a pivotal point in the genesis and proliferation of BL. I confirmed its nuclear location both in BL cell lines and *Myc*-driven mouse B cell tumors (Fig. 3.1, 3.2). Although clear circles, seen in naïve wild-type B cells (Fig. 3.2. A), reflect that the antibody is able to distinguish between nuclear or cytosolic localization, both antibodies used bind also unspecifically to cellular proteins (Western blot Fig. 3.9.). Thus, confocal microscopy of NFAT distribution - although giving valuable hints for translocations - has to be interpreted carefully.

Interestingly, protein levels and transcriptional expression of NFATc1 mRNA does not necessarily correlate with *MYC*-overexpression. In *Eμ-myc* induced mouse tumors, *Nfatc1* mRNA levels in tumor or pre-tumor cells are significantly lower than in control B cells (Fig. 3.13. B) (Biegging, Fish et al. 2011, Murti 2014). Moreover, its half-life time is elongated in Ramos and Namalwa cells, compared with naïve B cells (6.66 h against 4 h) and increases in P493-6 cells, if *MYC* is deregulated (8 h against 5 h) (Murti 2014). Intriguingly, in the human system, RNA levels of *NFATC1* are similar to resting B cells (Murti 2014), and protein levels remained unaffected by *MYC*-knockdown in P493-6 cells. However, both its distribution and molecular weight changed (Fig. 3.10A). All these observations indicate a pronounced post transcriptional up-regulation of NFATc1 by *MYC*, either on the translational or post-translational level.

In several human aggressive B and T tumor cell lines, CN inhibitors induce NFAT deactivation with a subsequent cell cycle inhibition and apoptosis (Medyouf, Alcalde et al. 2007). Probably, *MYC*-overexpression promotes a certain resistance against CN-dependent NFAT de-activation. This is observable in the BL cell lines (Fig. 3.8., 3.9.) or other *MYC*-overexpressing cancers, such as in the pancreatic cancer cell lines IMIM-PC-2 and TD-2 (Buchholz and Ellenrieder 2007). An apoptosis induction with high concentrations of CN inhibitors might be due to unspecific toxic effects. For instance, high concentrations of CsA (10 μ M or 12 μ g/ml) cause the release of TGF- β 1 in T cells, that counteracts *MYC* (Weinberg 2007). Nevertheless, CN inhibition caused alterations

in phosphorylation status of NFAT including a partial cytosolic translocation (Fig.3.3, 3.4). It remains unclear to what extent the nuclear portion is transcriptionally active. Hence, further investigations should concentrate on transcription properties or MYC affecting the nuclear export machinery.

In many hematologic malignancies, NF- κ B proteins provide the major pro-survival signals. But in BL, *c-Myc* overexpression predominantly activates their pro-apoptotic features: NF- κ B1 is dispensable for lymphomagenesis (Keller, Nilsson et al. 2005), NF- κ B2 must be suppressed to provide lymphoma genesis (Keller, Huber et al. 2010) and, only few NF- κ B target genes are expressed in BL (Dave, Fu et al. 2006, Klapproth, Sander et al. 2009). However, in the lymphoblastoid B cell line P493-6, activation of NF- κ B by estrogen (EBNA2 becomes active, induces the latent membrane protein (LMP)) should promote and activate NF- κ B (Abbot, Rowe et al. 1990, Ersing, Bernhardt et al. 2013)). However, apoptosis rates are nearly not altered (Fig. 3.12. G). In contrast, transgenic NF- κ B activation or its activation through anti-CD40 treatment induces apoptosis in Ramos cells (Klapproth, Sander et al. 2009). These examples show that P493-6 cells on the one hand help to understand MYC's influence on intracellular pathways, but on the other they differ from classical BL cell lines. Another proposed BL model are tumor cells grown in *E μ -myc* mice. Contrary to the BL that is germinal center-derived, these cells resemble a pre/pro-B cell lymphomas (as their surface markers differ from BL in IgM, CD5 and CD21 expression) and are mostly monoclonal (Murti 2014). By introducing constitutively active BCR signaling, mice developed much earlier tumors that are polyclonal (Refaeli, Young et al. 2008). Taken together, these examples show that BL is much more than a MYC-overexpression. It also needs additional mutations, such as in the PI3K pathway, cyclin D3, TCF3 or p53. And, another feature is the down regulation of NF- κ B. Even if many mice models might resemble BL, their surface marker expression, intracellular signaling or unknown mutations will always discriminate them from the original human BL.

In normal B cells, PI3K inhibition or depletion of its catalytic subunits, p110 δ , or of the "cofactors" Vav1, Vav2 and Vav3 attenuates the BCR-mediated calcium influx, the intracellular calcium levels and finally NFAT activation, whereas overexpression of Vav1 or Vav2 is known to increase them (Doody, Billadeau et al. 2000, Martin, Wang et al.

2012). Furthermore, AKT kinase is known to down regulate NFATc2 levels via ubiquitination in breast cancer cell lines. On the one hand, this resulted in tumor progression and increase of cell survival, but on the other it inhibited migration and invasion (Yoeli-Lerner, Yiu et al. 2005). As many BL have deregulated PI3K signaling (Schmitz, Young et al. 2012), and PI3K inhibitors induce apoptosis in BL (Schmitz, Young et al. 2012, Niemann and Wiestner 2013) and, together with IgM stimulation, in BL cell lines like Ramos (Padmore, Radda et al. 1996), I could show that this does not affect the NFATc1 pathway. Until now, the PI3-kinase inhibitor Idelalisib is approved for patients with CLL, and many others are in clinical trials (Niemann and Wiestner 2013).

Do the “starry sky“ histiocytes derive from BL cells?

In “normal” germinal centers, the tingible-body macrophages phagocyte dying B cells (Victora and Nussenzweig 2012). The “starry sky” appearance in sections of tumors is a histological hallmark for diagnosis of BL. Numerous apoptotic cells, due to very high proliferation rates (Ki-67 > 95%), are cleared by macrophage isles embedded and scattered in the malignant tissue. Until now, we cannot rule out that these macrophages arise from transformed BL cells. In synopses with our findings and findings from other laboratories, under certain conditions murine *Myc*-driven lymphoma B cells can transform into macrophage-like cells (Yu and Thomas-Tikhonenko 2002).

Clearing of necrotic cells and toxic cell debris does not only support preventing self-destruction of the tumor mass, it is also known that *MYC* expression in tumor associated macrophages (TAM) leads to bigger tumors, lower T cell infiltration, and higher angiogenesis. Moreover, *MYC* provokes the expression of proteins like VEGF, MMP9 and HIF1 α (Pello and Andres 2013). *MYC*-induced tumors like BL harbor the genetic basis for these features and a transformation into macrophage-like cells is a potential “method” to create environmental conditions for a better survival of tumor cells.

Plasticity of *Myc*-driven tumor cells is already known as the first *E μ -myc* mice were established: tumor B cells that derived from pre-B cell stage and thus were surface Immunoglobulin negative (sIg-), became sIg+ after 3 weeks in culture, meaning that

differentiation does not need to be “frozen” at one stage (Adams, Harris et al. 1985). Much earlier, first in vitro morphing of a B lymphoma cell line into macrophage-like cell line was described (Dawe CJ, 1957). In 2002, Yu et al. discovered macrophage markers on B cell lymphoma cells that derived from *MYC*-encoding retrovirus-infected p53-null bone marrow progenitor cells, after long time of culturing in vitro (Yu and Thomas-Tikhonenko 2002). The myeloid and lymphoid phenotype oscillation seems to be related with EBF and Pax-5 expression that decreases automatically after several weeks of in vitro culturing. Low Pax-5 levels correlate with down-regulation of B cell markers, like B220 or CD19, but to up-regulation of CD11b or F4/80. Conversely, retrovirally encoded expression of PAX-5 can prevent macrophage-like transformation. In addition to PU.1, E2A and EBF, PAX-5 is one of the key transcription factors in B cell differentiation and usually inhibits GM-CSF receptor (Nutt, Heavey et al. 1999, Yu, Allman et al. 2003).

Alterations in surface marker expression, behavior and phagocytosis properties of our established *E μ -myc* B cell lines M1542 and M29, also represents the plasticity of lymphoma cells depending on environmental conditions. Moreover, there is evidence that it depends on changes in calcium signaling. On the one hand, calcium dependent oscillation directly points to NFAT appearing as another pivotal point for B cell lineage commitment. Moreover, on the other, it shows that uncontrolled *Myc* overexpression induces both myeloid differentiation and inhibition of terminal B cell differentiation. By the way, *Myc* is known to be overexpressed during commitment of stem cells to the monocyte lineage and in proliferating myeloblastic cells (Valledor, Borrás et al. 1998). Taken together, *Myc* overexpression generally prevents terminal B cell differentiation, induces lineage commitment of myeloid cells and is known to be expressed in tumor macrophages. The calcium dependence of oscillation between malignant B cells and macrophage-like cells points to NFAT factors playing a crucial role in this situation.

To confirm the origin of the “starry sky” macrophages, one could search for their *Myc*-translocation with fluorescence in situ hybridization under the microscope. Another possibility would be the creation of *E μ -myc* mice that also express *mb1-cre*, and eGFP or eYFP in floxed sites. Green or yellow fluorescent macrophage isles within the tumor mass then excludes their B cell origin, whereas no signal would confirm it.

7. Summary

Burkitt's lymphoma (BL) is a very aggressive, germinal center-derived B cell lymphoma. It mostly occurs in children from equatorial Africa who carry both the Epstein-Barr virus and the pathogens for malaria. Aside from this endemic form, there are also sporadic and immunosuppressive forms of BL. The most important characteristics are both the “starry sky” macrophages - from a histological point of view - and the translocation of *MYC* to one of the immunoglobulin enhancers at the molecular level. In addition to *MYC* overexpression several mutations, e.g. in p53 or cyclin D3, or constitutive active PI3-kinase signaling contribute to lymphoma genesis.

Furthermore, NFAT factors seem also to play a crucial role. In human BL cell lines and murine *Myc*-driven tumors, the pro survival factor NFATc1 is highly expressed and present in the nuclei. To interfere with the NFAT pathway in lymphoma formation, I tested the “classical” way by inhibition of calcineurin (CN) with CsA, FK506 or VIVIT. Surprisingly, CN inhibition was not sufficient to induce a complete cytoplasmic translocation of NFATc1. Furthermore, CN inhibitors affected cellular survival and proliferation only at atypical high concentrations. Investigation of other pathways, like the PI3-kinase or JAK3, excluded the possibility that they promote NFATc1 activity. Finally, I treated NFATc1 over-expressing BL and pancreatic cancer cell lines with gallium nitrate that turned out to be a very potent inhibitor of cell survival. Gallium nitrate suppressed *NFATc1* and *MYC* transcription though protein stability was not affected.

Regarding the regulation of NFATc1 by *MYC*-overexpression, the data obtained in my work suggested that (1) *NFATc1* mRNA level is down-regulated in murine cells, (2) NFATc1 protein level is up-regulated in both human and murine cells, and (3) *MYC* supports NFATc1's nuclear residence.

Finally, I discovered *Myc*-driven tumor cells as potential “starry sky” macrophages. Under certain conditions, mainly concerning calcium signaling, they change their outward appearance, surface marker expression, and gain the ability for phagocytosis.

For the future, the discovery that gallium acts through NFATc1 in BL and probably numerous other cancer types opens up new strategies for therapeutic interventions.

6. Table of Figures

	Title	Page
Fig. 1.1.	B cell differentiation: First steps of B cell maturation occur antigen-independent in the bone marrow.	2
Fig. 1.2.	The B cell receptor activates MAPK, NFAT, mTOR and NF- κ B pathways.	3
Fig. 1.3.	The germinal center.	5
Table 1.1.	Entities of BL	7
Fig. 1.4.	B cell differentiation steps and their malignant counterparts.	8
Fig. 1.11.	Frequently mutated genes and their context.	9
Fig. 1.6.	Scheme of the <i>Myc</i> gene.	10
Table 1.2.	Overview of the properties of NFAT factors.	14
Fig. 1.7.	Scheme of the five members of the NFAT family.	15
Fig. 1.8.	Overview: Target genes of NFAT factors.	16
Fig. 1.9.	Regulation of NFAT.	17
Fig. 1.10.	Scheme of the murine P1 promoter, the <i>Nfatc1</i> gene and NFATc1 α A.	19
Fig. 3.1.	Nuclear location of NFATc1 proteins, and of its inducible isoforms NFATc1 α , in Burkitt's lymphoma cell lines.	40
Fig. 3.2.	Nuclear location of NFATc1 α in tumors derived from E μ -myc mice.	42
Fig. 3.3.	Gallium inhibits the proliferation and induces the cell death of cell lines Ramos, Namalwa and Jurkat.	44
Fig. 3.4.	Gallium treatment leads to a reduction in protein levels of NFATc1, MYC and slightly p65 in BL cell lines Ramos and Namalwa. Moreover, a cytosolic translocation of NFATc1 is detectable.	46
Fig. 3.5.	Gallium treatment of Ramos cells does not significantly reduce protein stability of NFATc1, NFATc1 α or MYC, but mRNA levels directed by the inducible promoter P1 are decreased.	48
Fig. 3.6.	Pancreas carcinoma cell lines are sensitive to gallium. Their proliferation rate is diminished, apoptosis is induced and NFATC1 expression is down-regulated.	50
Fig. 3.7.	Only atypical high concentrations of CN-inhibitors affect the proliferation of BL cells.	52
Fig. 3.8.	The calcineurin inhibitor CsA, but not FK506 or VIVIT peptide, leads to a slight cytosolic translocation of NFATc1 and NFATc1 α in Burkitt's lymphoma cell lines.	54
Fig. 3.9.	CsA treatment induces translocation of NFATc1 isoforms from nucleus to cytosol and increases their molecular weights.	55

Fig. 3.10.	Inhibition of PI3K in BL cell line cells leads to proliferation inhibition, cell death and slight cytosolic translocation of NFATc1.	57
Fig. 3.11.	JAK3 Inhibition reduces proliferation of Ramos cells without affecting NFATc1 distribution but leading to a translocation of the NF- κ B protein family member RelA/p65 from nucleus to cytosol in Ramos cells.	59
Fig. 3.12.	CsA does not induce the cytosolic translocation of NFATc1 in P493-6 cells, but high concentrations inhibit their proliferation.	62
Fig. 3.13.	Overexpression of MYC induces nuclear location of NFATc1 in P49-6 cells and down-regulates NFATc1 mRNA levels in tumors derived from E μ -myc mice.	64
Fig. 3.14.	Appearance, surface marker expression and nuclear NFATc1 distribution of macrophage-like tumor cells from the E μ -myc mice 2229 and 1542.	66
Fig. 3.15.	Different treatments modulate surface marker expression of M29 cells.	67
Fig. 3.16.	CD11b down regulation correlates with high calcium signaling and nuclear translocation of NFATc1 or NFATc1 α in M29 cells.	69
Fig 3.17.	„M“ cells are competent for phagocytosis.	70
Fig. 4.1.	Putative molecular ways of gallium to suppress NF- κ B and NFAT dependent cancer types.	71

7. Bibliography

- Abbot, S. D., M. Rowe, K. Cadwallader, A. Ricksten, J. Gordon, F. Wang, L. Rymo and A. B. Rickinson (1990). "Epstein-Barr virus nuclear antigen 2 induces expression of the virus-encoded latent membrane protein." *J Virol* **64**(5): 2126-2134.
- Adams, J. M., A. W. Harris, C. A. Pinkert, L. M. Corcoran, W. S. Alexander, S. Cory, R. D. Palmiter and R. L. Brinster (1985). "The c-myc oncogene driven by immunoglobulin enhancers induces lymphoid malignancy in transgenic mice." *Nature* **318**(6046): 533-538.
- Adamson, R. H., G. P. Canellos and S. M. Sieber (1975). "Studies on the antitumor activity of gallium nitrate (NSC-15200) and other group IIIa metal salts." *Cancer Chemother Rep* **59**(3): 599-610.
- Akimzhanov, A., L. Krenacs, T. Schlegel, S. Klein-Hessling, E. Bagdi, E. Stelkovic, E. Kondo, S. Chuvpilo, P. Wilke, A. Avots, S. Gattenlohner, H. K. Muller-Hermelink, A. Palmetshofer and E. Serfling (2008). "Epigenetic changes and suppression of the nuclear factor of activated T cell 1 (NFATC1) promoter in human lymphomas with defects in immunoreceptor signaling." *Am J Pathol* **172**(1): 215-224.
- Aramburu, J., M. B. Yaffe, C. Lopez-Rodriguez, L. C. Cantley, P. G. Hogan and A. Rao (1999). "Affinity-driven peptide selection of an NFAT inhibitor more selective than cyclosporin A." *Science* **285**(5436): 2129-2133.
- Austyn, J. M. and S. Gordon (1981). "F4/80, a monoclonal antibody directed specifically against the mouse macrophage." *Eur J Immunol* **11**(10): 805-815.
- Baksh, S., H. R. Widlund, A. A. Frazer-Abel, J. Du, S. Fosmire, D. E. Fisher, J. A. DeCaprio, J. F. Modiano and S. J. Burakoff (2002). "NFATc2-mediated repression of cyclin-dependent kinase 4 expression." *Mol Cell* **10**(5): 1071-1081.
- Berridge, M. J. (2011). "Cell signalling biology; doi:10.1042/csb0001004."
- Bhattacharyya, S., J. Deb, A. K. Patra, D. A. Thuy Pham, W. Chen, M. Vaeth, F. Berberich-Siebelt, S. Klein-Hessling, E. D. Lamperti, K. Reifenberg, J. Jellusova, A. Schweizer, L. Nitschke, E. Leich, A. Rosenwald, C. Brunner, S. Engelmann, U. Bommhardt, A. Avots, M. R. Muller, E. Kondo and E. Serfling (2011). "NFATc1 affects mouse splenic B cell function by controlling the calcineurin--NFAT signaling network." *J Exp Med* **208**(4): 823-839.
- Bieging, K. T., K. Fish, S. Bondada and R. Longnecker (2011). "A shared gene expression signature in mouse models of EBV-associated and non-EBV-associated Burkitt lymphoma." *Blood* **118**(26): 6849-6859.
- Bjerke, K., T. S. Halstensen, F. Jahnsen, K. Pulford and P. Brandtzaeg (1993). "Distribution of macrophages and granulocytes expressing L1 protein (calprotectin) in human Peyer's patches compared with normal ileal lamina propria and mesenteric lymph nodes." *Gut* **34**(10): 1357-1363.
- Blum, K. A., G. Lozanski and J. C. Byrd (2004). "Adult Burkitt leukemia and lymphoma." *Blood* **104**(10): 3009-3020.
- Buchholz, M. and V. Ellenrieder (2007). "An emerging role for Ca²⁺/calcineurin/NFAT signaling in cancerogenesis." *Cell Cycle* **6**(1): 16-19.
- Buchholz, M., A. Schatz, M. Wagner, P. Michl, T. Linhart, G. Adler, T. M. Gress and V. Ellenrieder (2006). "Overexpression of c-myc in pancreatic cancer caused by ectopic activation of NFATc1 and the Ca²⁺/calcineurin signaling pathway." *EMBO J* **25**(15): 3714-3724.

Chitambar, C. R. (2012). "Gallium-containing anticancer compounds." Future Med Chem **4**(10): 1257-1272.

Chitambar, C. R., D. P. Purpi, J. Woodliff, M. Yang and J. P. Wereley (2007). "Development of gallium compounds for treatment of lymphoma: gallium maltolate, a novel hydroxypyronone gallium compound, induces apoptosis and circumvents lymphoma cell resistance to gallium nitrate." J Pharmacol Exp Ther **322**(3): 1228-1236.

Chitambar, C. R., J. P. Wereley and S. Matsuyama (2006). "Gallium-induced cell death in lymphoma: role of transferrin receptor cycling, involvement of Bax and the mitochondria, and effects of proteasome inhibition." Mol Cancer Ther **5**(11): 2834-2843.

Dave, S. S., K. Fu, G. W. Wright, L. T. Lam, P. Kluin, E. J. Boerma, T. C. Greiner, D. D. Weisenburger, A. Rosenwald, G. Ott, H. K. Muller-Hermelink, R. D. Gascoyne, J. Delabie, L. M. Rimsza, R. M. Braziel, T. M. Grogan, E. Campo, E. S. Jaffe, B. J. Dave, W. Sanger, M. Bast, J. M. Vose, J. O. Armitage, J. M. Connors, E. B. Smeland, S. Kvaloy, H. Holte, R. I. Fisher, T. P. Miller, E. Montserrat, W. H. Wilson, M. Bahl, H. Zhao, L. Yang, J. Powell, R. Simon, W. C. Chan, L. M. Staudt and P. Lymphoma/Leukemia Molecular Profiling (2006). "Molecular diagnosis of Burkitt's lymphoma." N Engl J Med **354**(23): 2431-2442.

Dominguez-Sola, D. and R. Dalla-Favera (2012). "Burkitt lymphoma: much more than MYC." Cancer Cell **22**(2): 141-142.

Dominguez-Sola, D., C. Y. Ying, C. Grandori, L. Ruggiero, B. Chen, M. Li, D. A. Galloway, W. Gu, J. Gautier and R. Dalla-Favera (2007). "Non-transcriptional control of DNA replication by c-Myc." Nature **448**(7152): 445-451.

Doody, G. M., D. D. Billadeau, E. Clayton, A. Hutchings, R. Berland, S. McAdam, P. J. Leibson and M. Turner (2000). "Vav-2 controls NFAT-dependent transcription in B- but not T-lymphocytes." EMBO J **19**(22): 6173-6184.

Ersing, I., K. Bernhardt and B. E. Gewurz (2013). "NF-kappaB and IRF7 pathway activation by Epstein-Barr virus Latent Membrane Protein 1." Viruses **5**(6): 1587-1606.

Felsher, D. W. and J. M. Bishop (1999). "Transient excess of MYC activity can elicit genomic instability and tumorigenesis." Proc Natl Acad Sci U S A **96**(7): 3940-3944.

Ferry, J. A. (2006). "Burkitt's lymphoma: clinicopathologic features and differential diagnosis." Oncologist **11**(4): 375-383.

Gachet, S. and J. Ghysdael (2009). "Calcineurin/NFAT signaling in lymphoid malignancies." Gen Physiol Biophys **28 Spec No Focus**: F47-54.

Greenough, A. and S. S. Dave (2014). "New clues to the molecular pathogenesis of Burkitt lymphoma revealed through next-generation sequencing." Curr Opin Hematol **21**(4): 326-332.

Habib, T., H. Park, M. Tsang, I. M. de Alboran, A. Nicks, L. Wilson, P. S. Knoepfler, S. Andrews, D. J. Rawlings, R. N. Eisenman and B. M. Iritani (2007). "Myc stimulates B lymphocyte differentiation and amplifies calcium signaling." J Cell Biol **179**(4): 717-731.

Hecht, J. L. and J. C. Aster (2000). "Molecular biology of Burkitt's lymphoma." J Clin Oncol **18**(21): 3707-3721.

Hernandez, G. L., O. V. Volpert, M. A. Iniguez, E. Lorenzo, S. Martinez-Martinez, R. Grau, M. Fresno and J. M. Redondo (2001). "Selective inhibition of vascular endothelial growth factor-mediated angiogenesis by cyclosporin A: roles of the nuclear factor of activated T cells and cyclooxygenase 2." J Exp Med **193**(5): 607-620.

Hoelzer, D., J. Walewski, H. Dohner, A. Viardot, W. Hiddemann, K. Spiekermann, H. Serve, U. Dührsen, A. Huttmann, E. Thiel, J. Dengler, M. Kneba, M. Schaich, I. G. Schmidt-Wolf, J. Beck, B. Hertenstein, A. Reichle, K. Domanska-Czyz, R. Fietkau, H.

A. Horst, H. Rieder, S. Schwartz, T. Burmeister, N. Gokbuget and L. German Multicenter Study Group for Adult Acute Lymphoblastic (2014). "Improved outcome of adult Burkitt lymphoma/leukemia with rituximab and chemotherapy: report of a large prospective multicenter trial." Blood **124**(26): 3870-3879.

Jauliac, S., C. Lopez-Rodriguez, L. M. Shaw, L. F. Brown, A. Rao and A. Toker (2002). "The role of NFAT transcription factors in integrin-mediated carcinoma invasion." Nat Cell Biol **4**(7): 540-544.

Keller, U., J. Huber, J. A. Nilsson, M. Fallahi, M. A. Hall, C. Peschel and J. L. Cleveland (2010). "Myc suppression of Nfkb2 accelerates lymphomagenesis." BMC Cancer **10**: 348.

Keller, U., J. A. Nilsson, K. H. Maclean, J. B. Old and J. L. Cleveland (2005). "Nfkb 1 is dispensable for Myc-induced lymphomagenesis." Oncogene **24**(41): 6231-6240.

Klapproth, K., S. Sander, D. Marinkovic, B. Baumann and T. Wirth (2009). "The IKK2/NF- κ B pathway suppresses MYC-induced lymphomagenesis." Blood **114**(12): 2448-2458.

Kondo, E., A. Harashima, T. Takabatake, H. Takahashi, Y. Matsuo, T. Yoshino, K. Orita and T. Akagi (2003). "NF-ATc2 induces apoptosis in Burkitt's lymphoma cells through signaling via the B cell antigen receptor." Eur J Immunol **33**(1): 1-11.

Kurosaki, T., H. Shinohara and Y. Baba (2010). "B cell signaling and fate decision." Annu Rev Immunol **28**: 21-55.

Levens, D. (2010). "You Don't Muck with MYC." Genes Cancer **1**(6): 547-554.

Liu, J., J. D. Farmer, Jr., W. S. Lane, J. Friedman, I. Weissman and S. L. Schreiber (1991). "Calcineurin is a common target of cyclophilin-cyclosporin A and FKBP-FK506 complexes." Cell **66**(4): 807-815.

Löffler, P., Heinrich (2007). Biochemie & Pathobiochemie, Springer.

Mackay, F., W. A. Figgett, D. Saulep, M. Lepage and M. L. Hibbs (2010). "B-cell stage and context-dependent requirements for survival signals from BAFF and the B-cell receptor." Immunol Rev **237**(1): 205-225.

Marafioti, T., M. Pozzobon, M. L. Hansmann, R. Ventura, S. A. Pileri, H. Roberton, S. Gesk, P. Gaulard, T. F. Barth, M. Q. Du, L. Leoncini, P. Moller, Y. Natkunam, R. Siebert and D. Y. Mason (2005). "The NFATc1 transcription factor is widely expressed in white cells and translocates from the cytoplasm to the nucleus in a subset of human lymphomas." Br J Haematol **128**(3): 333-342.

Martin, V. A., W. H. Wang, A. M. Lipchik, L. L. Parker, Y. He, S. Zhang, Z. Y. Zhang and R. L. Geahlen (2012). "Akt2 inhibits the activation of NFAT in lymphocytes by modulating calcium release from intracellular stores." Cell Signal **24**(5): 1064-1073.

Medyouf, H., H. Alcalde, C. Berthier, M. C. Guillemin, N. R. dos Santos, A. Janin, D. Decaudin, H. de The and J. Ghysdael (2007). "Targeting calcineurin activation as a therapeutic strategy for T-cell acute lymphoblastic leukemia." Nat Med **13**(6): 736-741.

Medyouf, H. and J. Ghysdael (2008). "The calcineurin/NFAT signaling pathway: a novel therapeutic target in leukemia and solid tumors." Cell Cycle **7**(3): 297-303.

Mognol, G. P., P. S. de Araujo-Souza, B. K. Robbs, L. K. Teixeira and J. P. Viola (2012). "Transcriptional regulation of the c-Myc promoter by NFAT1 involves negative and positive NFAT-responsive elements." Cell Cycle **11**(5): 1014-1028.

Molkentin, J. D. (2004). "Calcineurin-NFAT signaling regulates the cardiac hypertrophic response in coordination with the MAPKs." Cardiovasc Res **63**(3): 467-475.

Murti, K. (2014). The Role of NFATc1 in Burkitt Lymphoma and in Eu-Myc-induced B Cell Lymphoma, Universität Würzburg.

Nayak, A., J. Glockner-Pagel, M. Vaeth, J. E. Schumann, M. Buttman, T. Bopp, E. Schmitt, E. Serfling and F. Berberich-Siebelt (2009). "Sumoylation of the transcription factor NFATc1 leads to its subnuclear relocalization and interleukin-2 repression by histone deacetylase." *J Biol Chem* **284**(16): 10935-10946.

Neal, J. W. and N. A. Clipstone (2003). "A constitutively active NFATc1 mutant induces a transformed phenotype in 3T3-L1 fibroblasts." *J Biol Chem* **278**(19): 17246-17254.

Nie, Z., G. Hu, G. Wei, K. Cui, A. Yamane, W. Resch, R. Wang, D. R. Green, L. Tessarollo, R. Casellas, K. Zhao and D. Levens (2012). "c-Myc is a universal amplifier of expressed genes in lymphocytes and embryonic stem cells." *Cell* **151**(1): 68-79.

Niemann, C. U. and A. Wiestner (2013). "B-cell receptor signaling as a driver of lymphoma development and evolution." *Semin Cancer Biol* **23**(6): 410-421.

Nutt, S. L., B. Heavey, A. G. Rolink and M. Busslinger (1999). "Commitment to the B-lymphoid lineage depends on the transcription factor Pax5." *Nature* **401**(6753): 556-562.

O'Shea, J. J., H. Park, M. Pesu, D. Borie and P. Changelian (2005). "New strategies for immunosuppression: interfering with cytokines by targeting the Jak/Stat pathway." *Curr Opin Rheumatol* **17**(3): 305-311.

Oikawa, T., A. Nakamura, N. Onishi, T. Yamada, K. Matsuo and H. Saya (2013). "Acquired expression of NFATc1 downregulates E-cadherin and promotes cancer cell invasion." *Cancer Res* **73**(16): 5100-5109.

Padmore, L., G. K. Radda and K. A. Knox (1996). "Wortmannin-mediated inhibition of phosphatidylinositol 3-kinase activity triggers apoptosis in normal and neoplastic B lymphocytes which are in cell cycle." *Int Immunol* **8**(4): 585-594.

Pajic, A., D. Spitkovsky, B. Christoph, B. Kempkes, M. Schuhmacher, M. S. Staeger, M. Brielmeier, J. Ellwart, F. Kohlhuber, G. W. Bornkamm, A. Polack and D. Eick (2000). "Cell cycle activation by c-myc in a burkitt lymphoma model cell line." *Int J Cancer* **87**(6): 787-793.

Patra, A. K., A. Avots, R. P. Zahedi, T. Schuler, A. Sickmann, U. Bommhardt and E. Serfling (2013). "An alternative NFAT-activation pathway mediated by IL-7 is critical for early thymocyte development." *Nat Immunol* **14**(2): 127-135.

Pello, O. M. and V. Andres (2013). "Role of c-MYC in tumor-associated macrophages and cancer progression." *Oncoimmunology* **2**(2): e22984.

Pillai, S. (2005). "Birth pangs: the stressful origins of lymphocytes." *J Clin Invest* **115**(2): 224-227.

Refaeli, Y., R. M. Young, B. C. Turner, J. Duda, K. A. Field and J. M. Bishop (2008). "The B cell antigen receptor and overexpression of MYC can cooperate in the genesis of B cell lymphomas." *PLoS Biol* **6**(6): e152.

Robbs, B. K., A. L. Cruz, M. B. Werneck, G. P. Mognol and J. P. Viola (2008). "Dual roles for NFAT transcription factor genes as oncogenes and tumor suppressors." *Mol Cell Biol* **28**(23): 7168-7181.

Rodig, S. J., A. Shahsafari, B. Li and D. M. Dorfman (2005). "The CD45 isoform B220 identifies select subsets of human B cells and B-cell lymphoproliferative disorders." *Hum Pathol* **36**(1): 51-57.

Sander, S., D. P. Calado, L. Srinivasan, K. Kochert, B. Zhang, M. Rosolowski, S. J. Rodig, K. Holzmann, S. Stilgenbauer, R. Siebert, L. Bullinger and K. Rajewsky (2012). "Synergy between PI3K signaling and MYC in Burkitt lymphomagenesis." *Cancer Cell* **22**(2): 167-179.

Schmitz, R., M. Ceribelli, S. Pittaluga, G. Wright and L. M. Staudt (2014). "Oncogenic mechanisms in Burkitt lymphoma." *Cold Spring Harb Perspect Med* **4**(2).

Schmitz, R., R. M. Young, M. Ceribelli, S. Jhavar, W. Xiao, M. Zhang, G. Wright, A. L. Shaffer, D. J. Hodson, E. Buras, X. Liu, J. Powell, Y. Yang, W. Xu, H. Zhao, H. Kohlhammer, A. Rosenwald, P. Kluin, H. K. Muller-Hermelink, G. Ott, R. D. Gascoyne, J. M. Connors, L. M. Rimsza, E. Campo, E. S. Jaffe, J. Delabie, E. B. Smeland, M. D. Olgwang, S. J. Reynolds, R. I. Fisher, R. M. Braziel, R. R. Tubbs, J. R. Cook, D. D. Weisenburger, W. C. Chan, S. Pittaluga, W. Wilson, T. A. Waldmann, M. Rowe, S. M. Mbulaiteye, A. B. Rickinson and L. M. Staudt (2012). "Burkitt lymphoma pathogenesis and therapeutic targets from structural and functional genomics." Nature **490**(7418): 116-120.

Serfling, E., A. Avots, S. Klein-Hessling, R. Rudolf, M. Vaeth and F. Berberich-Siebelt (2012). "NFATc1/alphaA: The other Face of NFAT Factors in Lymphocytes." Cell Commun Signal **10**(1): 16.

Serfling, E., F. Berberich-Siebelt, S. Chuvpilo, E. Jankevics, S. Klein-Hessling, T. Twardzik and A. Avots (2000). "The role of NF-AT transcription factors in T cell activation and differentiation." Biochim Biophys Acta **1498**(1): 1-18.

Shapiro-Shelef, M. and K. Calame (2005). "Regulation of plasma-cell development." Nat Rev Immunol **5**(3): 230-242.

Shi, Y., F. Nikulenkov, J. Zawacka-Pankau, H. Li, R. Gabdoulline, J. Xu, S. Eriksson, E. Hedstrom, N. Issaeva, A. Kel, E. S. Arner and G. Selivanova (2014). "ROS-dependent activation of JNK converts p53 into an efficient inhibitor of oncogenes leading to robust apoptosis." Cell Death Differ **21**(4): 612-623.

Solovjov, D. A., E. Pluskota and E. F. Plow (2005). "Distinct roles for the alpha and beta subunits in the functions of integrin alphaMbeta2." J Biol Chem **280**(2): 1336-1345.

Taylor, K. H., J. Liu, J. Guo, J. W. Davis, H. Shi and C. W. Caldwell (2006). "Promoter DNA methylation of CD10 in lymphoid malignancies." Leukemia **20**(10): 1910-1912.

Torgerson, T. R., A. Genin, C. Chen, M. Zhang, B. Zhou, S. Anover-Sombke, M. B. Frank, I. Dozmorov, E. Ocheltree, P. Kulmala, M. Centola, H. D. Ochs, A. D. Wells and R. Q. Cron (2009). "FOXP3 inhibits activation-induced NFAT2 expression in T cells thereby limiting effector cytokine expression." J Immunol **183**(2): 907-915.

Valledor, A. F., F. E. Borrás, M. Culléll-Young and A. Celada (1998). "Transcription factors that regulate monocyte/macrophage differentiation." J Leukoc Biol **63**(4): 405-417.

Vazquez, B. N., T. Laguna, J. Carabana, M. S. Krangel and P. Lauzurica (2009). "CD69 gene is differentially regulated in T and B cells by evolutionarily conserved promoter-distal elements." J Immunol **183**(10): 6513-6521.

Verron, E., A. Loubat, G. F. Carle, C. Vignes-Colombeix, I. Strazic, J. Guicheux, N. Rochet, J. M. Bouler and J. C. Scimeca (2012). "Molecular effects of gallium on osteoclastic differentiation of mouse and human monocytes." Biochem Pharmacol **83**(5): 671-679.

Verron, E., M. Masson, S. Khoshniat, L. Duplomb, Y. Wittrant, M. Baud'huin, Z. Badran, B. Bujoli, P. Janvier, J. C. Scimeca, J. M. Bouler and J. Guicheux (2010). "Gallium modulates osteoclastic bone resorption in vitro without affecting osteoblasts." Br J Pharmacol **159**(8): 1681-1692.

Victoria, G. D. and M. C. Nussenzweig (2012). "Germinal centers." Annu Rev Immunol **30**: 429-457.

Viola, J. P., L. D. Carvalho, B. P. Fonseca and L. K. Teixeira (2005). "NFAT transcription factors: from cell cycle to tumor development." Braz J Med Biol Res **38**(3): 335-344.

Weinberg, R. A. (2007). The biology of cancer. New York, Garland Science.

Wilson, W. H., K. Dunleavy, S. Pittaluga, U. Hegde, N. Grant, S. M. Steinberg, M. Raffeld, M. Gutierrez, B. A. Chabner, L. Staudt, E. S. Jaffe and J. E. Janik (2008). "Phase II study of dose-adjusted EPOCH and rituximab in untreated diffuse large B-cell lymphoma with analysis of germinal center and post-germinal center biomarkers." J Clin Oncol **26**(16): 2717-2724.

Yoeli-Lerner, M., G. K. Yiu, I. Rabinovitz, P. Erhardt, S. Jauliac and A. Toker (2005). "Akt blocks breast cancer cell motility and invasion through the transcription factor NFAT." Mol Cell **20**(4): 539-550.

Young, R. M. and L. M. Staudt (2013). "Targeting pathological B cell receptor signalling in lymphoid malignancies." Nat Rev Drug Discov **12**(3): 229-243.

Yu, D., D. Allman, M. H. Goldschmidt, M. L. Atchison, J. G. Monroe and A. Thomas-Tikhonenko (2003). "Oscillation between B-lymphoid and myeloid lineages in Myc-induced hematopoietic tumors following spontaneous silencing/reactivation of the EBF/Pax5 pathway." Blood **101**(5): 1950-1955.

Yu, D. and A. Thomas-Tikhonenko (2002). "A non-transgenic mouse model for B-cell lymphoma: in vivo infection of p53-null bone marrow progenitors by a Myc retrovirus is sufficient for tumorigenesis." Oncogene **21**(12): 1922-1927.

Yu, H., T. J. van Berkel and E. A. Biessen (2007). "Therapeutic potential of VIVIT, a selective peptide inhibitor of nuclear factor of activated T cells, in cardiovascular disorders." Cardiovasc Drug Rev **25**(2): 175-187.

Danksagung

Ich möchte allen Personen, die mich auf der Reise zur Promotion unterstützt haben und mir sowohl tatkräftig als auch emotional zur Seite standen, herzlich danken.

Dabei gilt Prof. Dr. Edgar Serfling ein besonderer Dank. Es war mir eine große Ehre in seinem Labor arbeiten zu dürfen und seinen Ideenreichtum und Enthusiasmus für die Forschung spüren zu können.

Ich bedanke mich weiterhin bei Dr. Andris Avots, der mir die ganze Zeit als mein Betreuer, Lehrer und Freund zur Seite stand. Es hat mir wirklich große Freude bereitet mit ihm zu arbeiten, zu diskutieren, zu scherzen und so vieles von ihm zu lernen.

Allen Mitarbeitern des pathologischen Institutes, insbesondere den Mitarbeitern der molekularen Pathologie, danke ich für die vielen Hilfestellungen und für die freundliche Atmosphäre. Besonders danken möchte ich dabei meinen vielen Helfern und Mitstreitern, wie Rhoda Busch, Tobias Pusch, Krisna Murti, Doris Michel, Hani Alrefai, Amiya Patra, Stefan Klein-Heßling, Khalid Muhammad und Friederike Berberich-Siebelt.

Ein großer Dank gebührt auch meinen Geschwistern und Großeltern. Vor allem meinen Eltern möchte ich ganz herzlich für die Möglichkeit der Verwirklichung meiner Vorstellungen, sowie die ständige moralische und finanzielle Unterstützung während und vor meines Studiums und während der Durchführung der Promotionsarbeit danken.

Curriculum vitae

Persönliche Daten

Hendrik Eike Fender

Geburtstag: 06.08.1988

Geburtsort: Göttingen



Bildungsgang

Grundschule: 1994-1998 Besuch der Grundschule Herberhausen

Orientierungsstufe: 1998-2000 Besuch der Orientierungsstufe Nord in Göttingen

Gymnasium: 2000-2007 Besuch des Felix-Klein-Gymnasiums in Göttingen

Abschluss: Juli 2007 Abitur mit GdCh-Auszeichnung im Fach Chemie

Zivildienst: Innere Medizin Krankenhaus Neu-Mariahilf Göttingen

Studium: 2008-2014 Studium der Humanmedizin in Würzburg

Physikum am 8.4.2010

Staatsexamen am 21.11.2015

Promotion: Seit 2011 in der Abteilung für Molekularpathologie des Pathologischen Instituts der Universität Würzburg unter der Leitung von Prof. Dr. Edgar Serfling. Thema: NFATc1 as a Therapeutic Target in Burkitt's Lymphoma.